Contents

Introduction **4**

1 Random spin-glasses **7**

1.1 Spin-glass materials 7

1.1.1 Main experimental features 7

1.1.2 Edward-Anderson model and disorder averages 10

1.2 Sherrington-Kirkpatrick model 11

1.2.1 TAP mean field equations 12

1.2.2 Exponential number of solutions of the TAP equations 16

1.2.3 Non-trivial broken ergodicity and order parameters 19

1.2.4 The replica approach 24

1.2.5 Replica symmetric solution 27

1.2.6 Stability analysis and AT line 29

1.2.7 Parisi solution: replica symmetry breaking 30

1.3 Others infinite ranged models 35

1.3.1 p-spin model and the Random Energy Model 35

1.4 Realistic spin-glasses 38

2 Deterministic models with glassy behavior **40**

2.1 General features of deterministic models 40

2.2 Frustration 42

2.3 A random approach to deterministic models 43

2.4 Low Autocorrelation Model 44

2.4.1 Static equilibrium transition 45

2.4.2 Dynamical glassy transition 46

2.4.3 Introduction of a random model 48
2.5 The Sine Model and the Random Orthogonal Model 49
2.6 Another deterministic models 50

3 High temperature expansions for deterministic models 53
3.1 Introduction 53
3.2 Mean field equations 53
3.2.1 Case A: the sine model 56
3.2.2 Case B: the "quadratic" model 57
3.3 Ising model of arbitrary spin s 58
3.4 Conclusions 62

4 Statistics of energy levels and zero temperature dynamics for the Sine model 64
4.1 Introduction 64
4.2 Metastable states in the Random Orthogonal model 65
4.3 The limiting distribution of the rescaled energy levels 68
4.4 Legendre symbols as ground states in the sine model 71
4.5 Flipping spins from the ground state and statistics of levels 73
4.6 Zero temperature dynamics and metastable states. 78
4.7 Analytical estimate of the number of metastable states 79
4.8 Numerical checks of the analytical estimate 87
4.9 Conclusions 89

5 Chiral and spin order of the random XY model on a tube lattice 91
5.1 Introduction 91
5.2 The XY spin-glass model 92
5.3 Domain Wall Renormalization Group 94
5.4 Coulomb gas representation 97
5.5 Numerical Results 99
5.6 Conclusion 102

6 Spin-glasses and portfolio optimization 104
6.1 Introduction 104

6.2 The model 107
6.2.1 "Complexity" of the model 109
6.2.2 Constructing the efficient frontier 110
6.3 A worked example 112
6.3.1 Data 113
6.3.2 Multiple solutions 113
6.3.3 Exponential growth of solutions in the number of assets . . . 116
6.3.4 The efficient frontier 117
6.4 A few remarks on the variances/covariances matrix 119
6.5 Conclusions 122

A Proof of formulas (4.47) and (4.48) **127**

B Proof of formula (4.54) **129**

Acknowledgments **132**

References **133**

Introduction

The thermodynamical behavior of uniform systems showing phase transition, like ideal solids, is well explained by statistical mechanics. Despite the fact that only a few models can be solved exactly, the general mechanism underlining the passage from a disordered state to a ordered one is clear in translationally invariant systems and it has been formalized at the higher level in the theory of renormalization group. Real materials are seldom, if ever, the idealized pure systems that are considered by usual statistical mechanics. For example, magnetic crystals invariably contain defects and non-magnetic impurities. Liquids, which are generally taken to be composed of a single component, invariably have impurities dissolved in them. Thus it is important to understand the effect of disorder on the properties of materials.

Spin glasses are the current frontier in the study of magnetic disordered systems. They are systems of a collections of spins (magnetic moments) as a conventional ferromagnet or antiferromagnet. However, the low-temperature state is not the uniform or periodic configuration that is characteristic of conventional magnets. Therefore in spin glasses there is no long range order such as ferromagnetism or anti-ferromagnetism, but a new *frozen ordered state*. From the theoretical point of view it is believed that in order to reproduce such a state two new ingredients (absent in usual magnets) are essential: *frustration* and *randomness*. The frustration means that there is competition among the interactions between spins, so that there is no single spin configuration which minimize all the interactions simultaneously.

Randomness is usually introduced in pure (periodic) systems with the aim of producing competition between positive and negative bonds between spins: the former tend to align spins and the latter to antialigne them. Although there have been many efforts devoted to understand the physics of the random spin glasses for more than two decades, they are still far from fully understood due to the lack of

rigorous theoretical predictions. Since the upper critical dimension of these models is believed to be six, the behaviour in the real two and three dimensions could be far from the mean field theory, which is so far the only well-established theory. Thus one has to rely more and more on the numerical studies. At the present moment, the outcome of these studies is a convincing evidence that a finite temperature transition to an ordered spin-glass phase does exist in the Ising spin glass in three dimensions. More controversial is the situation for the XY and Heisenberg spin glass, where is still open the question if the lower critical dimension is three or four.

There has been also a great deal of study of periodic frustrated systems in which disorder is not present (these are called fully frustrated model, an example of which is the two-dimensional nearest-neighbour Ising model on a triangle lattice with all bonds antiferromagnetic). In these cases apparently the effective free energy landscape is too smooth to reproduce the complex spin-glass behaviour. The general belief is that frustration, although necessary, is not sufficient alone to produce a non-trivial broken ergodicity. Nevertheless, in recent years it has been considered *deterministic* non-random models that, at least at the mean field level, show the main properties typical of spin-glasses, in particular the existence of a huge number of "metastable" states (valleys in the free energy landscape).

In this dissertation we study both deterministic model with glassy behaviour and random spin-glasses. The outline of this work is the following:

- Chapters 1 and 2 are introductory. In the first it is reviewed the general theoretical concepts and models in spin glasses theory, within the random approach. After a brief Section in which experimental features are treated, the main focus is on the mean field Sherrington-Kirkpatrick model, which is at the present moment, the only well established theory. Other infinite range models, like the $p-$spin models and the Random Energy Model, are treated as well. Some remark on realistic short-range spin glasses are presented. In Chapter 2 we review the "state of the art" for non-random models with a glassy behaviour, showing the connection both with with structural glass transition and with disordered systems.

- In the context of deterministic models, the *sine* model introduced in ref. [69] and the *"quadratic"* model introduced in ref. [70] are our main concern

in Chapters 3 and 4. The high-temperature phase is studied by means of high-temperature expansions. In particular we extend previous analysis for dichotomic spin variables to the case of Ising variables of arbitrary spin. Furthermore we study analytically the statistics of energy levels, giving a full characterization of the energy distribution in the phase space. In the low-temperature limit we investigate, both numerically and analytically, the metastable states. At exactly zero temperature this amount to study the 1-flip stable stable states, due to the long range behaviour of the interactions.

- Within the realm of the random spin glasses, the XY model on a tube lattice is considered in Chapter 5. We employ the zero temperature domain wall, or defect energy scaling, to study it. Our motivation comes from the notice that this one-dimensional model, though does not exhibit broken symmetry at finite temperature, has been analyzed analytically, so that it could represent a sort of test for the existing numerical techniques. On the other hand, we will see that, applying numerical analysis, we gained some new informations that enabled us to cure some wrong assumptions that were employed in the analytical study.

- The underlying ideas of mean field spin glass theory have also proved to be fruitful in optimization problems and others research fields originally not related to condensed matter theory, such as biology, neural networks, optimization problems, digital images reconstruction and many others. New applications of these ideas have been proposed in a continuous way and still nowadays the "physics of complexity" is a growing subject. Following the pioneering study of ref. [119], one of the original contribution of this dissertation is to establish a strong connection between mean field spin-glasses (random or deterministic) and portfolio optimization in futures markets. We will deal with this issue in the last Chapter of this work.

Chapter 1

Random spin-glasses

1.1 Spin-glass materials

The classical examples of spin glass materials are noble metals (Au, Ag, Cu, Pt) weakly diluted with transition metal (Fe, Mn, Cr) impurities carrying local magnetic moments, which interact each other by Ruderman-Kittel-Kasuya-Yoshida (RKKY) interaction [5, 6, 7]. The transition metal moments produce a magnetic polarization of the host metal conduction electrons around them which is positive at some distance and negative at others. Other impurity moments then fell the local magnetic field produced by the polarized conduction electrons and try to align themselves along it. Because of the random placements of the impurities, the result is competing interactions. Many other materials (including magnetic insulators and amorphous alloys) have been identified as having a transition of the spin glass type. In this case the dependence of the interactions on the distance is completely different from that in the crystalline metallic systems. Moreover also non-magnetic materials, as ferroelectric-antiferroelectric mixtures and disordered molecular crystals, are known to display a kind of oriental freezing. In these cases the role of magnetic moments is played by electric dipole and quadrupole moments, respectively. We remand the reader to ref. [1] for a comprehensive list of spin-glass materials.

1.1.1 Main experimental features

Experimental signature of spin glasses was first observed by Cannella and Mydosh in 1972 [8]. They observed a sharp cusp in susceptibility at a temperature T_c (see

Fig. (1.1)). This suggested that there was a continuous phase transition from a paramagnetic phase to an ordered phase. Subsequently, more refined experiments showed that the cusp in $\chi_{a.c.}$ is very sensitively field-dependent and is not completely sharp [9, 10]. The freezing temperature T_c depends on the frequency of the applied magnetic field, so that the "true" T_c should be defined by the limit of vanishing frequency. This qualitative feature of frequency dependence is peculiar of spin glass materials and is absent in conventional magnets. This is related to the glassy nature of spin glasses, with long characteristic time and the presence of metastable states.

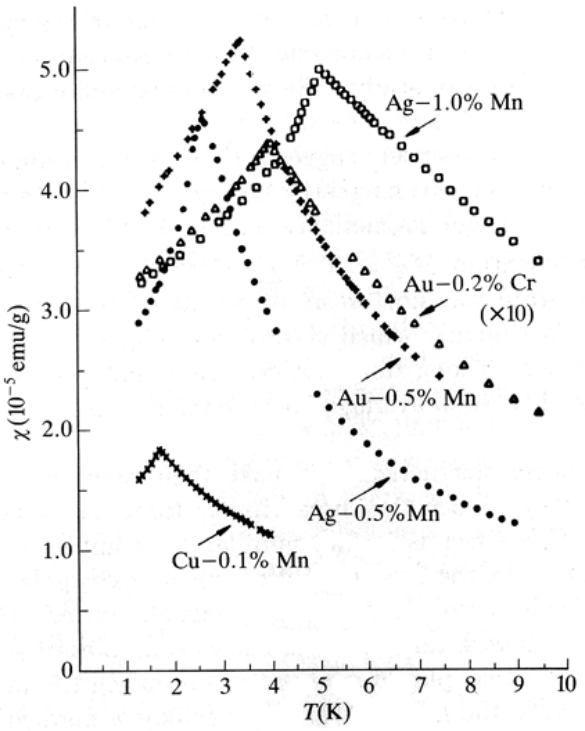

Figure 1.1: The ac susceptibility of Cu-0.1% Mn (×), Ag-0.5% Mn (•), Au-0.5% Mn (+), Au-0.5% Cr (△) and Ag-1.0% Mn (□) versus temperature for a magnetic field $H = 20$ Oe and 100 Hz (from ref. [8])

Another important feature that is a signature of the glassy properties in spin glasses is the remanence and irreversibility below the transition temperature T_c [11]. As it is clear from Fig. (1.2), the resulting susceptibility depends on how to perform the experiment, *i.e.* there is a difference between the "field-cooled" susceptibility and the "zero-field-cooled" susceptibility. The "field-cooled" means that the sample is cooled down below T_c in the filed which is applied above T_c. The "zero-field-cooled" is the case where the sample is cooled below T_c in zero field and then the field is applied. The former is, to a very good approximation [12, 13], independent of its history, but the latter is not for $T < T_c$. The fact that the magnetic response is history dependent can be qualitatively ascribed to the existence of many roughly equivalent (but very different!) spin configuration, so that the state which is reached depends crucially on details of the experiment such as the frequency and magnitude of the applied field, the speed with one cools down and whether one cools in zero or finite field.

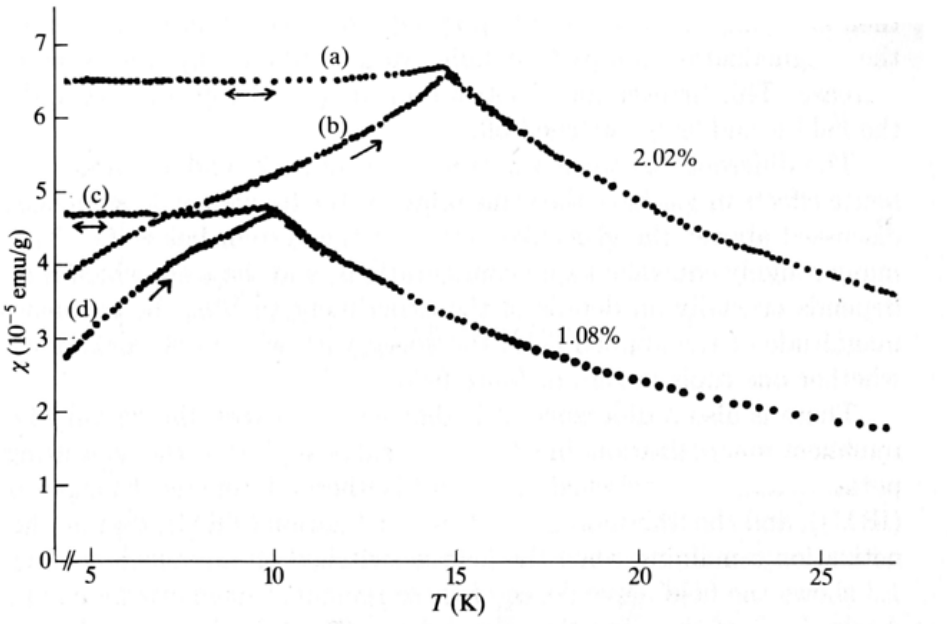

Figure 1.2: The static susceptibility of CuMn vs temperature for 1.08 and 2.02% Mn. After zero-field cooling ($H < 0.05Oe$), initial susceptibilities (b) and (d) were taken for increasing temperature in a field of $H = 5.90$ Oe. The susceptibilities (a) and (c) were obtained in the field $H = 5.90$ Oe, which was applied above T_c before cooling the samples (from ref. [11])

Other experimental properties of spin glasses below T_c are the following [3]:

- ⋆ The remanent magnetization decays very slowly with time.
- ⋆ A hysteresis curve, laterally shifted from the origin, appears.
- ⋆ No magnetic Bragg scattering is observed in neutron scattering experiments, thereby demonstrating the absence of long range order.
- ⋆ No sharp anomaly is detected in the specific heat that only shows a broad maximum at T_c.

1.1.2 Edward-Anderson model and disorder averages

The most simple model that has the two essential features, *i.e.* disorder and frustration, necessary to describe the spin glass transition was introduced by Edward and Anderson (EA) [14]. They put the spins on lattice sites (square in $2d$ and cubic in $3d$) and took the coupling between nearest neighbors spins to be independent random variables J_{ij} from some assigned distribution $P(J_{ij})$. Then they proposed a model Hamiltonian for spin glass as

$$H = -\frac{1}{2} \sum_{<ij>} J_{ij} \, S_i \cdot S_j \tag{1.1}$$

where S_i are n-component spins. When $n = 1$ the system becomes Ising spin glass,while the XY spin glass and Heisenberg spin glass are defined by $n = 2$ and $n = 3$, respectively. The standard choices for the coupling distribution are the symmetric Gaussian

$$P(J_{ij}) = \frac{1}{\sqrt{2\pi J^2}} \exp\left[-\frac{J_{ij}^2}{2J^2}\right] \tag{1.2}$$

and the double delta-function ($\pm J$ *model*)

$$P(J_{ij}) = \frac{1}{2}\delta(J_{ij} - J) + \frac{1}{2}\delta(J_{ij} + J) \tag{1.3}$$

In any case, the EA model is *short-ranged*: the J_{ij} are different from zero only for nearby pairs of spins, so that a spin interact only with its neighbors. The *long-ranged* version of the model (known as "SK model") is obtained by letting all the spin interact with the others and it will extensively treated in the next Section.

Since EA model is random, the free energy and thus any thermodynamic quantities calculated from the free energy will be different from sample to sample. This requires to perform an other average, the disorder average, in addition to the usual thermal average for each realization of disorder. We denote by $\langle \cdots \rangle$ the thermal average over spins configurations weighted with Boltzmann factor and by $\overline{\cdots}$ the average over the disordered couplings. There are two kinds of disorder average, the "annealed" and "quenched" averages. In the former, the disorder is treated on the same footing as the statistical variable such as spins, and can be used to describe the annealed systems, where the random variables reach their thermal equilibrium. On the other hand, if the random disorder is quenched and thus takes unique value independently from the temperature, one has to consider the quenched average, which is the case for spin glasses. The main difficulty in averaging comes from the fact that one has to average the free energy $\sim \ln Z$, not Z itself. There is a nice trick to do this difficult task, called the "replica method", that will be diffusively applied to the SK model in the next Section.

1.2 Sherrington-Kirkpatrick model

The first step in order to get some comprehension of the new physics of spin-glass was to analyze the mean-field theory. It turns out to be highly nontrivial and has been developed over more than a decade. Insofar it is the only well-established spin-glass theory, even if a *rigorous* solution (from the mathematical point of view) is still lacking.

The Hamiltonian of the infinite-range model introduced in 1975 by Sherrington and Kirkpatrick [15] (nowadays referred as SK model) is defined as

$$H = -\frac{1}{2} \sum_{i,j=1}^{N} J_{ij} \sigma_i \sigma_j - h \sum_{i=1}^{N} \sigma_i \tag{1.4}$$

where J_{ij} are symmetric ($J_{ij} = J_{ji}$) gaussian random variables with mean J_0 and variance J^2:

$$p(J_{ij}) = \frac{1}{\sqrt{2\pi J^2}} e^{-(J_{ij}-J_0)^2/2J^2} \tag{1.5}$$

and $\sigma_i = \pm 1$ are dichotomic Ising spin variables. The sum runs over all the possible pairs of particles in a one dimensional lattice of N sites. The physical sensible scaling

of J_0 and J^2 in order the energy to be an extensive quantity is

$$J_0 = \tilde{J}_0/N \tag{1.6}$$

$$J = \tilde{J}/\sqrt{N} \tag{1.7}$$

where $\tilde{J}_0$ and $\tilde{J}$ are $\mathcal{O}(1)$ quantities. In the following we will restrict to the case $J_0 = 0$: including a non-zero mean value as in the original articles [15] would yield a competition between ferromagnetic and spin-glass order, without appreciable physical consequences but with some complication of the formulas.

For a given disorder realization, one expect that in the high temperature phase the local magnetization $m_i = \langle \sigma_i \rangle$ is different from zero only if a magnetic field is present and it vanishes when the magnetic field goes to zero; on the other hand one naively expect that in the low temperature region there should be (as in the case of ferromagnets) some freezing of the spin in the position which is mostly favored energetically, hence the m_i should be different from zero also at zero external field. However the local magnetization m_i depends on the coupling realization and it will sometimes be positive and sometimes negative, that means the global magnetization density $(1/N)\sum_i m_i$ is zero. Therefore it is convenient to characterize the system in terms of the so-called Edward-Anderson parameter

$$q_{EA} = \frac{1}{N}\sum_{i=1}^{N} m_i^2 \tag{1.8}$$

1.2.1 TAP mean field equations

We start by considering the mean field equations of the SK model which were introduced by Thouless, Anderson and Palmer [18]. The TAP proposal was to compute the mean magnetizations directly from the mean field equations for a given choice of the bonds $\{J_{ij}\}$ and then to average over disorder. Their starting point was a high-temperature expansion of the free energy, originally derived by diagram expansion:

$$\begin{aligned} -\beta F(m_i) &= -\sum_i \left[\left(\frac{1+m_i}{2}\right) \ln \left(\frac{1+m_i}{2}\right) + \left(\frac{1-m_i}{2}\right) \ln \left(\frac{1-m_i}{2}\right) \right] \\ &\quad + \frac{\beta}{2}\sum_{ij} J_{ij} m_i m_j + \frac{\beta^2}{4}\sum_{ij} J_{ij}^2 (1-m_i^2)(1-m_j^2) \end{aligned} \tag{1.9}$$

Rigorous derivation of this expression through diagrammatic analysis can be found in ref. [19, 20, 21], while a different approach, known as "cavity method", is given in chapter 5 of ref. [2]. The physical interpretation of Eq. (1.9) is the following: the first line is the entropy of a set of Ising spin constrained to have means m_i; the second term is the naive internal energy of a frozen lattice; and the last term is the correlation energy of the fluctuations. This last term is usually called "Onsanger" or "*reaction*" term, for reason that will be clear in a while.

The mean field TAP equations are then obtained from the extremization condition $\partial F/\partial m_i = 0$. They read

$$m_i = \tanh\left[\beta \sum_j J_{ij} m_j - \beta^2 \sum_j J_{ij}^2 (1 - m_j^2) m_i\right] \tag{1.10}$$

The first two terms on the r.h.s. describe the conventional internal field in normal ferromagnets. The third term describes the contribution to the internal field from the spin s_i itself. Following the argument made by Onsanger, the magnetization m_i at site i produces a mean field $m_i J_{ij}$ at site j, which induces a magnetization $\chi_{jj} m_i J_{ij}$ at site j. The ordering of the spin s_i is induced by the internal fields of the spin s_j in the absence of the s_i, so this term has to be subtracted from the full mean field $\sum_j J_{ij} m_j$ in computing m_i:

$$m_i = \tanh\left[\beta \sum_j J_{ij} (m_j - \chi_{jj} m_i J_{ij})\right] \tag{1.11}$$

Eq. (1.10) are recovered after inserting in the last expression the fluctuation-response relation

$$\chi_{jj} = \beta \langle (s_j - \langle s_j \rangle)^2 \rangle = \beta (1 - m_j^2) \tag{1.12}$$

In normal ferromagnets the reaction field can be ignored, since it is smaller than the ordinary molecular field by a factor $1/N$. On the other hand in spin-glasses the reaction field, being quadratic in the couplings, is of the same order of magnitude of the molecular field.

TAP equations (1.10) are N coupled non linear equations for the local magnetization m_i and their exact solution is an hopeless task. They can be considerably simplified if one assume *self averaging*, that is, the error introduced by substituting m_j^2 by the EA order parameter $q_{EA} = N^{-1} \sum_j m_j^2$ vanishes in the

thermodynamical limit. Then the Onsanger term can be simplified and the equations become

$$m_i = \tanh\left[\beta \sum_j J_{ij} m_j - \beta^2 \tilde{J}^2 (1 - q_{EA}) m_i\right] \tag{1.13}$$

An analytic solution can be obtained in the critical region ($T \sim T_c$), while in the low-temperature region ($T \sim 0$) an approximated solution can be found by means of numerical computations.

For T near T_c, one expects m_i to be small and similar to the eigenvector M_i belonging to the largest eigenvalue $J_\lambda^{max} = 2\tilde{J}$ of the exchange matrix J_{ij}, so that one can linearize Eq. (1.13) near $q_{EA} = 0$. Any eigenvector M_i yields a solution if

$$1 - 2\beta\tilde{J} + \beta^2 \tilde{J}^2 = 0 \tag{1.14}$$

Its only positive zero $\beta = 1/\tilde{J}$ determines the critical temperature $T_c = \tilde{J}$. Therefore, for $T > T_c = \tilde{J}$ there is only the paramagnetic solution $q_{EA} = 0$, while for $T < T_c$ there is another solution (the physical one with the lower free energy) where q_{EA} is different from zero. Note that without the reaction term the critical temperature would be have been overestimated of a factor 2, that is the critical temperature would have been $T = 2\tilde{J}$. For T just below T_c, expanding to higher order Eq. (1.13) near $q_{EA} = 0$, one finds:

$$q_{EA}(T) = 1 - \frac{T}{T_c} + \mathcal{O}((T_c - T)^2) \tag{1.15}$$

In the low temperature regime, $T \ll T_c$, TAP characterized the low-energy excitations by the distribution $p(\tilde{h}_i)$ of the total molecular field $\tilde{h}_i = \sum_j J_{ij} m_j$, neglecting possible excitations which might require the simultaneous reversal of more than one spin. In fact, in the limit $T \to 0$, Eq.(1.10) greatly simplify to

$$m_i = \text{sign}(\tilde{h}_i) \tag{1.16}$$

Numerically they found that the probability distribution of the local field is linear in $\tilde{h}$ [18] (see also ref. [22])

$$p(\tilde{h}) = \frac{\tilde{h}}{h_0^2} \qquad (\tilde{h} \to 0, T \to 0) \tag{1.17}$$

Following the hint from Monte Carlo simulations, they further supposed a quadratic dependence for $q_{EA}(T)$, instead of the linear T dependence given by (1.15):

$$q_{EA}(T) = 1 - \alpha \left(\frac{T}{T_c}\right)^2 \tag{1.18}$$

Inserting this expression in Eq. (1.13) one has

$$m_i = \tanh\left[\beta\tilde{h}_i - \alpha m_i\right] \tag{1.19}$$

A relation between the coefficients α and h_0^2 can then be obtained by imposing the self-consistency equation

$$\begin{aligned} q_{EA} &= \int_0^\infty m^2(\tilde{h}) p(\tilde{h}) d\tilde{h} \\ &= h_0^{-2} \int_0^1 m^2 \tilde{h}(m) \frac{d\tilde{h}}{dm} dm \end{aligned} \tag{1.20}$$

which, after some integration, leads to the relation

$$\frac{h_0^2}{\tilde{J}^2} = \frac{1}{4}\alpha + \frac{2\ln 2 + 1}{3} + \frac{\ln 2}{\alpha} \tag{1.21}$$

which leaves the only unknown parameter α. TAP argued that the physical relevant value of α was the one which minimized h_0, *i.e.* the one which gave the maximum density of low-energy excitations. They found $\alpha = 2\sqrt{\ln 2} \approx 1.665$. Once α is determined, thermodynamic quantities in the low-temperature region ($T \ll T_c$) can be obtained from the free energy (Eq. (1.9))

$$\chi(T) \sim \alpha \left(\frac{T}{T_c}\right) \tag{1.22}$$

$$c(T) \sim \frac{1}{2}\alpha^2 \left(\frac{T}{T_c}\right)^2 \tag{1.23}$$

$$s(T) \sim \frac{1}{4}\alpha^2 \left(\frac{T}{T_c}\right)^2 \tag{1.24}$$

Unfortunately, because of the complicated structure of the TAP equations, it has not been possible to find analytically any general solution valid at all temperature. Moreover the stability analysis, performed by Bray and Moore in ref. [23], showed that the condition for the Hessian matrix $\partial^2 F/\partial m_i \partial m_j$ not to have negative eigenvalues is given by:

$$1 - \beta^2 \tilde{J}^2 (1 - 2q_{EA} + r) > 0 \tag{1.25}$$

where $q_{EA} = \frac{1}{N}\sum_i m_i^2$ and $r = \frac{1}{N}\sum_i m_i^4$. So we see that the system of TAP equations (1.10) makes sense only if the $\{m_i\}$ belong to a certain part of phase space. We will see later, in the replica approach, that this part of phase space correspond to the region above the so-called AT line in the $(h - T)$ plane. The solutions for which the eigenvalue spectrum is not positive, *i.e.* the one for which condition (1.25) is not satisfied, are on and below the AT line. They are called *marginally stable* in the sense that one has a divergent response everywhere along and below this line. The physical quantity that display this divergence is the spin glass susceptibility defined as

$$\chi_{SG} = \frac{1}{N}\sum_{ij}\chi_{ij}^2 = \frac{\beta^2}{N}\sum_{ij}(\langle\sigma_i\sigma_j\rangle - \langle\sigma_i\rangle\langle\sigma_j\rangle)^2 \tag{1.26}$$

It is worth mentioning that the condition (1.25) is identical with that for the convergence of the free energy expansion [21], because the TAP solutions can not be stable unless the subexstensive terms in the free energy expansion converge.

1.2.2 Exponential number of solutions of the TAP equations

Even if the complicate structure of TAP equations allow only for an heuristic treatment, these equations have been very important because they gave the first analytical indication of the complex structure of the free energy landscape in mean field spin-glasses. It turned out that TAP equations have an *exponential number of solution N_s below T_c* [24, 25, 26]. At that time it was already suspected from Monte Carlo simulations [16] that in SK model the free energy landscape is very complicated, in the sense that there are many local minima corresponding to pure states and ergodicity is broken in a non trivial way. The discover of an exponential number of solutions of TAP equations was the first direct hint of this complex behaviour: one can associate to each "state" or "phase" a solution of the TAP equation. On the contrary the inverse relation does not hold. There are many solutions of the TAP equations which do not correspond to stable states. These are called *metastable states*. Exactly at zero temperature, it can be shown that in models with long-range couplings, as SK, metastable states coincides with 1-flip-stable spin configurations, *i.e.* with configurations whose energy can not be decreased by flipping any of the spins. According to the folklore a TAP solution

corresponds to a stable state only if it is separated from other solutions by a barrier whose height diverges with the volume, so that the systems is trapped forever in the free energy valley associated with that solution. The number N_0 of solutions representing pure phases is considerably smaller than the total number of solutions N_s. Indeed in ref. [27] it was proved that ultrametricity does not allow N_0 to exceed N.

The calculation of N_s for the SK model will be presented in Sec. (4.2), where it will obtained as a by-product of the same computation for the Random Orthogonal Model. For the moment we give only the result at zero temperature [24, 25, 26]

$$\overline{N_s} = \exp(0.1992N) \tag{1.27}$$

and we show in Fig. (1.3) the total number of solutions as a function of the temperature. For $T > T_c$ one has only the paramagnetic solution $m_i = 0$. With decreasing temperature one has a sharp increase in the number of solutions.
Once that it was realized the existence of the exponential number of solutions, it soon became clear that the heuristic analysis performed by TAP should be modified in order to take in account this new information. A natural proposal was to assume that the statistical expectation value of a quantity is the average of the values that such a quantity takes in all possible solutions of the TAP equation, each solution contributing with a given weight. In particular, the local magnetization is given by

$$\langle s_i \rangle = m_i = \sum_{\alpha=1}^{N_s} w_\alpha m_\alpha^i$$

$$\sum_{\alpha}^{N_s} w_\alpha = 1 \tag{1.28}$$

where the different solutions of the TAP equations are labeled by α. The delicate point was the choice of the weights w_α. The first tentative was to perform a white average (all the w equal to each other) [20, 26]. In view of the above discussion, it is clear that the thermodynamical results are necessarily wrong (one finds a negative specific heat at low temperature!) because the solutions do not contribute all in the same way to thermodynamics. The right choice for the weight is

$$w_\alpha = \frac{\exp(-\beta F_\alpha)}{\sum_{\gamma=1}^{N_s} \exp(-\beta F_\gamma)} \tag{1.29}$$

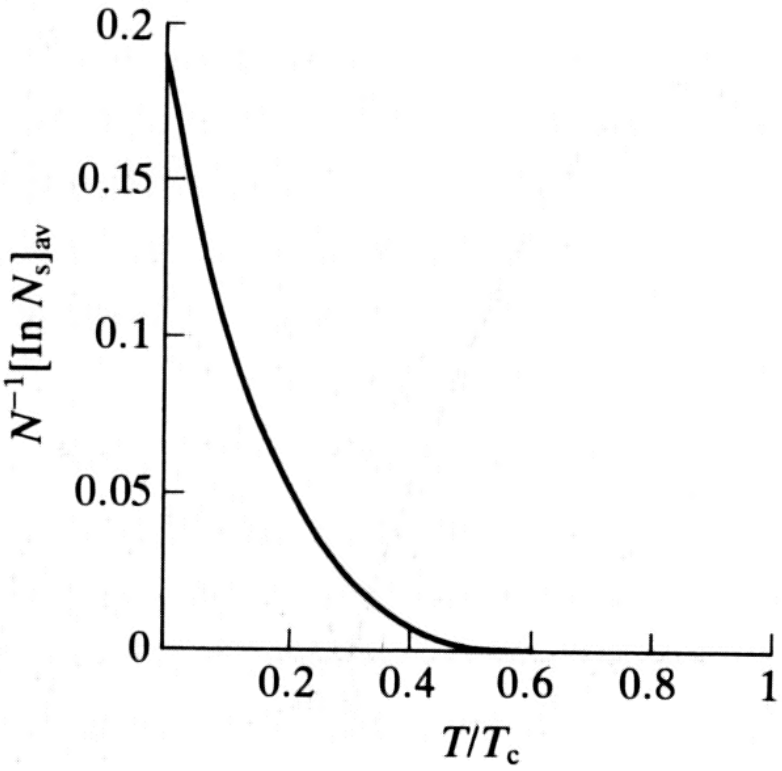

Figure 1.3: Logarithm of the total number N_s of TAP solutions, divided by N, as a function of the temperature (from ref. [24])

F_α being the total free energy of the α-th solution. In this way the only solutions which are relevant in the limit $N \to \infty$ are those which have a low value of the free energy. It finally turned out that it is very difficult to avoid the use of replicas and such a computation is at least as complex as the evaluation of the free energy using the replica approach. However introducing replicas one can shows that the weighted average of the TAP equations gives the same thermodynamics as the replica approach [28].

TAP equations are very tricky also from the numerical point of view. Nemoto and Takayama [29, 30, 31] have investigated the stationary points of the TAP free energy $F\{m_i\}$ (1.9) as defined by minimizing $|\nabla F| = \sqrt{\sum_i (\partial F/\partial m_i)^2}$. Starting from the freezing temperature T_c, they found an increasing number of solutions,

80% of which are marginally stable.

1.2.3 Non-trivial broken ergodicity and order parameters

In normal ferromagnets, when the phase transition takes place, the ergodicity is broken in a trivial way: one has only *two* "pure states" or "thermodynamic phases", *i.e.* the one with positive magnetization and the one with negative magnetization. They are related by an overall spin flip. Above the Curie critical temperature the free energy has only one minimum, corresponding to the paramagnetic phase of zero magnetization. Below the critical temperature the free energy develops two minima, corresponding to the states up- or down-magnetized, and the system select one of this state and will never be found later in the other one. The notion that the system can find itself in a state which breaks the symmetry of the Hamiltonian is a very profound one. It means that the ergodic hypothesis is violated. The system motion is restricted to the part of configuration space with positive or negative magnetization. In calculating the thermal averages through statistical mechanics one has to put the broken ergodicity by hand, restricting the trace used to define thermal averages to configurations having positive or negative magnetization. Alternatively one can achieve this restricted trace formally in the ferromagnet by keeping a very small magnetic field in the Hamiltonian, calculating the trace over all configurations space, taking the thermodynamical limit and *in the end* letting the magnitude of the magnetic field to zero. The order of the limit is crucial and is essential to develop an infinite barrier between the two minima of the free energy. More explicitly, in a system of size N to select the positive magnetization state one needs a positive symmetry-breaking field that is large compared to T/N in order to give a negligible relative thermal weight to the negative magnetization state.

From the TAP analysis described in the previous Sections, it emerges the picture of a *very complex* free energy landscape in the SK model, so that one has at least to address the possibility of *non-trivial broken ergodicity*. In the $(N+1)$ dimensional space whose axes are labeled by the m_i and $F(\{m_i\})$, the free energy function has an exponential number of local minima, *i.e.* solutions of $\partial F/\partial m_i = 0$ with the eigenvalues of the matrix $\partial^2 F/\partial m_i \partial m_j$ all positive. If, in the limit of large N, some of the barriers between these locally stable magnetization configurations become infinite, one can partition the entire state space into mutually inaccessible

"valleys". Each of these valleys corresponds to a thermodynamic phase. Within such a state there can be several sub-valleys which are local minima of F, but with finite barriers separating them. All but the lowest of these correspond to metastable magnetization configurations. When a system finds itself in one of this valleys it will exhibit properties which in general are specific to that valley. They differ from true equilibrium properties which involve averages over all valleys with appropriate relative thermal weights. For example, there might be valleys (or at least metastable sub-valleys) with very different magnetizations; this is the origin of the remanence observed in all spin-glasses. In order to calculate the properties of the system in a single valley, the trace over configurations in the partition function must be restricted to the appropriate valley. If there are many possible states, whose free energies are expected to be the almost the same, the imposition of an infinitesimal external field uncorrelated with any m_i^α will no longer select out a single phase. Furthermore, we are handicapped in trying to use infinitesimal external fields h_i^α proportional to the m_i^α to try to generate appropriately restricted trace because we do not know this conjugate fields a priori.

Thus broken ergodicity makes the definition of relevant thermal averages in general, and that of order parameters in particular, a highly non-trivial one. A natural consequence of the existence of many phases is that a spin glass can not be described by a single order parameter, but rather requires many of them. If we regard ergodicity breaking as essentially dynamical in nature, the most natural order parameter to consider is the one introduced originally by Edward and Anderson [14]:

$$q_{EA} = \lim_{t\to\infty} \lim_{N\to\infty} \overline{\langle s_i(t_0) s_i(t_0+t)\rangle} \tag{1.30}$$

where the average is over a long (eventually infinitely so) set of reference times t_0. This will clearly be zero if the system is ergodic, and will be nonzero if it is trapped in a single phase. One must take the $N \to \infty$ limit before the $t \to \infty$ one, since for a finite system the correlation will eventually die out as true equilibrium is reached. Since an infinite system can never escape the valley it is, q_{EA} measures the mean square single-valley local spontaneous magnetization, averaged over all possible valleys. That is, in terms of thermal averages:

$$q_{EA} = \overline{\sum_\alpha w_\alpha (m_i^\alpha)^2} \tag{1.31}$$

where the weights w_α are given by formula (1.29). It can be shown that, in the mean field SK model, q_{EA} is *self-averaging* in the thermodynamical limit, *i.e.* it does not depend on the disorder realization, so that one can also write

$$q_{EA} = \frac{1}{N} \sum_i \sum_\alpha w_\alpha (m_i^\alpha)^2 \tag{1.32}$$

q_{EA} is not, of course, the mean square local *equilibrium* magnetization. The true equilibrium or statistical mechanics order parameter is defined as:

$$q = \overline{m_i^2} = \overline{\left(\sum_\alpha w_\alpha m_i^\alpha \right)^2} = \overline{\sum_{\alpha\beta} w_\alpha w_\beta m_i^\alpha m_i^\beta} \tag{1.33}$$

or, equivalently,

$$q = \frac{1}{N} \sum_i \overline{\sum_{\alpha\beta} w_\alpha w_\beta m_i^\alpha m_i^\beta} \tag{1.34}$$

One can see immediately that q differs from q_{EA} in having inter-valley contributions. Moreover q is *not* self-averaging, so it is convenient to define it also for a single sample:

$$q_J = \frac{1}{N} \sum_i m_i^2 = \frac{1}{N} \sum_i \sum_{\alpha\beta} w_\alpha w_\beta m_i^\alpha m_i^\beta \tag{1.35}$$

One can picture the difference between q and q_{EA} dynamically by imagining N large but finite, so that transition across the barriers are allowed. On a time-scale long enough for the system to pass statistically many times through all valleys having significant thermal weight, true equilibrium is reached and all inter-valley terms in q contributes. On a short time-scale, no transitions between valleys have time to occur, so q_{EA} is the physical relevant quantity. One can also imagine intermediate time scales, where certain groups of valleys are accessible to each other, but there is not time to climb over the higher barriers separating one group from another. Then a quantity between these two limiting case is the physically relevant one. This picture of a gradual interpolation between complete broken ergodicity and full equilibrium is the physical basis of the Simpolinsky dynamical formulation of mean field theory [32, 33]. The relation between the experimental measurement and the order parameter can be given by the relation

$$\chi = \beta(1 - q) \tag{1.36}$$

where χ is the uniform susceptibility, which is equal to the local susceptibility χ_{ii} for a symmetric bond distribution [34]. Of course, if the system is a particular valley, what one measures is $\chi = \beta(1 - q_{EA})$, not an equilibrium susceptibility.
Coming back to the definitions of order parameters, it is clear that, since one has many phases, it is interesting to ask not only about the mean square magnetization in a single state, such as occurs in q_{EA}, but also about the correlation between states One can consider the *overlap* (for a single sample) defined as

$$q_{\alpha\beta} = \frac{1}{N}\sum_i m_i^\alpha m_i^\beta \tag{1.37}$$

By definition one has $-1 \leq q_{\alpha\beta} \leq 1$. In order to characterize the distribution of overlaps between states, it is useful to introduce the probability distribution of overlap [43]:

$$P_J(q) \equiv \langle \delta(q - q_{\alpha\beta}) \rangle \equiv \sum_{\alpha\beta} w_\alpha w_\beta \delta(q - q_{\alpha\beta}) \tag{1.38}$$

One can also define the corresponding disorder averaged probability distribution

$$P(q) \equiv \overline{P_J(q)} \equiv \overline{\sum_{\alpha\beta} w_\alpha w_\beta \delta(q - q_{\alpha\beta})} \tag{1.39}$$

Through the $P(q)$ one can see that the equilibrium order parameter q is nothing else that the average overlap between pure states:

$$\begin{aligned} q &= \frac{1}{N}\sum_i \overline{\sum_{\alpha\beta} w_\alpha w_\beta m_i^\alpha m_i^\beta} \\ &= \overline{\sum_{\alpha\beta} w_\alpha w_\beta q_{\alpha\beta}} \\ &= \int_{-1}^{1} P(q) q dq \end{aligned} \tag{1.40}$$

On the argument that the correlation between phases cannot be greater than the mean square magnetization in a single phase, it is natural to identify q_{EA} as the largest value of q for which $P(q)$ has support. The form of the probability distribution of overlap $P(q)$ can be used as a valuable tool to distinguish between systems with conventional broken ergodicity and those with nontrivial broken ergodicity. Below the critical temperature, for a normal ferromagnet $P(q)$ is just the sum of a pair of delta functions centered at $q = \pm m^2$, where m is the spontaneous

magnetization. This is because there are only two equilibrium states related by an overall symmetry. On the other hand, for a spin-glass $P(q)$ may have a continuous part, indicating the possibility of a continuum of possible overlaps between various phases. The non-triviality of the function $P(q)$ is the main characteristic of the spin glass phase. Moreover we expect that the weights w_α strongly fluctuate from one realization of the disorder to another because the weights are sensitive to variations in the total free energy of order one, *i.e.* of relative order $1/N$. As a consequence the function $P_J(q)$ defined for one sample will also fluctuate when J_{ij} changes and it will not be self-averaging. The higher moments of the overlap are defined as:

$$q_J^{(k)} = \int_{-1}^{1} P_J(q) q^k dq \tag{1.41}$$

and

$$q^{(k)} = \overline{q_J^{(k)}} = \int_{-1}^{1} P(q) q^k dq \tag{1.42}$$

Just as $q_J^{(1)}$ is not self-averaging if there is non-trivial broken ergodicity, neither, in general, are the higher moments $q_J^{(k)}$. Using the property that in the pure states the connected correlation functions of two spins are generally negligible in the thermodynamical limit, one has:

$$q^{(k)} = \frac{1}{N^k} \sum_{i_1} \cdots \sum_{i_k} \overline{[\langle s_{i_1} \ldots s_{i_k} \rangle]^2} \tag{1.43}$$

For example, considering the second moment, one has:

$$\begin{aligned}
q^{(2)} &= \int_{-1}^{1} P(q) q^2 dq \\
&= \overline{\sum_{\alpha\beta} w_\alpha w_\beta [q_{\alpha\beta}]^2} \\
&= \overline{\sum_{\alpha\beta} w_\alpha w_\beta \left[\frac{1}{N} \sum_i \langle s_i \rangle_\alpha \langle s_i \rangle_\beta\right] \left[\frac{1}{N} \sum_j \langle s_j \rangle_\alpha \langle s_j \rangle_\beta\right]} \\
&= \frac{1}{N^2} \sum_i \sum_j \overline{\left[\sum_\alpha w_\alpha \langle s_i s_j \rangle_\alpha\right] \left[\sum_\beta w_\beta \langle s_i s_j \rangle_\beta\right]} \\
&= \frac{1}{N^2} \sum_i \sum_j \overline{\langle s_i s_j \rangle \langle s_i s_j \rangle}
\end{aligned} \tag{1.44}$$

1.2.4 The replica approach

The TAP approach presented in the previous paragraphs is the most direct method to grasp the complicated structure of the free-energy landscape that is characteristic of spin-glasses at the mean field level. On the other hand it does not allow for a full treatment of the problem. In fact the solution of the model can be achieved through a different approach, called *replica method.* The main thermodynamical quantity to be calculated is the quenched free energy

$$f = -K_B T \lim_{N\to\infty} \frac{1}{N} \overline{\ln Z} \tag{1.45}$$

Since the disorder average of the logarithm of the partition function can not be carried out, the solution is based on the following identity ("replica trick")

$$\overline{\ln Z} = \lim_{n\to 0} \frac{1}{n} \left[\overline{Z^n} - 1\right] \tag{1.46}$$

so that one obtains

$$f = -K_B T \lim_{N\to\infty} \lim_{n\to 0} \frac{1}{nN} \left[\overline{Z^n} - 1\right] \tag{1.47}$$

The replica trick, *introducing the limit* $n \to 0$, moves the problem of calculating the disorder average of the logarithm of the partition function to the one of calculating the disorder average of the n-th power of the partition function. This can be carried out in a straightforward way for general integer n. Of course, one has to take the limit $n \to 0$ in the result, which is the main problem of this method. If one knows the solution for a finite number of replicas, the analytic continuation from integer n's to $n \to 0$ is not unique (see later).
For positive integer n one can write

$$Z^n(\{J_{ij}\}) = Tr_{\{\sigma^1,\sigma^2,\ldots,\sigma^n\}} \exp\left[-\beta \sum_{\alpha=1}^{n} H(\sigma^\alpha, \{J_{ij}\})\right] \tag{1.48}$$

where we have introduced n replicas of the system with the *same* disorder realization $\{J_ij\}$. Indeed the partition function of n non-interacting replicas of the same system is the partition function of the original system to the power n; the spin variables σ_i^α carry two indices: the upper one denotes the replica and goes from 1 to n and the lower one denotes the site and goes from 1 to N. In the SK model, performing the

gaussian integration over the disorder, one simply has:

$$\begin{aligned}\overline{Z^n} &= \int \prod_{ij} dJ_{ij} P(J_{ij}) Z^n(\{J_{ij}\}) \\ &= Tr_{\{\sigma^1,\sigma^2,\ldots,\sigma^n\}} \exp\left[\frac{\tilde{J}^2\beta^2}{4N}\sum_{ij}\sum_{\alpha\beta}\sigma_i^\alpha\sigma_j^\alpha\sigma_i^\beta\sigma_j^\beta + h\beta\sum_i\sum_\alpha\sigma_i^\alpha\right] \quad (1.49)\end{aligned}$$

Then we have converted the disordered problem into a non-random one involving 4-spin interactions. One can proceed further: rearranging terms in the summations and extracting in the double sum over α and β the term with $\alpha = \beta$, one has

$$\overline{Z^n} = Tr_{\{\sigma^1,\sigma^2,\ldots,\sigma^n\}} \exp\left[\frac{\tilde{J}^2\beta^2 Nn}{4} + \frac{\tilde{J}^2\beta^2}{4N}\sum_{(\alpha\beta)}\left(\sum_i \sigma_i^\alpha\sigma_i^\beta\right)^2 + h\beta\sum_{\alpha i}\sigma_i^\alpha\right] \quad (1.50)$$

where (α,β) means summation over $\alpha \neq \beta$. Using the gaussian identity

$$\exp\left[\frac{1}{2}\lambda a^2\right] = \left(\frac{\lambda}{2\pi}\right)^{1/2}\int_{-\infty}^{+\infty} dx \exp\left[-\frac{1}{2}\lambda x^2 + a\lambda x\right] \quad (1.51)$$

with $a = \sum_i \sigma_i^\alpha\sigma_i^\beta$ and $\lambda = \frac{1}{2}\beta^2\tilde{J}^2$ and introducing a set of dummy variables $\{y^{\alpha\beta}\}$, one has

$$\begin{aligned}\overline{Z^n} &= \exp\left[\frac{\tilde{J}^2\beta^2 Nn}{4}\right]\int_{-\infty}^{+\infty}\prod_{(\alpha\beta)}\left(\frac{N\beta^2\tilde{J}^2}{2\pi}\right)^{1/2} dy^{\alpha\beta}\exp\left[-\frac{1}{2}N\beta^2\tilde{J}^2\sum_{(\alpha\beta)}(y^{\alpha\beta})^2\right] \\ &\quad Tr_{\{\sigma^1,\sigma^2,\ldots,\sigma^n\}}\exp\left[\beta^2\tilde{J}^2\sum_{i(\alpha\beta)} y^{\alpha\beta}\sigma_i^\alpha\sigma_i^\beta + h\beta\sum_{i\alpha}\sigma_i^\alpha\right] \quad (1.52)\end{aligned}$$

Thus the spin have been decoupled and one now has a single site problem. In return for this simplification, one has to deal with couplings between spins in different replicas. The single-spin property allow to evaluate the trace over all state of the nN spins σ_i^α as the trace over all state of the n spins on a single site σ^α raised to the power N. In formula one has:

$$Tr_{\{\sigma^1,\sigma^2,\ldots,\sigma^n\}}\exp[\sum_i g(\sigma_i^\alpha)] = \exp[N\ln Tr_{\{\sigma^\alpha\}}\exp g(\sigma^\alpha)] \quad (1.53)$$

where g is an arbitrary function. In the end, recalling Eq. (1.47), one is left with the following expression for the free energy:

$$f = -KT\lim_{N\to\infty}\lim_{n\to 0}\frac{1}{Nn}\left\{\int\prod_{\alpha\beta}\left(\frac{N\beta^2\tilde{J}^2}{2\pi}\right)^{1/2} dy^{\alpha\beta}\exp(-NA[Y]) - 1\right\}$$

with

$$A[Y] = -\frac{\tilde{J}^2\beta^2 n}{4} + \frac{\beta^2\tilde{J}^2}{2}\sum_{(\alpha\beta)}(y^{\alpha\beta})^2 - \ln Tr_{\{\sigma^\alpha\}}\exp\left[\frac{\beta^2\tilde{J}^2}{2}\sum_{(\alpha\beta)} y^{\alpha\beta}\sigma^\alpha\sigma^\beta + \beta h\sum_\alpha \sigma^\alpha\right] \tag{1.54}$$

Here we have denoted by Y the $n \times n$ symmetric matrix whose elements are $y_{\alpha\beta}$. Assuming that the two limits $n \to 0$ and $N \to \infty$ can be interchanged, the saddle-pint method can be applied in the thermodynamical limit $N \to \infty$:

$$\int dY \exp(-NA[Y]) \approx \exp(-NA[Y_0]) \tag{1.55}$$

where Y_0 is the matrix that minimize the function $A[Y]$, that is, the matrix elements $y_0^{\alpha\beta}$ are the solution of the $n(n-1)$ saddle-point equations

$$\frac{\partial A}{\partial y^{\alpha\beta}} = 0 \tag{1.56}$$

This equations can be written under the form of self consistent equations:

$$y_0^{\alpha\beta} = \overline{\langle\sigma^a\sigma^\beta\rangle} \tag{1.57}$$

Once the solutions $y_0^{\alpha\beta}$ of the saddle point Equations (1.56) have been found, then the free energy reads:

$$\begin{aligned} f &= -KT\lim_{n\to 0}\left\{\frac{\beta^2\tilde{J}^2}{4}\left[1 - \frac{1}{n}\sum_{(\alpha\beta)}(y_0^{\alpha\beta})^2\right]\right. \\ &\left. + \frac{1}{n}\ln Tr_{\{\sigma^\alpha\}}\exp\left[\frac{\beta^2\tilde{J}^2}{2}\sum_{(\alpha\beta)} y_0^{\alpha\beta}\sigma^\alpha\sigma^\beta + \beta h\sum_\alpha\sigma^\alpha\right]\right\} \end{aligned} \tag{1.58}$$

Before going ahead with the solution of the saddle point equations, one has to express in the replica formalism the spin glass order parameters that have been introduced in previous Section. It can be easily shown that the spin glass equilibrium order parameter q is the $n = 0$ limit of the spin-spin correlation function between replicas for any arbitrary site i, provided that $\alpha \neq \beta$:

$$q = \lim_{n\to 0}\overline{\langle\sigma_i^\alpha\sigma_i^\beta\rangle} \tag{1.59}$$

Comparing Eq. (1.57) and Eq. (1.59) one realize that

$$q = \lim_{n\to 0} y_0^{\alpha\beta} \tag{1.60}$$

In the same manner one gets for higher overlap moments

$$q^{(k)} = \lim_{n\to 0} \left\{ \overline{\langle \sigma_i^\alpha \sigma_i^\beta \rangle} \right\}^k = \lim_{n\to 0} \left\{ y_0^{\alpha\beta} \right\}^k \tag{1.61}$$

The previous equation is not ambiguous if all $y_0^{\alpha\beta}$ are equal (this means that the replica symmetry is not broken as it will be shown in the next paragraph). In the case where the replica symmetry is broken the various matrix elements $y_0^{\alpha\beta}$ are not all equal and one must be a bit more careful. It turned out that one must average over all possible ways of breaking the replica symmetry. The generalization of Eq. (1.61) is the following [20, 43]:

$$q^{(k)} = \lim_{n\to 0} \frac{1}{n(n-1)} \sum_{\alpha\neq\beta} \left\{ y_0^{\alpha\beta} \right\}^k \tag{1.62}$$

The correct replica expression for the overlap probability distribution is

$$P(q) = \lim_{n\to 0} \frac{1}{n(n-1)} \sum_{\alpha\neq\beta} \delta(q - y_0^{\alpha\beta}) \tag{1.63}$$

That is, comparing Eq. (1.38) and Eq. (1.63), the distribution of the values of the matrix elements $y_0^{\alpha\beta}$ in a replica-symmetry breaking solution must be the same as the distribution of overlaps between different pure states when there are many states. This show the intimate connection between broken ergodicity and broken replica symmetry. Finally, we can identify the Edward-Anderson order parameter q_{EA} with the largest $y_0^{\alpha\beta}$ in a broken replica symmetric solution:

$$q_{EA} = \max_{\alpha\beta} y_0^{\alpha\beta} \tag{1.64}$$

1.2.5 Replica symmetric solution

The simplest approach for solving the saddle point equations (1.56) is the so-called *replica symmetric* ansatz, originally proposed by Sherrington and Kirkpatrick [15, 16]. Since the n replicas are indistinguishable (the function $A[Y]$ is left invariant when we exchange some of the lines or the rows of the matrix Y), it is natural to parameterize the matrix Y in the following form:

$$y^{\alpha\beta} = \begin{cases} q & \text{if } \alpha \neq \beta \\ 0 & \text{otherwise} \end{cases} \tag{1.65}$$

With this parameterization, carrying out the calculations, one finds:

$$f = -\frac{\beta\tilde{J}^2}{4}(1-q^2) - \int \frac{dz}{\sqrt{2\pi}} e^{-\frac{1}{2}z^2} \ln[2\cosh(\beta\tilde{J}\sqrt{q}z + \beta h)] \tag{1.66}$$

where the value of q is determined self-consistently by the unique saddle-point equation

$$q = \int \frac{dz}{\sqrt{2\pi}} e^{-\frac{1}{2}z^2} [\tanh(\beta\tilde{J}\sqrt{q}z + \beta h)]^2 \tag{1.67}$$

Considering the case of zero magnetic field, the previous equation locate the transition temperature of the model. Expanding the r.h.s. in powers of q one has:

$$\begin{aligned} q &= \int \frac{dz}{\sqrt{2\pi}} e^{-\frac{1}{2}z^2} \left[z^2\beta^2\tilde{J}^2 q - \frac{2}{3} z^4\beta^4\tilde{J}^4 q^2 + \ldots \right] \\ &= q(\beta\tilde{J})^2 - 2q^2(\beta\tilde{J})^4 + \ldots \end{aligned} \tag{1.68}$$

from which we find $T_c = \tilde{J}$ and $q(T) = 1 - \frac{T}{T_c} + \mathcal{O}((T_c - T)^2)$ for T just below T_c, as in the heuristic TAP analysis.

Eq.(1.67) can be solved numerically at any temperature T. The solution is very appealing because the root mean square local magnetization $q^{1/2}$ behaves roughly the way the magnetization does in the ferromagnetic case (see Fig.(1.4)). Similarly the susceptibility obtained from this q using the relation (1.36) seems very reasonable, having at $T = T_c$ the cusp revealed in experiments (see Fig.(1.4)). The specific heat, calculated through the free energy (1.66) displays a cusp at T_c, in disagreement with the experimental data. However this is not a serious drawback because a mean-field model does not necessarily represent a real spin-glass material.

Despite the appealing results found by Sherrington and Kirkpatrick (in particular it would seem that the spin-glass transition fit nicely into the standard theory of phase transition, the role of the order parameter being played by the root mean square local magnetization), this mean-field solution is unphysical at low temperatures. It gives a negative entropy while in a discrete system the entropy must always be positive (it is the logarithm of the number of allowed configurations!). This can be seen expanding Eq. (1.67) to the first order in the temperature for $T \to 0$. One finds a linear temperature dependence for q

$$q(T) = 1 - \sqrt{\frac{2}{\pi}}\frac{T}{T_c} + o(T) \tag{1.69}$$

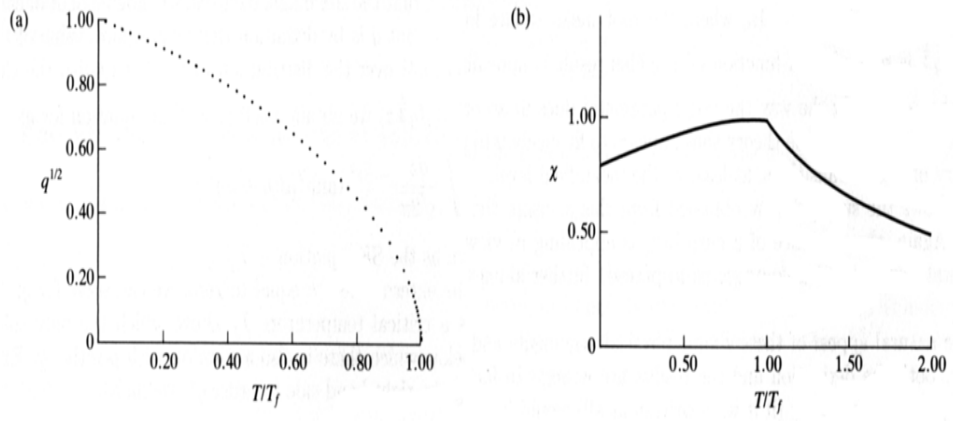

Figure 1.4: (a) The root mean square local magnetization $q^{1/2}$ vs. T/T_c. (b) The susceptibility $\chi(T)/\chi(T_c)$ vs. T/T_c (from ref. [16])

so that the free energy is given by

$$f(T) = -\sqrt{\frac{2}{\pi}}\tilde{J} + \frac{T}{2\pi} + o(T) \tag{1.70}$$

and the entropy at $T = 0$ is $s(T = O) = -1/2\pi$.

1.2.6 Stability analysis and AT line

From the computational point of view, the reason for the unphysical low temperature behaviour of the replica symmetric solution, can be traced back to the fact that the Hessian matrix $\partial^2 A/\partial y^{\alpha\beta}\partial y^{\gamma\delta}$ evaluated at the SK saddle point is not positive definite, so that the steepest descendent procedure is meaningless. De Almeida and Thouless [17] performed a stability analysis of the SK solution, calculating all the eigenvalues of the Hessian matrix and imposing that they are positive. They found the following condition:

$$1 \geq (\beta\tilde{J})^2 \int \frac{dz}{\sqrt{2\pi}} e^{-\frac{z^2}{2}} [\mathrm{sech}(\beta\tilde{J}\sqrt{q}z + \beta h)]^4 \tag{1.71}$$

This equation defines a line $T(h)$ in the $h - T$ plane, known as *AT line*, marking the boundary of the region where the SK solution is stable, as shown in Fig.(1.5). This is exactly the same condition we have already noticed for the stability of the TAP free energy, Eq. (1.25). It can been shown that the latter equation coincide

also with the condition for the spin-glass susceptibility χ_{SG} to not be negative. The naive replica symmetric approach to evaluate the integral is correct for every $n > 1$, but fails in the region $0 < n < 1$: this means that the analytic continuation of the integral from its values on the integers down to its value at $n = 0$ is unjustified. The replica symmetric ansatz gives the correct saddle point for evaluating the integral only above a certain temperature $T(h)$. At low temperature one must look for a new solution of the Eq. (1.56) such that the Hessian matrix has no negative eigenvalues. This requires to break the replica symmetry.

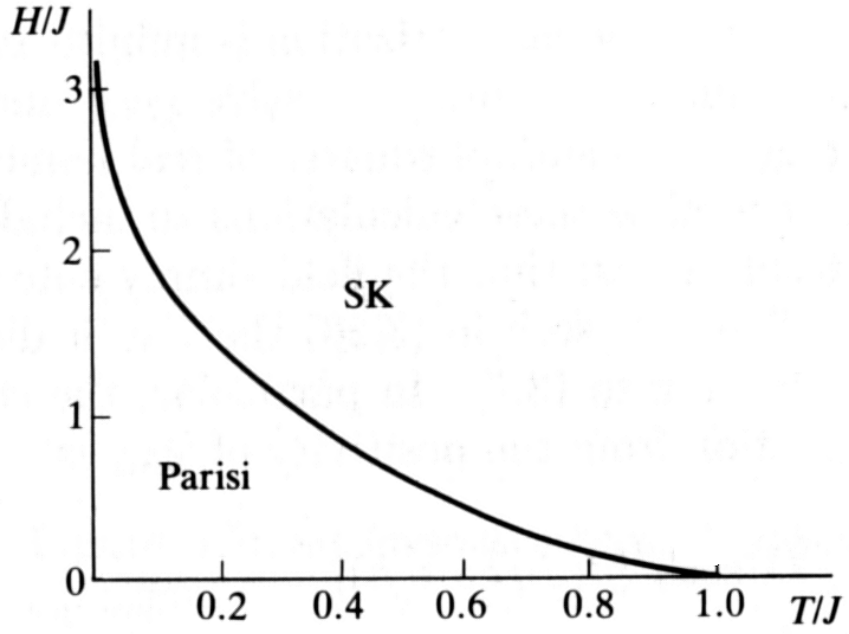

Figure 1.5: Plot of the Almeida-Thouless (AT) line for SK model. To the right of the line, the SK solution with a single order parameter is correct, while to the left of the line the Parisi solution (see Section 1.2.7) is believed exact. The Parisi solution represents the many valley structure of the phase space and non-ergodic behaviour. The AT line, therefore, signals the onset of irreversibility (from ref.[17])

1.2.7 Parisi solution: replica symmetry breaking

Since the replica symmetric ansatz for the saddle point matrix Y_0 gives an instable solution, there have been several attempts to exhibit a different ansatz such that

the solution is stable [35, 36, 37, 38]. At the present moment only one form of the matrix is known which satisfies the requirement of having all Hessian eigenvalues non negative. This have been formulated by Parisi [39, 40, 41, 42, 43]. There is a widespread agreement that this choice is the correct one: the results of this approach agree with the existing numerical simulations of the SK model. The stability of Parisi solution has been explicitly checked in ref. [44].

Parisi ansatz has the following hierarchical form. One starts with the SK form, in which all elements of the Y_0 matrix have the same value q_0 (except the diagonal one which are taken to be zero). One the break the big $n \times n$ matrix into $n/m_1 \times n/m_1$ blocks of size $m_1 \times m_1$. In the off-diagonal blocks one leaves q_0, but in the diagonal blocks one replaces q_0 by q_1 One then does the same thing within each of the blocks along the diagonal: they are broken into $m_1/m_2 \times m_1/m_2$ subblocks, each of size $m_2 \times m_2$, and in each of these along the diagonal one replaces q_1 by q_2. This procedure is then repeated infinitely many times. A typical form of the Y matrix with two level of replica symmetry breaking is the following (here $n = 8$, $m_1 = 4$, $m_2 = 2$):

$$\begin{bmatrix} 0 & q_2 & q_1 & q_1 & q_0 & q_0 & q_0 & q_0 \\ q_2 & 0 & q_1 & q_1 & q_0 & q_0 & q_0 & q_0 \\ q_1 & q_1 & 0 & q_2 & q_0 & q_0 & q_0 & q_0 \\ q_1 & q_1 & q_2 & 0 & q_0 & q_0 & q_0 & q_0 \\ q_0 & q_0 & q_0 & q_0 & 0 & q_2 & q_1 & q_1 \\ q_0 & q_0 & q_0 & q_0 & q_2 & 0 & q_1 & q_1 \\ q_0 & q_0 & q_0 & q_0 & q_1 & q_1 & 0 & q_2 \\ q_0 & q_0 & q_0 & q_0 & q_1 & q_1 & q_2 & 0 \end{bmatrix}$$

If one imagines doing this iterative construction for positive-integral-dimensional matrix, then each m_i has to be evenly divisible by m_{i+1}, which requires

$$n > m_1 > m_2 > \ldots > 1 \tag{1.72}$$

But in the $n \to 0$ limit, one must turn this around and take

$$0 < m_1 < m_2 < \ldots < 1 \tag{1.73}$$

instead. In the limit where the procedure is done infinitely many times, the m_i become continuous: $m_i \to x$, $0 < x < 1$. The information in the set of q_i's and m_i's

is then contained in a unit function on the unit interval defined as

$$q(x) = q_i \qquad \text{if} \quad m_i < x < m_{i+1} \tag{1.74}$$

The overlap probability distribution is so expressed as

$$P(q) = \lim_{n\to 0} \frac{1}{n(n-1)} \sum_{\alpha\neq\beta} \delta(q - y_0^{\alpha\beta}) = \int_0^1 dx \delta(q - q(x)) = \frac{dx(q)}{dq} \tag{1.75}$$

where $x(q)$ is the inverse function of $q(x)$. It is evident that $q(x)$ must be a non-decreasing function in order that this inversion can be performed.

Within the Parisi parameterization the free energy becomes a functional of $q(x)$ and it must maximized with respect to $q(x)$. Although the exact solution requires an infinite number of steps of replica symmetry breaking, good results are already obtained for small values of the number of steps (for example the entropy becomes $-.003$ to be compared with SK solution $-.17$ and with the exact 0 value). The free energy can be explicitly computed using the whole symmetry breaking pattern near the critical temperature by expanding the functional $A[q]$ in powers of q [41]. The main result is that $q(x)$ is continuous function with the following properties

$$\begin{cases} q(x) = q(0) & \text{for } 0 < x < x_0 \\ q(x) = 2x & \text{for } x_0 < x < x_1 \\ q(x) = q(1) & \text{for } x_1 < x < 1 \end{cases} \tag{1.76}$$

where

$$\begin{cases} q(0) = \frac{3}{4}\left[h^2/\tilde{J}^2\right]^{\frac{2}{3}} & x_0 = \frac{1}{2}q(0) \\ q(1) = q_{EA} & x_1 = \frac{1}{2}q(1) \end{cases} \tag{1.77}$$

Physically, being $q(1)$ the largest overlap it must be identified with the single-phase order parameter q_{EA}. When the magnetic field becomes zero the function $q(x)$ vanishes at $x = 0$. As the field increase, the plateau at $q(0)$ rises, and once it reaches the height of the second plateau at $q(1)$, the only solution is x independent. That is the replica symmetry breaking disappears and one is back to the SK solution. One recognizes the point at which this happens as the AT *line* discussed in the previous Section. The solution is shown in Fig. (1.6), including the behaviour for finite field h. As a consequence of the behaviour or $q(x)$, the function $P(q)$ has two

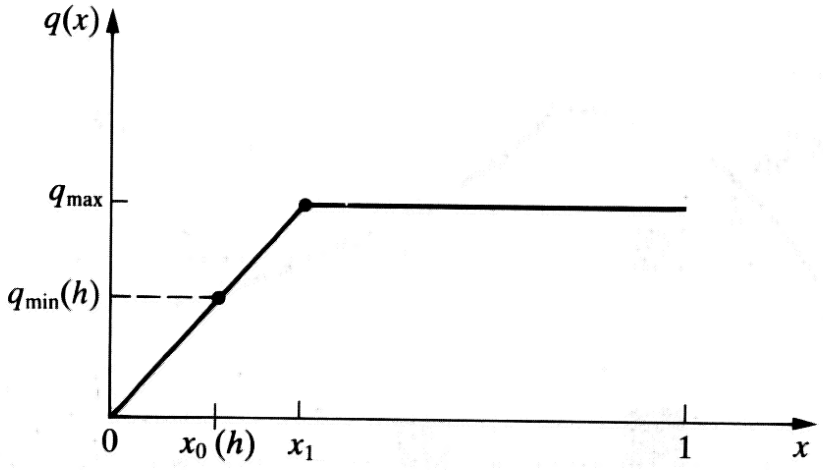

Figure 1.6: The Parisi solution for $q(x)$ close to $T = T_c$. The solid line is for $h = 0$ and the broken line for small h (from ref.[41])

delta functions, one at $q = q(0)$ and the other one at $q = q(1)$, plus a smooth part with support in the interval $q(0) < q < q(1)$. In the limit $h \to 0$ the delta function at $q(0)$ disappears while when h increases and reaches the critical magnetic field of the AT line the two delta functions collapse into a single one. The agreement between the form of $P(q)$ obtained by Monte Carlo simulations [47] and the one obtained from Parisi $q(x)$ is striking (see Fig. (1.7)). The important point about the form of this solution is the presence, in addition to the delta function spike at $q = q(1)$ of a continuous part extending down to $q = 0$. There therefore must exist very many states resembling each other in all possible degrees. Another important feature of the Parisi theory is the lack of self-averaging of certain quantities, like the single sample equilibrium order parameter q_J, the probability $P_J(q)$ and all other overlap moments, and the susceptibility. On the other hand, one can see very simply that quantities such as equilibrium energy, free energy, or magnetization, which do not involve inter-valley correlations, will be self-averaging. An even more dramatic and celebrated feature than the lack of self-averaging which has been discovered in Parisi solution is *ultrametricity* [45, 46, 2]. This is the terminology for a very special hierarchical structure in the overlaps between the various phases. It is revealed by

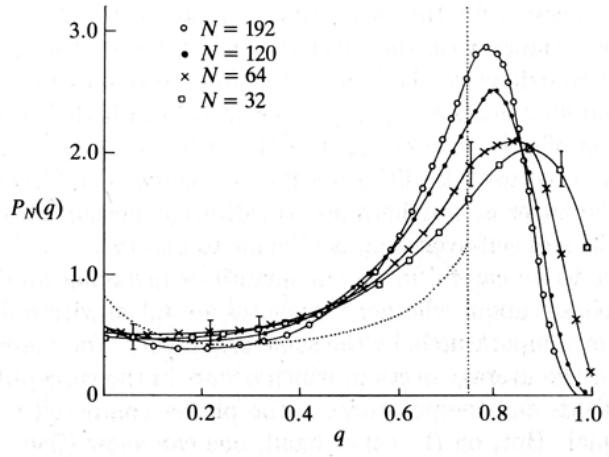

Figure 1.7: Data for $P_N(q)$ for the SK model for several size at $T = 0.4T_c, h = 0$. The distribution has been symmetrized, so only $q \geq 0$ is shown. The dotted line is the prediction of an approximate solution of Parisi's equations (from ref. [47]).

computing the joint distribution of the mutual overlaps between three randomly chosen states:

$$P_J(q_1, q_2, q_3) = \sum_{\alpha\beta\gamma} w^\alpha w^\beta w^\gamma \delta(q_1 - q_{\alpha\beta})\delta(q_2 - q_{\beta\gamma})\delta(q_3 - q_{\gamma\alpha}) \tag{1.78}$$

In replica formalism the disorder average of this quantity is

$$\begin{aligned} P(q_1, q_2, q_3) &= \overline{P_J(q_1, q_2, q_3)} \\ &= \frac{1}{n(n-1)(n-2)} \sum_{(\alpha\beta\gamma)} \delta(q_1 - y_0^{\alpha\beta})\delta(q_2 - y_0^{\beta\gamma})\delta(q_3 - y_0^{\gamma\alpha}) \end{aligned} \tag{1.79}$$

and in the Parisi parameterization it becomes

$$\begin{aligned} P(q_1, q_2, q_3) &= \frac{1}{2} P(q_1) x(q_1) \delta(q_1 - q_2)\delta(q_3 - q_1) + \\ &\quad \frac{1}{2} \left[P(q_1)P(q_2)\theta(q_1 - q_2)\delta(q_2 - q_3) + \text{permutations} \right] \end{aligned} \tag{1.80}$$

Defining the distance between two configurations in the N-dimensional spin configuration space to be the fraction of spins which are different in the two states,

i.e. $d_{\alpha\beta} = \frac{1}{2}(1 - q_{\alpha\beta})$, then the previous expression says that, if one take any three states, either they are mutually equidistant or two of the separations are equal and greater than the third. This implies that the space of states has a sort of family tree structure in which the degree of relatedness in the family is associated with the degree of overlap.

1.3 Others infinite ranged models

1.3.1 p-spin model and the Random Energy Model

The SK model discussed so far is a special case of the more general *p-spin model*. One can generalize the SK model by replacing the random pair interaction in Eq. (1.4) by random p-spin interaction. The Hamiltonian is then

$$H = -\sum_{(i_1,i_2,\cdots,i_p)} J_{i_1,i_2,\ldots,i_p}\sigma_{i_1}\sigma_{i_2}\cdots\sigma_{i_p} \tag{1.81}$$

Here again, the spins are Ising variables, the summation is over different indexes and the probability distribution of the couplings has to be scaled with N in order to ensure an extensive free energy as

$$P(J_{i_1,i_2,\ldots,i_p}) = \left(\frac{N^{p-1}}{\pi p!}\right)\exp\left[-\frac{(J_{i_1,i_2,\ldots,i_p})^2 N^{p-1}}{\tilde{J}^2 p!}\right] \tag{1.82}$$

The SK model is recovered in the case $p = 2$. The relation between all these p-spin models can be seen in the statistics of the energy levels. Considering an arbitrary spin configuration $\sigma^{(1)}$, the probability density that the energy of this configuration is E can be written as

$$P(E) = \overline{\delta(E - H[(\sigma^{(1)})])} \tag{1.83}$$

For symmetrical bond distribution, using gauge transformations, it can be shown that this average does not depend on the configuration for which it is evaluated. Therefore it can be calculated over any configuration, for example the one with all spins up. The result is the same for any value of p:

$$P(E) = \frac{1}{\sqrt{N\pi\tilde{J}^2}}\exp\left(-\frac{E^2}{N\tilde{J}^2}\right) \tag{1.84}$$

Thus, at this level, all random p-spin behave identically. To see the difference between them, it is necessary to go to higher order statistics, *e.g.* the joint probability

$P(E_1, E_2)$ that two given configuration of spins $\sigma^{(1)}$ and $\sigma^{(2)}$ have, respectively, energies E_1 and E_2

$$P(E_1, E_2) = \overline{\delta(E - H[(\sigma^{(1)})])\delta(E - H[(\sigma^{(2)})])} \tag{1.85}$$

It turns out that this probability distribution depends only on the distance between the two configurations, namely, on the number of identical spin, *i.e.* on the overlap

$$q^{(1,2)} = \frac{1}{N}\sum_i \sigma^{(1)}\sigma^{(2)} \tag{1.86}$$

One finds

$$P(E_1, E_2) = \frac{1}{\sqrt{N\pi\tilde{J}^2(1+q^p)(1-q^p)}} \exp\left[-\frac{(E_1+E_2)^2}{2N(1+q^p)\tilde{J}^2} - \frac{(E_1-E_2)^2}{2N(1-q^p)\tilde{J}^2}\right] \tag{1.87}$$

Now, the important thing which was pointed out by Derrida [48], is that, in the limit $p \to \infty$, $q^p \to 0$, so that

$$P(E_1, E_2) \to P(E_1)P(E_2) \tag{1.88}$$

One can consider also the probability distributions of three or more levels and again when p is large these probabilities factorize. In this sense, the limit $p \to \infty$ of the random p-spin model is equivalent to the Random Energy Model (REM) defined by the following three properties:

1. It has 2^N energy levels E_i.

2. The energy levels are distributed according to Eq. (1.84).

3. The energy levels are independent random variables.

The thermodynamics of the model is most easily evaluated in the microcanonical ensemble. The average number of level with energy E is just $P(E)$ multiplied by the total number 2^N of levels:

$$n(E) = \frac{1}{\sqrt{N\pi\tilde{J}^2}} \exp\left[N\left(\ln 2 - \frac{E^2}{N^2\tilde{J}^2}\right)\right] \tag{1.89}$$

One can notice a critical dependence on E: for $|E| < E_0 = N\tilde{J}\sqrt{\ln 2}$, there is an exponentially large number of levels, and therefore a finite entropy

$$S(E) = N\left[\ln 2 - \frac{E^2}{N^2\tilde{J}^2}\right] \tag{1.90}$$

On the other hand, for $|E| > E_0$, there are *no* levels left in the thermodynamic limit, and therefore no entropy. Using $1/T = dS/dE$ one finds that the free energy is

$$f = \begin{cases} -T\ln 2 - \tilde{J}^2/4T & T > T_c \\ -\sqrt{\ln 2} & T < T_c \end{cases} \tag{1.91}$$

where the critical temperature is

$$T_c = \frac{\tilde{J}}{2\sqrt{\ln 2}} \tag{1.92}$$

Below T_c, the system get stuck in the lowest available energy level, $E = -E_0$ and the entropy vanishes.

The similarities and differences between the REM model and the SK model were illuminated very elegantly by Gross and Mezard [49], by solving the $p \to \infty$ of the p-spin model explicitly in the replica formalism. They found broken replica symmetry, but only one level of the Parisi hierarchical replica-symmetry-breaking scheme is necessary, rather than the infinite number required in the SK ($p = 2$) case. The restricted nature of the replica symmetry breaking in this case means that Parisi order function $q(x)$ consists of two flat portions at values $q_0 = 0$ and $q_1 = 1$ (in zero external field), with a discontinuous jump between them at $x = T/T_c$. Thus the overlap distribution function $P(q)$ for the REM consists of a pair of delta-functions (see Fig.(1.8))

$$P(q) = \frac{T}{T_c}\delta(q) + \left(1 - \frac{T}{T_c}\right)\delta(q-1) \tag{1.93}$$

In this sense the REM is much simpler than the SK model; Gross and Mezard called it "the simplest spin glass". On the other hand, it also exhibits more generic behaviour: the first order behaviour of the order parameter $q(1) = q_{EA}$, which jumps discontinuously at T_c, occurs for all p-spin models with $p > 2$ [50, 51]. The SK case is the only one with a continuous q_{EA}. To be more precise, for finite $p > 2$ there is a transition from the disordered phase to a partially frozen phase characterized by a step function $q(x)$ with values 0 and $q_1 < 1$. As the temperature is lowered

further, a second transition occurs, leading to a phase described by a continuous order parameter function. Also of interest is the spherical p-spin interaction spin glass model whose static properties have been throughly using the replica method [52] (see [53] for an analysis of the relaxational dynamics). In particular, the spin glass phase of this continuous model is described by a step order parameter function, *i.e.* the one-step replica symmetry breaking is the most general solution within the Parisi scheme.

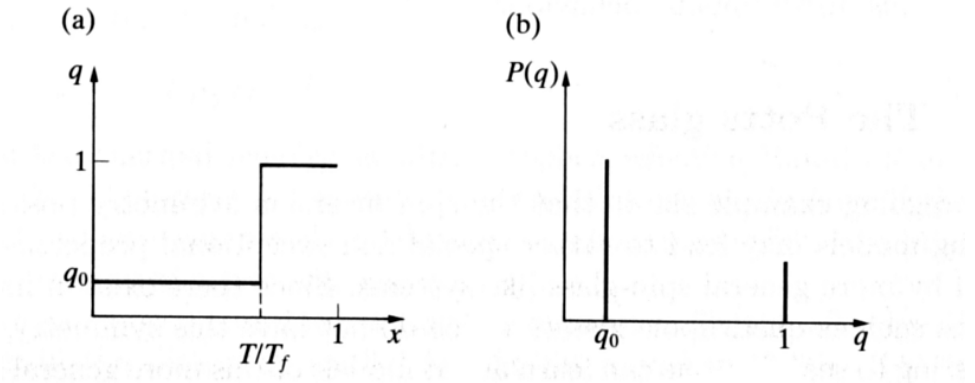

Figure 1.8: $q(x)$ (a) and $P(q)$ (b) for the random energy model.

1.4 Realistic spin-glasses

Although the spin glasses have been the subject of considerable attention for a long time, the description of the realistic case with short-range interaction is still controversial a issue. The upper critical dimension d_u, above which the mean field theory becomes valid, is believed to be $d_u = 6$. Hence, the properties of the real two and three dimensional spin glasses are far from trivial. As we know from the critical phenomena of conventional pure systems, the phase behaviour depends on the spin dimension as well as the spatial dimension. The Ising spin glass, which has been studied most among spin glass models because it is the simplest among them, is now believed to have a finite temperature phase transition in three dimension, but not in two dimensions. Thus, the lower critical dimension (LCD) for Ising spin

glass has been believed $2 < d_l < 3$.

For vector spin glass such as XY spin glass and Heisenberg spin glass, their LCD have been suggested $d_l = 4$, which means that only Ising spin glass order is possible in the three dimension. However, the situation has not been clear as Ising spin glass since one has to deal with continuous variables in addition to randomness and a growing numerical evidence in favor of spin glass order in the tree dimensional vector spin glass is accumulating. Furthermore, there is an additional feature in a vector spin glass, the existence of two-fold symmetry like Ising in addition to the obvious rotational symmetry, which was at first pointed out by Villain [92] and which is one of the issues that will be studied in Chapter 5.

Concerning the nature of the spin glass phase in short-ranged models, two principal theories have been investigated: the "droplet model" proposed by Fisher and Huse [54, 55, 56, 3] and the replica symmetry breaking of Parisi. The main difference between these theories consists in the number of large-scale, low energy excitations. RSB theory follows the exact solution of the infinite range SK model in predicting that there are excitations which involve turning over a finite fraction of the spins and which cost only a *finite* amount of energy in the thermodynamical limit. The droplet theory argues that the lowest energy excitation involving a given spin and which has linear spatial extent L typically costs an energy L^θ, where θ is a positive exponent. Hence in the thermodynamical limit, excitations which flip a finite fraction of the spins cost an *infinite* amount of energy. The difference between the RSB scenario and the droplet model seen in the form of the order parameter function $P(q)$. In the former, as already said, $P(q)$ has delta functions at (plus or minus) the Edward-Anderson order parameter q_{EA}, corresponding to ordering within a single valley, and a tail with a finite weight extending down to $q = 0$. In the latter $P(q)$ is trivial, *i.e.* it has only delta functions at $\pm q_{EA}$. Unfortunately in the finite systems which are employed in numerical simulations finite size effects are always present so that it has been impossible till now to identify which of the two conjectures are applicable to the real short-range case.

Chapter 2

Deterministic models with glassy behavior

2.1 General features of deterministic models

A main issue in glassy systems is the analogy between glass-forming liquids and discontinuous spin-glasses, first pointed out in the pioneering works by Kirkpatrick, Thirumalai and Wolynes [59, 60, 61, 62, 63]. In both cases the thermodynamical properties can be indeed related to the dynamical evolution in an energy landscape. In liquid theory one can define the notion of *inherent structures* [64] (local minima of the potential energy, each one surrounded by its attraction basin or valley) and *configurational entropy*, *i.e.* the logarithm of the number of these minima divided by the number of particles in the system. Then the low-temperature dynamical evolution can be described as a superposition of an intra-basin "fast" motion and a "slow" crossing of energy barriers. If the temperature of the system is small enough, namely less than the Mode Coupling critical temperature T_{MC}, the system gets trapped in one of the basins. Since the number of energy minima diverges exponentially with the size of the system, a thermodynamic transition can be associated with an entropy crisis: the Kauzmann temperature T_K of the glassy transition corresponds to the vanishing of the configurational entropy. We refer the reader to [65] for an overview on equilibrium thermodynamics of glasses.

Consider now the class of discontinuous spin glasses, i.e. the mean-field models involving a random p-spin interaction. Also these models show a dynamical transition at a temperature T_D (corresponding to T_{MC}) where dynamical ergodicity

breaks down; a thermodynamic entropy-driven transition takes place at a lower temperature T_{1RSB} (corresponding to T_K), at which replica symmetry breaks down with a "one step" pattern. Here the local minima of the free energy correspond to the solutions of the mean field TAP equations. Anyway, in infinitely connected spin glasses at temperature $T = 0$, metastable states with respect to any dynamics reduce to 1-spin-flip stable states.

The main gap in the analogy between structural glasses and discontinuous spin-glasses is that in the latter models, unlike the former, the couplings between spins are quenched random variables. A significant, recent step in filling this gap has been made by the introduction of *deterministic*, i.e. non-random, spin models which show a complex thermodynamical behaviour very similar to the one of discontinuous spin-glasses [67, 68, 69, 82, 70, 71]. In the low temperature phase, these systems have a very slow dynamic and ageing effects and there exists a very large number of metastable configurations. Nevertheless they are completely deterministic, in the sense that the couplings are fixed in the very beginning and not taken from a random distribution (as it is, for example, in the SK model which has been presented in the previous chapter). It is the high degree of frustration among the couplings, *not* the disorder, to generate a huge number of metastable states and thus the glassy behaviour. The discovery of these models proved that disorder is not necessary to reproduce a complex free energy landscape.

In general, in these models, the following scenario holds:

- There exists a *dynamical* phase transition to a glassy phase. At this temperature T_D the order parameter experiences a jump, correlation time diverges (*i.e.* correlations functions do not decay exponentially as they do in the high temperature regime) and aging effects start to appear.

- At a lower temperature, there is a *static* equilibrium phase transition associated with the vanishing of the high-temperature entropy. Below this temperature T_S there are many equilibrium states available to the system and the system freezes in one of them.

2.2 Frustration

The idea underlying the introduction of deterministic models is that highly and irregularly oscillating couplings among the spins enable to reproduce frustration, yielding a complex landscape for the free energy of the system: one says that disorder is "self-induced". The concept of frustration was introduced by Toulose in ref. [57]. Consider a two dimensional $\pm J$ EA model on a square lattices. The elementary unit of lattice, namely the square of 4 spins and their mutual 4 couplings, is called a "plaquette". Since the bonds are random and independent, it is equally like to find an even or an odd number of negative bonds around the contour of the plaquette. If this number is even, then it is always possible to find a pair of spin configuration (related by an overall flip) which satisfy all the bonds. But if this number is odd, one can not satisfy all bond simoultaneously, so that there will an extra ground state degeneracy corresponding to the freedom to break any one of the bonds. In the former case one says that the plaquette is unfrustated, in the latter it is *frustrated*. The situation is depicted in Fig. (2.1). If the magnitude of

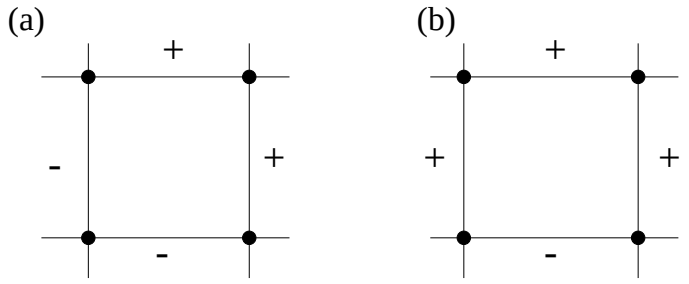

Figure 2.1: Frustration in a square lattice: (a) an unfrustated plaquettes (b) a frustrated plaquette.

the bonds is also random (as, for example, in the gaussian EA model), the exact degeneracy will be broken. Nevertheless the frustration still gives a possibility of low-lying metastable configurations that would be absent in the unfrustated case. On the other hand, true frustration requires more than a simple mixture of positive and negative interactions. The classical example of a system having positive and negative interactions but which is not frustrated is the Mattis model [58]. One takes

the bonds as $J_{ij} = J\xi_i\xi_j$ where ξ_i are independent and takes on the values ± 1 with equal probabilities. Half of the bond are indeed positive and half are negative, but they are not independent. In fact the product of the bonds around any plaquette is $J_{12}J_{23}J_{34}J_{41} = J^4\xi_1\xi_2\xi_2\xi_3\xi_3\xi_4\xi_4\xi_1 = J^4 > 0$. That is, all plaquettes in the Mattis model are unfrustrated. Indeed, by making a change in how to define "up" and "down" locally, *i.e.* defining new spins $\sigma_i' = \xi_i\sigma_i$, the Mattis model is equivalent (in zero external field) to a uniform ferromagnet.

2.3 A random approach to deterministic models

Due to the deep similarity between dynamical and thermodynamical properties of deterministic models and random systems (especially the random spin glasses with p-spin interactions), it has been conjectured that techniques from the realm of disorder, such as replica theory, can be used to solve deterministic models.

In Chapter 1 it has been reviewed how replica method has been applied quite successfully to the analysis of systems in which quenched randomness play a major role. There is nothing *a priori* random in deterministic models and the replica method seems definitively out of place. However, one can hope to use the replica method to gain informations on a deterministic system by introducing a random model which mimics its properties. One has to identify such a disordered system on the basis of some general principle. One possible approach [67, 68] is based on considering a Hamiltonian $H(\{J_{ij}\})$ which depends on quenched control parameters $\{J_{ij}\}$, which are randomly distributed. For a particular realization of the sequence $\{J_{ij}\}$ such a random Hamiltonian should coincide with the original deterministic Hamiltonian. If one is able to use the replica approach to compute the average of the thermodynamic functions for the random system, then one can hope that the result obtained for a generic realization of the random variables $\{J_{ij}\}$ is the same as one would have obtained by selecting the exact $\{J_{ij}\}$ sequences corresponding to the original deterministic Hamiltonian. Of course, this way of reasoning is potentially very dangerous and can lead to a disaster (it is enough to think about the three dimensional Edward Anderson model that has nothing to do with the ferromagnetic three dimensional model). The critical issue is *how generic* is the special $\{J_{ij}\}$ sequence which gives the original deterministic model. This problem cannot be

solved *a priori* . One can verify, *a posteriori* , if the deterministic and the random model have the same high-temperature expansion.

By applying the random approach to deterministic models it has been shown that the static transition is relegated to *replica symmetry breaking* [67, 68] , while the dynamical transition can be associated with the so-called *marginality condition* [69]. This condition corresponds to the search for certain saddle points of the free energy (not the true maxima like in the static case) such that one particular eigenvalue of the stability matrix vanishes (the so called replicon eigenvalue) [76, 77]. This condition corresponds to the temperature at which dynamical stability is lost.

2.4 Low Autocorrelation Model

The *Low Autocorrelation Model* (LAM) is an optimization problem in which one searches for string of binary digits with minimal autocorrelation. Sequences of this kind are important in favoring efficient communication, so the problem has relevant practical applications. One starts considering a sequence of length p of spin variable $\{\sigma_j\}, j = 1, \ldots, p$ that can take values ± 1 and the following Hamiltonian:

$$H = \frac{1}{p} \sum_{k=1}^{p} C_k^2, \tag{2.1}$$

where C_k are correlation functions which connect spins at distance k. The choice of the boundary conditions defines two different variants of the model

- The *periodic* and translationally invariant model is defined by using periodic boundary condition, i.e. $\sigma_{j+p} = \sigma_j$, so that one has

$$C_k = \sum_{j=1}^{p} \sigma_j \sigma_{j+k}, \tag{2.2}$$

- The *open* model is defined by using open boundary condition, so that one sums only on $p - k$ terms:

$$C_k = \sum_{j=1}^{p-k} \sigma_j \sigma_{j+k}. \tag{2.3}$$

2.4.1 Static equilibrium transition

The first studies of these models were performed by Golay [72, 73] and after by Bernasconi [74]. They show that the thermodynamics of the *open* model can be approximated by supposing that the correlation functions C_k are uncorrelated gaussian random variables. The Golay-Bernasconi approximation is based under the assumption that the σ_j are independent variables and then so are the C_k. This assumption is totally unjustified and obviously not true as the temperature of the system is finite. Nevertheless the Golay-Bernasconi approximation is quite good at high enough temperature and, overall, predicts the existence of a phase transition at a low temperature (the transition temperature corresponds at the point where the entropy becomes negative and it is $T_s \approx 0.047$). The same approximation can be applied also to the *periodic* model [67], and the results is $T_s \approx 0.1$. This is the *static transition.*

The high-temperature regime of the *periodic* model can be solved exactly [67]. Using the translational symmetry of the model one can rewrite the Hamiltonian in the dual Fourier space

$$H = \frac{2}{p} \sum_{l=1}^{p/2} |B(l)|^4, \tag{2.4}$$

where $B(l)$ are the Fourier space components

$$B(l) = \frac{1}{\sqrt{p}} \sum_{j=1}^{p} \sigma_j \exp\left(\frac{i2\pi jl}{p}\right) \tag{2.5}$$

and it has been used the relation

$$B(l) = \overline{B(-l)} \tag{2.6}$$

Here the bar denotes complex conjugate operation and property (2.6) follows from the fact that σ_i are real function, so that half of the Fourier components can be neglected . In the Fourier space one can shown that only certain kind of connected diagrams contribute to the free energy allowing for a Hartree-Fock resummation of the full high-temperature series. The exact computation of the various contributes at each order in a small-β expansion shows that the GB approximation is not exact (in the sense that does no reproduce the correct coefficients) but not so bad: basically the temperature at which the entropy obtained from the high-temperature

resummation vanishes is again $T_s \approx 0.1$. The result for the free energy obtained from high-temperature expansion is

$$f = \frac{1}{\beta} \ln \int_0^\infty r \exp(-\beta r^4 - \mu r^2) dr - \frac{1}{\beta} \ln(2) - 1 \tag{2.7}$$

where the value of μ is determined by the equation

$$\int_0^\infty r^3 \exp(-\beta r^4 - \mu r^2) dr = \int_0^\infty r \exp(-\beta r^4 - \mu r^2) dr \tag{2.8}$$

The last condition correspond to the closure condition

$$\sum_{l=1}^{p/2} \langle |B_l|^2 \rangle = 1 \tag{2.9}$$

where the mean values $\langle \ldots \rangle$ are evaluated using the effective Hamiltonian

$$H(\{B_l\}) = -\beta \sum_l |B_l|^4 - \mu \sum_l |B_l|^2 \tag{2.10}$$

The integration variables B_l are complex variables and the mean values $\langle \ldots \rangle$ are obtained integrating over the real and imaginary part of the B_l. Obviously this expression for the free energy is not valid for the open model for which a high-temperature resummation is still lacking.

2.4.2 Dynamical glassy transition

The static transition obtained using GB approximation and high-temperature expansion does not coincide with the temperature at which one observes a phase transition in computer simulations. In ref. [75], using Monte Carlo dynamics, it have been measured the main thermodynamical observables and dynamical quantities both in the periodic and open models. Doing annealings, starting from large temperatures down to low T region, one observes only a *dynamical glassy* transition at a temperature T_D where energy freezes and fluctuations vanish, not the static transition transition described in the previous paragraph. In fact, the dynamical transition is higher than the static transition and is related to the fact that the system remains trapped in metastable configurations. From the thermodynamic point of view this transition is second order: the energy and the entropy are continuous, while the specific heat and the susceptibility experiences a jump at

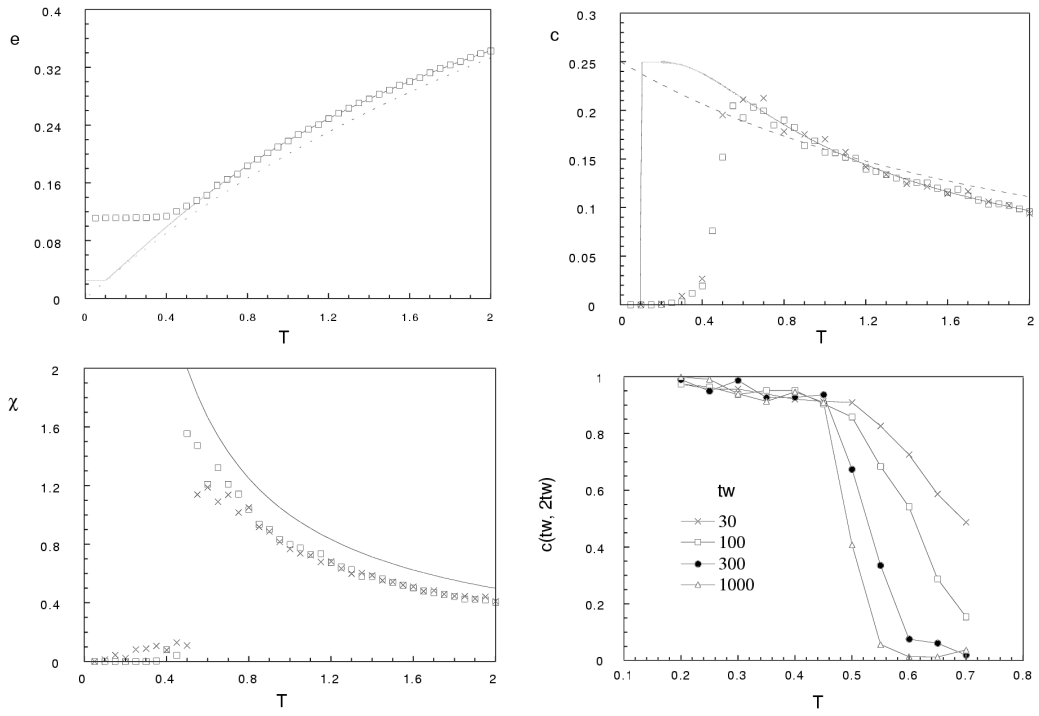

Figure 2.2: Simulations for the periodic LAM model. Energy (top left), specific heat (top right), susceptibility (bottom left) as a function of the temperature. The system size is $p = 100$ (squares) and $p = 500$ (crosses). The continuous line is the high-temperature result Eq. (2.7). The dashed line is the GB approximation. Bottom right: $C(t_w, 2t_w)$ vs. temperature for different values of $t_w = 30, 100, 300, 1000$. (from ref. [75])

the temperature $T_D = 0.45$ for periodic model (see Fig. (2.2)). The open model has a completely similar behaviour and the dynamical temperature is $T_D \approx 0.2$.
However, the main property of the glassy transition in low autocorrelation models regards the first order nature of this transition, which is seen in the discontinous behaviour of the dynamical order parameter. This can be defined as

$$q_1 = \lim_{t_w \to \infty} C(t_w, 2t_w) \tag{2.11}$$

where

$$C(t_w, t_w + t) = \frac{1}{p} \sum_{i=1}^{p} \sigma_i(t_w)\sigma_i(t_w + t) \tag{2.12}$$

is the correlation function between the spins configuration at time t_w and the configuration at time $t_w + t$. Above the glass transition, time homogeneity applies

(this means that $C(t_w, t_w + t)$ only depends on t) and the correlation function decays very fast in time, so that one has $q_1 = 0$. Below the glass transition the time behaviour of the correlation function drastically changes: time homogeneity hypothesis is lost and aging effects start to appear, that is, the decay of correlation function is very slow and depends on the previous history of the system. (more concretely, it depends on the time t_w at which the spins configuration is memorized). The system remains trapped in metastable states and it takes a very long time for the system to overcome the barriers and explore new configurations. The aging phenomena can be used as a precise method to locate the glass transition through finite size scaling. Just below T_G, q_1 jumps from zero to a finite value that is very close to 1 (see again Fig. (2.2)). The order parameter q_1 is physically related to the local order parameter associated to the metastable states and it is smaller than the local overlap associated to the true equilibrium configurations (the static Edward-Anderson order parameter). Because of the q_1's jump, the dynamical transition is of discontinuous type. This is very reminiscent of the REM.

2.4.3 Introduction of a random model

In references [67] and [68] it has been proposed for the first time to use the replica method to gain informations on the LAM, respectively for the periodic and open case. A disordered model has been introduced requiring that it does have the *same high-temperature expansion* of the periodic LAM. For the open case, since the high temperature expansion has not been resummed at the present moment, it has been required that the disorder model reproduces the high-temperature Golay-Bernasconi approximation. In both cases, the introduction of the random model amounts to substitute the Fourier transform of Eq. (2.5) with a generic unitary transformation

$$B(l) = \sum_j U_{lj}\sigma_j \tag{2.13}$$

where the U matrices are random unitary matrices. Fourier transform is one particular unitary transformation and one try to understand what happens if one substitute it with a random transformation. Taking into account the reality property,

Eq. (2.6), one is lead for the periodic model, to the following random Hamiltonian

$$H \equiv \sum_{l=1}^{p/2} |A(2l-1) + iA(2l)|^4 \tag{2.14}$$

where the A variables are defined from the spin variables σ_j as

$$A(l) \equiv \sum_{j=1}^{p} O_{lj}\sigma_j \tag{2.15}$$

and the O_{lj} are random orthogonal transformations over which has has to integrate. This model can be explicitly solved by replica approach. In the replica symmetric approximation one recovers the Hartree-Fock resummation (Eq. (2.7)) and the temperature of the static transition T_S is given by the temperature at which replica symmetric breaking happens. The explicit computation of the dynamical temperature through replicas has been performed not for the LAM but for a simpler model (*the sine model*) which is introduced in the next Section.

2.5 The Sine Model and the Random Orthogonal Model

The periodic LAM model can be seen as a fully 4-spin interaction: the 4-spin terms are given by the square of the two-point correlation functions that appear in Hamiltonian (2.1). The ground state of the model is not known in general. No systematic procedure for constructing ground-state configurations is known. A remarkable exception has been found for prime values of the system size p, such that $p = 4n + 3$, where n is a natural number. In this case it is possible to exhibit an explicit construction that is based on number theory [69]. The ground state is given by the so-called Legendre symbols (see Chapter 4). On such particular sequence σ, Gauss has proved that the Fourier transform is invariant, namely the Fourier-transformed variables are equal or proportional to the original spin variables:

$$B(l) = G(p)\sigma_l \tag{2.16}$$

where $G(p) = 1$ for $p = 4n+1$ and $G(p) = -i$ for $p = 4n+3$. By using this property, in ref. [69], it has been defined a simple model with 2-spin interaction which has the same ground state as the 4-spin interaction low autocorrelation model. The new

Hamiltonian has the form

$$H = \sum_l |G(p)\sigma_l - B(l)|^2 \tag{2.17}$$

This can be further simplified by noticing that the sequence of the Legendre σ is symmetric or antisymmetric around the point $\frac{1}{2}(p-1)$, depending on the value of $G(p)$. This allow to define a new model with half the number of the degree of freedom (that, from now on, we call N) which continues to admits, for selected N values, the Legendre symbols as ground states. This model has been called the *sine model* and is given by the following Hamiltonian

$$H = -\frac{1}{2}\sum_{i,j=1}^{N} J_{ij}\sigma_i\sigma_j \tag{2.18}$$

where J is the symmetric orthogonal $N \times N$ matrix

$$J_{ij} = \frac{2}{\sqrt{2N+1}} \sin\left(\frac{2\pi ij}{2N+1}\right) \tag{2.19}$$

This is the deterministic model that we are going to study in this work (another deterministic model will be introduced in the next Section). Being simpler, it shares the same properties of the periodic LAM. In ref. [69] it has been identified the static transition temperature $T_S = 0.065$ where the high-temperature entropy vanishes (equilibrium transition), while the higher dynamical temperature is $T_D = 0.134$.

The corresponding disordered version of the sine model has been introduced as well. It is the *Random Orthogonal Model* (ROM) defined by Hamiltonian (2.18) where the coupling matrix is chosen at random in the set of orthogonal symmetric matrices. The probability distribution (or integration measure) is defined by writing $J = ODO^{-1}$ with D a diagonal matrix composed of ± 1 and O a generic orthogonal matrix (not necessarily symmetric) whose probability distribution is defined by the Haar measure on the orthogonal group. In ref. [69] it has also been shown, using the replica formalism, that most of the thermodynamical properties of the sine model are the same as those of a generic symmetric orthogonal matrix.

2.6 Another deterministic models

It has been observed [78] that the matrix J of the sine model coincides with the imaginary part of the evolution operator V_A quantizing the elliptic dynamical system

given by the unit Hamiltonian sympletic matrix

$$A = \begin{pmatrix} 0 & 1 \\ -1 & 0 \end{pmatrix} \tag{2.20}$$

acting as a Hamiltonian map over the 2-torus T^2 [79]. The operator quantizing a Hamiltonian map of the torus is a $N \times N$ unitary matrix, N being the inverse of the Planck constant (the physical intuition is that the phase space has volume 1 and can accommodate at most N quantum states of volume h, so that $Nh = 1$). As a consequence, in this context the thermodynamical limit $N \to \infty$ is formally equivalent to the classical limit.

This algebraic identity suggested as more natural candidates for detecting deterministic glassy behaviour the coupling matrices defined by the quantization of hyperbolic maps over T^2. In ref. [70] it has been proposed to consider the model defined by Hamiltonian

$$H = -\frac{1}{2} \sum_{i,j=1}^{N} J_{ij} \sigma_i \sigma_j \tag{2.21}$$

where the coupling matrix is

$$J_{ij} = C_N \frac{1}{\sqrt{N}} \cos\left(\frac{2\pi}{N}(gi^2 - ij + gj^2)\right) \qquad g \in \mathbb{N} \tag{2.22}$$

that corresponds to the real part of the propagator V_B quantizing hyperbolic maps of the form [80]

$$B = \begin{pmatrix} 2g & 1 \\ 4g^2 - 1 & 2g \end{pmatrix} \tag{2.23}$$

Here C_N is an arbitrary phase factor, $|C_N| = 1$. We call this model *"quadratic"*, because, compared to the sine model, the coupling are the cosine of a fully quadratic form in the lattice indexes.

While for the sine model the linearization of the mean field equations obtained by resumming the high temperature expansion do not determine the critical temperature [85] (see Chapter 3), in the case of the model defined by (2.21) and (2.22) the critical temperature of a phase transition can be determined by linearization around the largest eigenvalue of J and is value is $T_c \sim 0.8$ [70]. The transition is of glassy type because the mean magnetization is zero for small values of the Edwards-Anderson parameter. We do not known whether the possibility of

locate the transition temperature is only a mathematical chance or if there is a deeper physical reason. By the way we observe that the dynamical system A (2.20) is periodic and, since J is orthogonal, the eigenvalues are only ± 1. In case B (2.23) the dynamical system is chaotic and, at the thermodynamical limit $N \to \infty$, the spectrum is equidistributed in $[-1, 1]$.

Chapter 3

High temperature expansions for deterministic models

3.1 Introduction

It has been suggested by Parisi et al. [82] that, unlike the random case, where the long ranged spherical model admits a critical temperature [81], the glass transition in deterministic spin models only exist for Ising-like variables. The numerical study of the XY case [82] (where the spin variables are complex numbers of modulo 1) and the analytical one for the spherical model [83] (where the spin variables are allowed to be continuous functions subject to the constraint $\sum_{i=1}^{N} \sigma_i^2 = N$) has strengthened this conjecture, showing that these systems are paramagnetic at all temperatures. In this Chapter, it is actually shown that it is the discrete nature of the spin variables in deterministic model that generate a phase transition associated with a non-trivial thermodynamical behaviour. We are going to generalize the dichotomic Ising case, considering the general case of spin s, so that the number of configurations available for each spin is $2s + 1$. For the sake of space, we will treat only the "quadratic" coupling (2.22). The calculation that will be given is essentially an adaption of the calculation of ref. [70], part of their work have, however, been simplified.

3.2 Mean field equations

Let us consider in this Section the mean field equation for the magnetizations in the case of deterministic models with dichotomic Ising spin variable $\sigma_i = \pm 1$. The

Hamiltonian is

$$H = -\frac{1}{2}\sum_{i,j=1}^{N} J_{ij}\sigma_i\sigma_j \tag{3.1}$$

where the deterministic coupling can be

- A: the sine model coupling

$$J_{ij} = \frac{2}{\sqrt{2N+1}}\sin\left(\frac{2\pi ij}{2N+1}\right) \tag{3.2}$$

- B: the "quadratic" model coupling

$$J_{ij} = C_N\frac{1}{\sqrt{N}}\cos\left(\frac{2\pi}{N}(gi^2 - ij + gj^2)\right) \tag{3.3}$$

The general strategy to obtain mean field equations for the magnetizations through high-temperature expansion is the following:

1. Compute the Helmotz free energy $F(\beta, h_i)$ expanding in powers of β and h_i the logarithm of the partition function and the resumming it.

2. Compute the Gibbs free energy $\Phi(\beta, m_i)$, passing from the variables h_i to m_i using a Legendre transform

$$\Phi(\beta, m_i) \equiv F(\beta, h_i) + \sum_i h_i m_i \qquad \text{with} \quad m_i = -\frac{\partial F}{\partial h_i} \tag{3.4}$$

3. Write down the mean field (TAP) equations for the magnetizations extremizating $\Phi(\beta, m_i)$ with respect to the m_i's

$$\frac{\partial\Phi(\beta, m_i)}{\partial m_i} = 0 \tag{3.5}$$

Let us start from the standard Helmotz free energy in zero external field:

$$\begin{aligned} e^{-\beta F(\beta)} &= \sum_{\{\sigma_i\}}\exp\left[\frac{\beta}{2}\sum_{i,j}J_{ij}\sigma_i\sigma_j\right] \qquad (3.6)\\ &= \frac{1}{\det^{1/2}(2\pi\beta J)}\int_{-\infty}^{+\infty}\prod_i\frac{dx_i}{\sqrt{2\pi}}\exp\left[-\frac{1}{2\beta}\sum_{i,j=1}^{N}J^{-1}_{ij}x_ix_j + \sum_i\ln\cosh x_i\right] \end{aligned}$$

where we have introduced N dummy variables x_i to perform the trace over spin variables. The high-temperature expansion for $\beta F(\beta)$ is generated out of the

integration of the expansion of the $\exp \ln \cosh x$. The well known diagrammatic representation of the nth-order term is obtained [84] by drawing all diagrams with n links, $2 < j+1 < n+1$ vertices and no external legs, whose individual contribution is given by the following rules:

(1) for any link between two consecutive vertices $l \neq k$ a factor βJ_{lk};

(2) for any vertex with m links the cumulant u_m, *i.e.* the mth coefficient of the Taylor expansion of $\ln \cosh x$

(3) any diagram has to divided by its order of symmetry

The contribution of each individual diagram D at order β^n is indeed

$$|D| = U(D)S(D)^{-1} \sum_{r_1, r_2, \ldots, r_{j+1}} J^{\alpha_1}_{r_1 r_2} J^{\alpha_2}_{r_2 r_3} \cdots J^{\alpha_j}_{r_j r_{j+1}} \qquad j = 1, \ldots, n \tag{3.7}$$

Here $j+1$ is the number of vertices, $\alpha_1 + \ldots \alpha_n = n$; $n - j + 1 = n - 1 \ldots, 1$ is the number of loops, $\alpha_i \geq 1$ the number of links between consecutive vertices, $S(D)$ the symmetry factor and $U(D) = u_1(\alpha_1) u_2(\alpha_1 + \alpha_2) \ldots u_j(\alpha_{j-1} + \alpha_j) u_{j+1}(\alpha_j)$. Note that $r_{n+1} = r_1$ for $j = n$.

To determine the Gibbs free energy $\Phi(\beta, m_i)$, we have to put a site-dependent magnetic field h_i in the Eq. (3.6)

$$e^{-\beta F(\beta, h_i)} = \frac{1}{\det^{1/2}(2\pi\beta J)} \int \prod_i \frac{dx_i}{\sqrt{2\pi}} \exp \left[-\frac{1}{2\beta} \sum_{i,j=1}^{N} J^{-1}_{ij} x_i x_j + \sum_i \ln \cosh(x_i + h_i) \right] \tag{3.8}$$

repeat the previous expansion (now in powers of β and h_i) and perform the Legendre transform Eq.(3.4). In standard field theory, the Legendre transform can be formulated in diagrammatical terms. The Gibbs free energy, also called the effective potential in particle physics, is given by the sum over connected one-particle-irreducible diagrams. This is not true in the present case, because the external field h_i does not appear as a linear source in Eq. (3.8), instead it appears inside the potential. A shift in x_i would not simplify matters since it would introduce a term quadratic in h_i sufficient to render invalid the usual $1PI$ derivation. It is, however, possible to perform the expansion of Gibbs free energy algebraically and to give it a diagrammatic representation [86]. The weak point of this method is that

the vertex weight and the combinatorial factors cannot be calculated systematically. Nevertheless, since we will see that in the expansions for deterministic models only a restricted class of diagrams survives the large-N limit, one can verify that, passing from Helmotz to Gibbs free energy, this class of non-vanishing diagrams appears with the same weight but with an extra factor of $(1 - m_{j_k}^2)$ for each vertex j_k. Assuming self-averaging for all the contributing terms (expect for the "entropic" and "energetic" one), one can further simplify the final result by substituting m_j^2 by $q \equiv \frac{1}{N}\sum_j m_j^2$.

3.2.1 Case A: the sine model

For the sine model, using the orthogonality relation $\sum_k J_{ij}J_{jk} = \delta_{ij}$, one obtains that all diagrams are zero in the thermodynamical limit expect for the so-called even "cactus" diagrams, which are trees made out of loops of even length joined at the vertices and whose contribution amounts to N [85]. In other words, the high temperature Helmotz free energy in zero external field is given by N times the sum over the combinatorial factors and powers of β of all even cactus diagrams. Evaluating this sum [85] one obtains

$$-\beta F(\beta) = N \ln 2 + N G_A(\beta) \tag{3.9}$$

where $G_A(\beta)$ is the function

$$G_A(\beta) = \frac{1}{4}\left[\sqrt{1+4\beta^2} - \ln\left(\frac{1+\sqrt{1+4\beta^2}}{2}\right) - 1\right] \tag{3.10}$$

It is important to note that this free energy is *independent* of the particular choice of the orthogonal matrix J, so it is also the free energy of the ROM model. In fact the same result can be obtained by solving the disordered ROM in the replica symmetric approach. Furthermore $G_A(\beta)$ has the following expansion in the vicinity of $\beta = 0$:

$$G(\beta) = \frac{\beta^2}{4} + \mathcal{O}(\beta^3), \tag{3.11}$$

which, by the way, coincides with what one obtains for the SK model. From the Eq. (3.9) and (3.10) one derives the other thermodynamical quantities at zero external field

$$U(\beta) = -\frac{N\beta}{1+\sqrt{1+4\beta^2}} \tag{3.12}$$

$$C(\beta) = \frac{N\beta^2}{1+4\beta^2+\sqrt{1+4\beta^2}} \tag{3.13}$$

$$S(\beta) = N\ln 2 - \frac{N}{4}\ln\left[\frac{1}{2}\left(1+\sqrt{1+4\beta^2}\right)\right] \tag{3.14}$$

In particular from the expression for the entropy one can locate the static equilibrium transition temperature $T_S \sim 0.065$: it is the point where entropy vanishes. The high temperature Gibbs free energy is given by

$$\begin{aligned}\beta F(\beta, m_i) &= \sum_i \left[\left(\frac{1+m_i}{2}\right)\ln\left(\frac{1+m_i}{2}\right) + \left(\frac{1-m_i}{2}\right)\ln\left(\frac{1-m_i}{2}\right)\right] \\ &\quad -\frac{\beta}{2}\sum_{ij} J_{ij}m_i m_j - NG_A(\beta(1-q))\end{aligned} \tag{3.15}$$

One can see that the first two terms (the "entropic" and "energetic" terms) are the same like in the TAP free energy (1.9) for the SK model. The third is the generalization of the Onsanger reaction term to the present case: now one can not retain (in the thermodynamical limit) only the β^2 contribution as for the SK model; one has instead to take in account the contributions from all the higher-order terms in the high temperature series. This is included in the function $G_A(\beta)$. Applying Eq. (3.5), the mean field equations read

$$m_i = \tanh\left[\beta\sum_j J_{ij}m_j + 2\beta G'_A(\beta(1-q))m_i\right] \tag{3.16}$$

where the prime denotes derivation of the function $G_A(x)$ with respect to its argument x.

3.2.2 Case B: the "quadratic" model

For the "quadratic" model, the class of diagrams contributing to the Helmotz free energy in the thermodynamical limit is even smaller. Using the basic estimates fulfilled by Gauss sums [90]

$$\left|\sum_{s_1,s_2,\ldots,s_l=1}^{N} \exp\left(\frac{2\pi i}{N}g(s_1,s_2,\ldots,s_l)\right)\right| \leq CN^{l/2} \tag{3.17}$$

where g is any quadratic form in the l integers $s_1, s_2, \ldots, s_l$ with integer coefficients and C a constant independent of g and N, one can prove [70] that the only surviving

diagrams are the ones at even order $n = 2p$, having $p + 1$ vertices, p loops and two links between consecutive loops. The results for the Helmotz free energy is [70]

$$-\beta F(\beta) = N \ln 2 + N G_B(\beta) \tag{3.18}$$

where $G_B(\beta)$ is now given by

$$G_B(\beta) = \frac{\beta^2}{8 + 4\beta^2} \tag{3.19}$$

As in the previous case, expanding to first order $-\beta F(\beta)$ we recover the SK Helmotz free energy, and the function $G_B(\beta)$ does not depend on the particular choice of the couplings, *i.e.* on the value of $g \in N$. In this case one derives the following expressions for the main thermodynamical quantities at zero external field

$$U(\beta) = -\frac{N\beta}{(2 + \beta^2)^2} \tag{3.20}$$

$$C(\beta) = \frac{N(2\beta^2 - 3\beta^4)}{(2 + \beta^2)^3} \tag{3.21}$$

$$S(\beta) = -\frac{N\beta^2}{(2 + \beta^2)^2} + \frac{N\beta^2}{8 + 4\beta^2} + N \ln 2 \tag{3.22}$$

This time the high-temperature entropy is well-defined at any temperature but we note that the specific heat becomes negative at the temperature $T \sim 1.22$. Analougsly to case A, the high temperature Gibbs free energy is given by

$$\begin{aligned} \beta F(\beta, m_i) &= \sum_i \left[\left(\frac{1 + m_i}{2} \right) \ln \left(\frac{1 + m_i}{2} \right) + \left(\frac{1 - m_i}{2} \right) \ln \left(\frac{1 - m_i}{2} \right) \right] \\ &\quad - \frac{\beta}{2} \sum_{ij} J_{ij} m_i m_j - N G_B(\beta(1 - q)) \end{aligned} \tag{3.23}$$

and the mean field equations are

$$m_i = \tanh \left[\beta \sum_j J_{ij} m_j + 2\beta G_B'(\beta(1 - q)) m_i \right] \tag{3.24}$$

3.3 Ising model of arbitrary spin s

Consider a system of N spins with only one component (the one along the z axis for example) of value s, which can be an integer or an half-integer. The possible

autostates of each spin are labelled by the quantum number s_z which ranges from $-s$ to s in unit steps. The Hamiltonian (normalized to the spin value) is:

$$H = -\frac{1}{2s^2}\sum_{i,j=1}^{N} J_{ij} s_i^z s_j^z - \frac{1}{s}\sum_{i=1}^{N} s_i^z h_i \tag{3.25}$$

The normalization is such that the maximal interaction between two parallel spins ($\uparrow\uparrow$) remains constant varying the spin value. If $s = 1/2$ we recover (3.1). The prefactor $1/2$ is conventional and is kept to compare with previous results. The partition function (at site-dependent magnetic field $h_i = 0$) is the trace of the Boltzmann factor:

$$Z(\beta) = \mathrm{Tr}\left(\exp(-\beta H)\right) = \sum_{\{s_i^z\}} \exp\left(\frac{\beta}{2s^2}\sum_{i,j=1}^{N} J_{ij} s_i^z s_j^z\right) \tag{3.26}$$

Using standard formulas for gaussian integrations we can rewrite the previous expression as a theory of N fields in zero dimension:

$$Z(\beta) = \sum_{\{s_z\}} \frac{1}{\det^{1/2}(2\pi\beta J)} \int_{R^N} dx \exp\left(-\frac{1}{2\beta}\sum_{i,j=1}^{N} J_{ij}^{-1} x_i x_j + \frac{1}{s}\sum_{i=1}^{N} s_i^z x_i\right) \tag{3.27}$$

The summation over the s_z is now decoupled and can be carried out; after some algebraic manipulations, we have

$$\begin{aligned} Z(\beta) \;=\; & \frac{1}{\det^{1/2}(2\pi\beta J)} \int_{R^N} dx \exp\left(-\frac{1}{2\beta}\sum_{i,j=1}^{N} J_{ij}^{-1} x_i x_j \right. \\ & \left. + \sum_{i=1}^{N} \log\left\{\frac{\sinh[(1+\frac{1}{2s})x_i]}{\sinh[(\frac{1}{2s})x_i]}\right\}\right) \end{aligned} \tag{3.28}$$

To obtain the mean-field equations we resume the high temperature expansion for the Gibbs (i.e. magnetization dependent) free energy. We start, as usual, from the Helmholtz free energy $-\beta F(\beta) = \log Z(\beta)$, representing its expansion in diagrammatic way. For convenience of the reader we remember the fundamental steps:

- in the diagrammatic representation we have to consider all the connected diagrams with the propagator βJ_{ij} for any link between two consecutive vertices

- the vertices factors are now generalized for any vertex with m links to the cumulant u_m (i.e. the m-th coefficient of Taylor expansion) of $\log\left\{\frac{\sinh[(1+\frac{1}{2s})x]}{\sinh[(\frac{1}{2s})x]}\right\}$
- any diagram has to be divided by its order of symmetry.

In the thermodynamical limit, due to the properties of quadratic Gauss sums, it can be shown (see [70] for a rigorous proof) that the set of diagrams contributing in order N are just those of even order $n = 2p$ with $p+1$ vertices and p loops. Equivalently these are all the diagrams having two vertices with two links (the extrema) and $p-1$ vertices with four links (all the remaining ones). At every order, ref [70] tell us that couplings gives an amount of $N2^{-p}$, the symmetry factor is 2^{p+1} and we only need to calculate the cumulants u_2 and u_4 :

$$u_2 = \frac{1}{3}\frac{s+1}{s} \tag{3.29}$$

$$u_4 = -\frac{1}{15}\frac{(s+1)(2s^2+2s+1)}{s^3} \tag{3.30}$$

Putting everything together, we can perform the summation and obtain the Helmholtz free energy:

$$\begin{aligned} -\beta F(\beta) &= N\log(2s+1) + N\sum_{p=1}^{\infty}(u_2)^2(u_4)^{(p-1)}\frac{1}{2^{p+1}}\frac{\beta^{2p}}{2^p} \\ &= N\log(2s+1) + \frac{5}{6}\frac{s(s+1)^2\beta^2}{60s^3+(s+1)(2s^2+2s+1)\beta^2} \\ &= N\log(2s+1) + NG(\beta) \end{aligned} \tag{3.31}$$

To determine the Gibbs free energy $\Phi(\beta, m_i)$, we have to put a magnetic field h_i, repeat the previous expansion and perform the Legendre transform

$$\Phi(\beta, m_i) \equiv F(\beta, h_i) + \sum_i h_i m_i \tag{3.32}$$

with $m_i = -\partial F/\partial h_i$. The class of non-vanishing diagrams has the same weights as in the $h_i = 0$ case but with an extra factor of $(1 - m_{i_k}^2)$ for each vertex i_k [86]. The hypothesis of self-averaging [85], namely $m_i^2 = q \equiv \lim_{N\to\infty} 1/N \sum_i m_i^2$ yields the same function $G(\beta)$ in (3.31), with β replaced by $\beta(1-q)$. In the final expression for $\Phi(\beta, m_i)$ we have to put by hand the usual terms given by the entropy of a set of

non-interacting spins constrained to have magnetization m_i and the "naive" mean field energy

$$\begin{aligned} -\beta\Phi(\beta, m_i) &= -\sum_i \log\left\{\frac{\sinh[(1+\frac{1}{2s})\mathcal{L}_s^{-1}(m_i)]}{\sinh[(\frac{1}{2s})\mathcal{L}_s^{-1}(m_i)]}\right\} - m_i\mathcal{L}_s^{-1}(m_i) \\ &\quad -\frac{\beta}{2}\sum_{ij} J_{ij}m_i m_j - NG(\beta(1-q)) \end{aligned} \tag{3.33}$$

where

$$\mathcal{L}_s(y) = \left(1+\frac{1}{2s}\right)\coth\left[\left(1+\frac{1}{2s}\right)y\right] - \left(\frac{1}{2s}\right)\coth\left[\left(\frac{1}{2s}\right)y\right] \tag{3.34}$$

is the so-called Langevin functions [87], which is typical of paramagnetism in non-metallic solids. Having the expression for the Gibbs free energy, the mean field equations of the model (that are presumably exact because of its infinite range) are given by direct differentiation of (3.33). These would be the analogous of TAP equations for SK model [18]. To see whether a "glass" phase transition exists we look for solutions of mean-field equations different from the trivial one $q = 0$. For T near T_c the magnetizations m_i and also the eigenvectors corresponding to the largest eigenvalue of J_{ij} are small so we can linearize in m_i. Using

$$\mathcal{L}_s^{-1}(m_i) = \frac{3s}{s+1}m_i + \frac{9}{10}\frac{s(1+2s+2s^2)}{(1+s)^3}m_i^3 + o(m_i^4) \tag{3.35}$$

the linearized equations read

$$\frac{3s}{s+1}m_i - \beta m_i + 2\beta G'(\beta)m_i = 0 \tag{3.36}$$

With some tedious algebra one can rewrite the previous equation as

$$\begin{aligned} 0 &= \beta^5[(1+s)^3(1+2s+2s^2)^2] - \beta^4[3s(1+s)^2(1+2s+2s^2)^2] \\ &\quad +\beta^3[120s^3(1+s)^2(1+2s+2s^2)] - \beta^2[40s^4(1+s)(14+28s+23s^2)] \\ &\quad +\beta[3600s^6](1+s) - 10800s^7 \end{aligned} \tag{3.37}$$

The critical temperature T_c is given by the zeros of (3.37). For fixed value of s we numerically solved it; in Fig. (3.1) we plot the critical inverse temperature β_c versus the spin value s. The numerical fit is consistent with the following law:

$$\beta_c \sim \frac{10}{3} - \frac{3}{s+1} \tag{3.38}$$

The inverse critical temperature grows with an inverse power law for increasing s, approaching a constant value for $s \to \infty$.

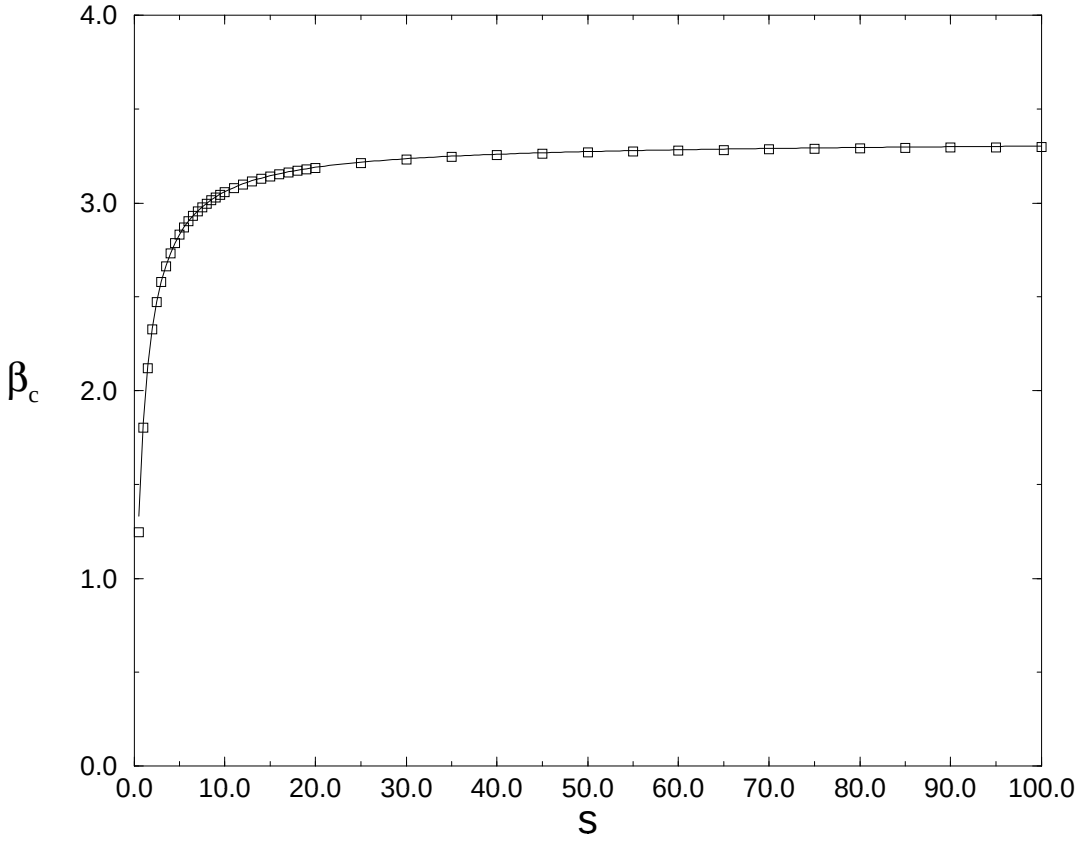

Figure 3.1: Plot of the inverse critical temperature β_c versus the spin value s. The solid line is the best numerical fit, (Eq. (3.38)).

3.4 Conclusions

By studying the dependence of the critical temperature in the "quadratic" model for the case of Ising spin values of arbitrary spin value, we have confirmed that discreteness of spin variable allow the existence of a phase transition in deterministic models. Its nature is "glassy" (in the sense that the pure magnetization states at zero temperature are neither ferromagnetic nor antiferromagnetic) by the same argument

of [70]: at $T = 0$ the averaged magnetization is zero because it is proved that

$$\lim_{N\to\infty} \frac{1}{N} \sum_{i=1}^{N} \mu_i = 0$$

if μ_i are the components of any normalized eigenvector of the matrix J corresponding to the eigenvalue 1. Even though the ground state is degenerate, none of the magnetization states generates long-range order. One would ask if the discreteness of spin variable is a necessary condition to a glass state exist. To obtain this conclusion one would have to rigorously shown that there is no transition in models with continuous symmetry (like the XY or Heisenberg models). This point goes beyond the aims of this work and will be discussed elsewhere.

Chapter 4

Statistics of energy levels and zero temperature dynamics for the Sine model

4.1 Introduction

Metastables states in infinite-range disordered spin-glasses have been extensively studied, both in the SK model [24, 25, 26] and in p-spin interaction spin-glasses [88]. Here we deal with the same question in deterministic models. By probabilistic arguments we will obtain, for the sine model a lower bound on the number of 1-spin-flip stable states, which increases exponentially with the size of the system. Hence this deterministic model exhibits the main feature of glassy behaviour.

The outline of this Chapter is the following. In Section (4.2) we calculate the number of metastable states at zero temperature for the Random Orthogonal Model, which is the disordered model associated to the sine model. In Section (4.3) we start our analysis on the sine model by studying the limiting distribution of the rescaled energy density, showing that it gets δ-distributed in the thermodynamic limit. This property, which holds for the Curie-Weiss case, is an indication of the mean-field nature of the model. In Section (4.4) we rigorously show that Legendre symbols are ground state configurations for the sine model when N is odd such that $p = 2N + 1$ is a prime of the form $4m + 3$. We deal with the state space of the system in Section (4.5), computing explicitly (for N prime analytically, for other values of N numerically) the distribution of the energy levels by flipping one spin at a time;

among other things we show that there can be a large number of states with almost zero overlap with the ground state but very close in energy to it. In Section (4.6) we relate metastable states to zero temperature dynamics and we numerically compute them. In Section (4.7) we derive the main result, that is a lower exponential bound for the number of metastable states at temperature $T = 0$. Finally, some numerical checks on the approximation that is made in the analytical calculation are presented in Section (4.8) and the concluding remarks are drawed in the last Section (4.9)

4.2 Metastable states in the Random Orthogonal model

We want to study the metastable states at temperature $T = 0$ in the Random Orthogoanl Model (ROM). As a by-produce we will obtain also the result for the SK model. The number of metastable state in the ROM model has been computed in ref. [85], calculating the number of solutions of the mean field equations through replicas. Here we rederive the result at zero temperature in a straightforward way. On the matrices of the random orthogonal group the following identity (which is useful to solve the model through replicas) holds in the large N limit

$$\int \mathcal{D}J \exp\left[\mathrm{Tr}\frac{JA}{2}\right] = \exp\left[N\mathrm{Tr}G\left(\frac{A}{N}\right)\right] \tag{4.1}$$

where Tr means the sum of diagonal elements, A is a symmetric matrix of finite rank and $G(x)$ is given by

$$G(x) = \frac{1}{4}\left[\sqrt{1+4x^2} - \log\left(\frac{1+\sqrt{1+4x^2}}{2}\right) - 1\right] \tag{4.2}$$

The fundamental formula (4.1) also applies to the case of random matrix with gaussian elements (SK model) with $G_{SK}(x)$ given by

$$G_{SK}(x) = \frac{x^2}{4} \tag{4.3}$$

Metastable states at zero temperature coincides with 1-flip stable states, *i.e.* configurations whose energy cannot be decreased by flipping any spin. The number of states subject to the stability condition against single spin flips for a fixed disorder realization J is given by

$$\mathcal{N} = \overline{\sum_{\{\sigma\}} \int_0^\infty \prod_i [d\lambda_i \; \delta(\lambda_i - \sum_j J_{ij}\sigma_i\sigma_j)]} \tag{4.4}$$

where as usual the bar denotes the average over disorder. Since we expect an exponential increase of the number of 1-flip stable states, the average over the bond distribution should be performed on the logarithm of this number, which is the extensive quantity, rather than on the number itself. This would lead us back to introducing replicas. However it turn out that for most of the states (actually for all states with energy ϵ above a critical value ϵ_c) the two computations coincide. Introducing integral representations for the δ functions

$$\delta(\lambda - \lambda_0) = \frac{1}{2\pi} \int_{-\infty}^{\infty} e^{-i\phi(\lambda-\lambda_0)}\, d\phi \tag{4.5}$$

we have

$$\mathcal{N} = \sum_{\{\sigma\}} \int_0^{\infty} \prod_i (d\lambda_i\ ) \int_{-\infty}^{\infty} \prod_i (\frac{d\phi_i}{2\pi}) e^{-i\sum_i \lambda_i \phi_i} \overline{\exp(i \sum_{i,j} J_{ij}\sigma_i\sigma_j\phi_i)} \tag{4.6}$$

We now do the simple change of variable $\phi_i \to \phi_i\sigma_i$ whose Jacobian is $\mathrm{Jac} = \prod_i \sigma_i$:

$$\mathcal{N} = \sum_{\{\sigma\}} \int_0^{\infty} \prod_i (d\lambda_i\ ) \int_{-\infty}^{\infty} \mathrm{Jac} \prod_i (\frac{d\phi_i}{2\pi}) e^{-i\sum_i \lambda_i \phi_i\sigma_i} \overline{\exp(i \sum_{i,j} J_{ij}\phi_i\sigma_j)} \tag{4.7}$$

Defining $A_{ij} = i(\phi_i\sigma_j + \phi_j\sigma_i)$ we have $i\sum_{i,j} J_{ij}\sigma_i\sigma_j = \mathrm{tr}(JA/2)$ and we can perform the average over disorder using formula (4.1). To this end we need the eigenvalues of A; it can be proved that the spectrum of A is composed by all zeros expect two eigenvalues $i\mu_+$ and $i\mu_-$ where

$$\mu_\pm = \langle \phi, \sigma \rangle \pm \|\phi\|\|\sigma\| \tag{4.8}$$

We obtain

$$\mathcal{N} = \sum_{\{\sigma\}} \int_0^{\infty} \prod_i (d\lambda_i\ ) \int_{-\infty}^{\infty} \mathrm{Jac} \prod_i (\frac{d\phi_i}{2\pi}) e^{-i\sum_i \lambda_i \phi_i\sigma_i} e^{N[G(i\mu_+/N)+G(i\mu_-/N)]} \tag{4.9}$$

We make again the elementary substitution $\phi_i \to \phi_i\sigma_i$ yielding $\mu_\pm/N \to v \pm \sqrt{w}$ with $v = 1/N\sum_i \phi_i$ and $w = 1/N\sum_i \phi_i^2$:

$$\mathcal{N} = \sum_{\{\sigma\}} \int_0^{\infty} \prod_i (d\lambda_i\ ) \int_{-\infty}^{\infty} [\mathrm{Jac}]^2 \prod_i (\frac{d\phi_i}{2\pi}) e^{-i\sum_i \lambda_i \phi_i} e^{N[G(i(v+\sqrt{w}))+G(i(v-\sqrt{w}))]} \tag{4.10}$$

Now the expression is independent of σ and the sum over spin configurations can be done: $\sum_{\{\sigma\}} = 2^N$. Note moreover that $[\mathrm{Jac}]^2 = 1$ so that

$$\mathcal{N} = \frac{1}{(\pi)^N} \int_0^\infty \prod_i (d\lambda_i\ ) \int_{-\infty}^\infty \prod_i (d\phi_i) e^{-i\sum_i \lambda_i \phi_i} e^{N[G(i(v+\sqrt{w}))+G(i(v-\sqrt{w}))]} \tag{4.11}$$

Now we want to perform the integration over the λ_i. To this end we introduce step functions to extend the integrals over the whole space.

$$\mathcal{N} = \frac{1}{(\pi)^N} \int_{-\infty}^\infty \prod_i [\theta(\lambda_i)\ d\lambda_i\ ] \int_{-\infty}^\infty \prod_i (d\phi_i) e^{-i\sum_i \lambda_i \phi_i} e^{N[G(i(v+\sqrt{w}))+G(i(v-\sqrt{w}))]} \tag{4.12}$$

Introducing integral representations for the step functions (from now on it is understood that the limit $\epsilon \to 0$ has to be taken)

$$\theta(\lambda) = \frac{1}{2\pi i} \int_{-\infty}^\infty \frac{e^{i\lambda k}}{k - i\epsilon}\, dk \tag{4.13}$$

we have

$$\begin{aligned} \mathcal{N} \;=\; & \frac{1}{(\pi i)^N} \int_{-\infty}^\infty \prod_i (d\phi_i) e^{N[G(i(v+\sqrt{w}))+G(i(v-\sqrt{w}))]} \\ & \int_{-\infty}^\infty \prod_i \left(\frac{dk_i}{k_i - i\epsilon}\right) \int_{-\infty}^\infty \prod_i \left(\frac{d\lambda_i}{2\pi}\right) e^{i\sum_i \lambda_i (k_i - \phi_i)} \end{aligned} \tag{4.14}$$

Now we recognize in the preceding expression the delta integral representation (4.5) so that

$$\mathcal{N} = \int_{-\infty}^\infty \prod_i \left(\frac{1}{i\pi}\, \frac{d\phi_i}{\phi_i - i\epsilon}\right) e^{N[G(i(v+\sqrt{w}))+G(i(v-\sqrt{w}))]} \tag{4.15}$$

The last step is to perform the integral over ϕ_i using the saddle point method. In order to do that we introduce again delta functions:

$$\begin{aligned} \mathcal{N} \;=\; & \int_{-\infty}^\infty dv\ \delta(v - 1/N \sum_i \phi_i) \int_{-\infty}^\infty dw\ \delta(w - 1/N \sum_i \phi_i^2) \\ & \int_{-\infty}^\infty \prod_i \left(\frac{1}{i\pi} \frac{d\phi_i}{\phi_i - i\epsilon}\right) e^{N[G(i(v+\sqrt{w}))+G(i(v-\sqrt{w}))]} \end{aligned} \tag{4.16}$$

and, using again the integral representation (4.5),

$$\begin{aligned} \mathcal{N} \;=\; & \frac{1}{(2\pi)^2} \int_{-\infty}^\infty dx \int_{-\infty}^\infty dy \int_{-\infty}^\infty dv \int_{-\infty}^\infty dw\ e^{i(vx+wy)} e^{N[G(i(v+\sqrt{w}))+G(i(v-\sqrt{w}))]} \\ & \int_{-\infty}^\infty \prod_i \left(\frac{1}{i\pi} \frac{\exp\left(-i\frac{\phi_i x}{N} - i\frac{\phi_i^2 y}{N}\right)}{\phi_i - i\epsilon} d\phi_i\right) \end{aligned} \tag{4.17}$$

Rescaling $x/N \to x$ and $y/N \to y$ and noticing that the integrals over ϕ_i are now decoupled, we obtain

$$\begin{aligned}\mathcal{N} &= \left(\frac{N}{2\pi}\right)^2 \int_{-\infty}^{\infty} dx \int_{-\infty}^{\infty} dy \int_{-\infty}^{\infty} dv \int_{-\infty}^{\infty} dw\; e^{N[i(vx+wy)+G(i(v+\sqrt{w}))+G(i(v-\sqrt{w}))]} \\ &\left(\int_{-\infty}^{\infty} \frac{1}{i\pi} \frac{\exp\left(-i\phi x - i\phi^2 y\right)}{\phi - i\epsilon} d\phi\right)^N \end{aligned} \tag{4.18}$$

The last integral can be directly evaluated completing the square in the exponential and using the identity

$$\text{erfc(-iz)} = e^{z^2} \int_{-\infty}^{\infty} \frac{1}{i\pi} \frac{\exp(-t^2)}{t - z} dt \tag{4.19}$$

where erfc(z) is the complementary error function. The final result is then obtained by applying the saddle-point method

$$\mathcal{N} \simeq \max_{\{v,w,x,y\}} \exp\left\{ N \left[G(v+\sqrt{w}) + G(v-\sqrt{w}) - vx - wy + \ln \text{erfc}\left(-\frac{x}{2\sqrt{y}}\right)\right]\right\} \tag{4.20}$$

Solving numerically the saddle point equations one finds

$$\mathcal{N} \simeq \exp(0.28N) \tag{4.21}$$

For the SK model, using the function $G_{SK}(x)$ of Eq. (4.3) instead of $G(x)$ one obtain the well known result [24, 25, 26] $\mathcal{N}_{SK} \simeq \exp(0.199N)$.

4.3 The limiting distribution of the rescaled energy levels

Before starting the analysis of metastable states in the sine model we study the distribution of energy levels. The basic setup is a probability space $(\Sigma_N, \mathcal{F}_N, \mathrm{P}_N)$. The sample space Σ_N is the configuration space, *i.e.* $\Sigma_N = \{-1, 1\}^N$ whose elements are the sequences $\sigma = (\sigma_1, \cdots, \sigma_N)$ with $\sigma_i = \pm 1$; $\mathcal{F}_N$ is the finite algebra with 2^{2^N} elements, and the *a priori* (or *infinite-temperature*) probability measure P_N is given by

$$\mathrm{P}_N(C) = \frac{1}{2^N} \sum_{\sigma \in C} 1. \tag{4.22}$$

The Hamiltonian is the function on Σ_N defined as

$$H(\sigma) = -\frac{1}{2}\sum_{xy} J_{xy}\,\sigma_x\,\sigma_y = -\frac{1}{2} < J\sigma, \sigma > \tag{4.23}$$

where $J = (J_{xy})$ is a symmetric real orthogonal $N \times N$ matrix given from the outset. Although many of the results presented here will hold for a generic symmetric matrix of the Random Orthogonal Matrices Group, in what follows we shall examine the particular example of *sine model* (2.19), that we report again for completeness:

$$J_{xy} = \frac{2}{\sqrt{2N+1}} \sin\left[\frac{2\pi xy}{2N+1}\right]. \tag{4.24}$$

which satisfies (we assume N odd) [1]

$$J\,J^T = \mathrm{Id} \quad \text{and} \quad \sum_{x=1}^{N} J_{xx} = \sum_{x=1}^{N} J_{xx}^2 = 1. \tag{4.25}$$

The knowledge of the eigenvalues of J imposes simple bounds on the energy of any spin configuration. Indeed a state vector σ can be decomposed into its projections on the various orthogonal eigenspaces relatives to different eigenvalues. Here, due to orthogonality, the possible eigenvalues are $+1, -1$ so that

$$-\frac{N}{2} \le H(\sigma) \le \frac{N}{2}. \tag{4.26}$$

Let us consider the rescaled and shifted Hamiltonian (representing the energy per site, or energy density of the model, plus the 'zero point' energy $1/2$)

$$h(\sigma) = \frac{H(\sigma)}{N} + \frac{1}{2} \tag{4.27}$$

which takes values in $[0, 1]$. We shall show that in the limit $N \to \infty$ the energy density h gets δ-distributed at $x = 1/2$. We point out that this property can be immediately proved for the Curie-Weiss model, thus indicating a mean field behaviour of the present model in the thermodynamic limit. To this end consider the partition function Z_N at inverse temperature β:

$$Z_N(\beta) = \sum_{\sigma \in \Sigma_N} \exp\left(-\beta H(\sigma)\right) = 2^N\, \mathrm{E}_N(e^{-\beta H}), \tag{4.28}$$

[1] One might also consider interaction matrices with zero diagonal terms, recovering orthogonality in large N limit. This amounts to put the average energy equal to zero (instead of $-1/2$) and may be convenient for particular purposes

where E_N denotes the expectation wrt P_N, and note that the characteristic function of h can be written as

$$\mathrm{E}_N(e^{-\lambda h}) = e^{-\lambda/2}\,\frac{Z_N(\lambda/N)}{2^N}. \tag{4.29}$$

This expression will prove useful to compute the limiting expression of the characteristic function of the energy density h without knowing the expression of all its moments. To see this, we first decouple the spins as follows: let B be an orthogonal matrix such that $B^T J B = D$ with $D = \mathrm{diag}\,(d_1, \ldots, d_N)$. Since $\det J \neq 0$ we have $d_i \neq 0$, $i = 1, \ldots, N$, and $\det J^{-1} = \prod_i d_i^{-1}$. Let $u \in I\!R^N$ be such that $\sigma = Bu$.We have $< J\sigma, \sigma > = < Bu, JBu > = < u, Du >$, and thus

$$\begin{aligned}
\exp(\frac{\lambda}{2N} < J\sigma, \sigma >) &= \prod_{i=1}^{N} \exp(\frac{\lambda}{2N} d_i u_i^2) \\
&= \prod_{i=1}^{N} \frac{1}{\sqrt{2\pi}} \int_{-\infty}^{\infty} \exp\left(-\frac{x_i^2}{2} + \sqrt{\frac{\lambda d_i}{N}}\; u_i x_i\right) dx_i \\
&= \frac{1}{(2\pi)^{N/2}} \int_{I\!R^N} \exp\left(-\frac{1}{2} < x, x > + \sqrt{\frac{\lambda}{N}}\; < u, D^{1/2} x >\right) dx \\
&= \frac{\det J^{-\frac{1}{2}}}{(2\pi\lambda)^{N/2}} \int_{I\!R^N} \exp\left(-\frac{1}{2\lambda} < y, J^{-1} y > + < \sigma, \frac{y}{\sqrt{N}} >\right) dy,
\end{aligned}$$

which, together with (4.23), (4.28) and (4.29) yields

$$\mathrm{E}_N(e^{-\lambda h}) = e^{-\lambda/2}\,\frac{\det J^{-\frac{1}{2}}}{(2\pi\lambda)^{N/2}} \int_{I\!R^N} \exp\left(-\frac{1}{2\lambda} < y, J^{-1} y > + \sum_i \log\cosh\frac{y_i}{\sqrt{N}}\right) dy \tag{4.30}$$

(As usual, the square roots appearing in the above formulas are only apparently ill defined: they disappear in the expansion because it contains only the even terms). The above integral can be evaluated by means of standard high-temperature expansion techniques which turn out to be considerably simpler if one assumes that $\sum_i J_{ii} = 0$ (see [85]). As we have already noted, this assumption amounts to fix at zero the mean value of the energy.Also, the division by N of the argument of the partition function leads to a convergence domain which is increasing as N itself. In this way, the asymptotic expression (for $N \to \infty$) of $\mathrm{E}_N(e^{-\lambda h})$ can be written in the form

$$\mathrm{E}_N(e^{-\lambda h}) = e^{-\lambda/2}\, e^{NG(\lambda/N)}\, \left(1 + \mathcal{O}(N^{-1})\right) \tag{4.31}$$

where the function $G(x)$ is an effective specific free energy. For the symmetric orthogonal interaction matrices and in particular for the sine model (4.24) one finds [85]:

$$G(x) = \frac{1}{4}\left[\sqrt{1+4x^2} - \log\left(\frac{1+\sqrt{1+4x^2}}{2}\right) - 1\right]. \tag{4.32}$$

This yields

$$e^{NG(\lambda/N)} = 1 + \frac{\lambda^2}{4N} + \mathcal{O}\left(\frac{\lambda^3}{N^2}\right). \tag{4.33}$$

Summarizing, we have found that for any fixed λ,

$$\mathrm{E}_N(e^{-\lambda h}) = e^{-\lambda/2}\left[1 + \mathcal{O}\left(\frac{1}{N}\right)\right], \qquad N \to \infty. \tag{4.34}$$

Using a well known theorem of probability theory [91] which says that a distribution function G_N converges weakly to G if and only if $\varphi_N(\lambda) \to \varphi(\lambda)$ for any λ (where $\varphi_N(\lambda)$ and $\varphi(\lambda)$ are the characteristic fcts of G_N and G respectively) and noting that $\varphi(\lambda) = e^{-\lambda/2}$ is the characteristic function of the distribution function $G(x) = \chi_{[\frac{1}{2},\infty)}$, we then conclude that the distribution of h tends to $\chi_{[\frac{1}{2},\infty)}$.

4.4 Legendre symbols as ground states in the sine model

As already noted in Chapter 2, for special values of N the ground state, i.e. the configuration $\sigma^0 \in \Sigma_N$ which minimizes the energy, can be explicitly constructed. Indeed, for N odd such that $p = 2N+1$ is prime of the form $4m+3$, where m is an integer, let σ^0 be the state given by the sequence of Legendre symbols, i.e.

$$\sigma^0_x = \left(\frac{x}{p}\right) = \begin{cases} +1, & \text{if } x = k^2 (\mathrm{mod} p), \\ -1, & \text{if } x \neq k^2 (\mathrm{mod} p), \end{cases} \tag{4.35}$$

with $k = 1, 2, \ldots, p-1$. Then, using basic results of number theory on the Gauss sums (see, for example, ref. [90]), we can prove that σ^0 is an eigenvector of J with eigenvalue 1 and so the value of the Hamiltonian on Legendre symbols is the lowest possible value

$$H(\sigma^0) = -\frac{1}{2} < J\sigma^0, \sigma^0 > = -\frac{1}{2} < \sigma^0, \sigma^0 > = -\frac{N}{2} \tag{4.36}$$

In fact we have:

$$
\begin{aligned}
(J\sigma^0)_y &= \frac{2}{\sqrt{p}} \sum_{x=1}^{N} \sin\left[\frac{2\pi xy}{p}\right] \left(\frac{x}{p}\right) \\
&= \frac{2}{\sqrt{p}} \sum_{x=1}^{N} \frac{1}{2i} \left(\exp\left[\frac{i2\pi xy}{p}\right] \left(\frac{x}{p}\right) - \exp\left[\frac{-i2\pi xy}{p}\right] \left(\frac{x}{p}\right)\right)
\end{aligned}
$$

changing $x \mapsto -x$ in the second summation

$$
= \frac{1}{i\sqrt{p}} \left[\sum_{x=1}^{N} \exp\left[\frac{i2\pi xy}{p}\right] \left(\frac{x}{p}\right) - \sum_{x=-N}^{-1} \exp\left[\frac{i2\pi xy}{p}\right] \left(\frac{-x}{p}\right)\right]
$$

using multiplicativity of Legendre symbols: $\left(\frac{-x}{p}\right) = \left(\frac{-1}{p}\right)\left(\frac{x}{p}\right)$
and the fact that $\left(\frac{-1}{p}\right) = -1$ if $p = 3(\mathrm{mod}4)$

$$
= \frac{1}{i\sqrt{p}} \left[\sum_{x=1}^{N} \exp\left[\frac{i2\pi xy}{p}\right] \left(\frac{x}{p}\right) + \sum_{x=-N}^{-1} \exp\left[\frac{i2\pi xy}{p}\right] \left(\frac{x}{p}\right)\right]
$$

using the periodicity of Legendre' symbols : $\left(\frac{x+p}{p}\right) = \left(\frac{x}{p}\right)$

$$
= \frac{1}{i\sqrt{p}} \left[\sum_{x=1}^{N} \exp\left[\frac{i2\pi xy}{p}\right] \left(\frac{x}{p}\right) + \sum_{x=N+1}^{2N} \exp\left[\frac{i2\pi xy}{p}\right] \left(\frac{x}{p}\right)\right]
$$

being $\left(\frac{p}{p}\right) = 0$ by definition

$$
= \frac{1}{i\sqrt{p}} \sum_{x=1}^{p} \exp\left[\frac{i2\pi xy}{p}\right] \left(\frac{x}{p}\right)
$$

using the separability for Gauss sums

$$
= \frac{1}{i\sqrt{p}} \left(\frac{y}{p}\right) \sum_{x=1}^{p} \exp\left[\frac{i2\pi x}{p}\right] \left(\frac{x}{p}\right)
$$

evaluating the Gauss sum

$$= \frac{1}{i\sqrt{p}} \left(\frac{y}{p}\right) i\sqrt{p} = \sigma_y^0 ,$$

which is the desired property. A typical ground state for p prime of the form $4m+3$ reflects the well known random distribution of the Legendre symbols (see Fig. (4.1), where a pair of ground states are shown for two different N values). No structure is present at any scale. Nevertheless, denoting by m^0 the *specific magnetization* of the ground state, *i.e.*

$$m^0 = \frac{1}{N} \sum_{x=1}^{N} \sigma_x^0 = \frac{1}{N} \sum_{x=1}^{N} \left(\frac{x}{p}\right) , \tag{4.37}$$

one observes that it tends to be a positive function of N, fluctuating around the value $1/\sqrt{N}$. To let the reader better appreciate this fact we plot in Fig. (4.2) the total magnetization Nm^0 versus N.

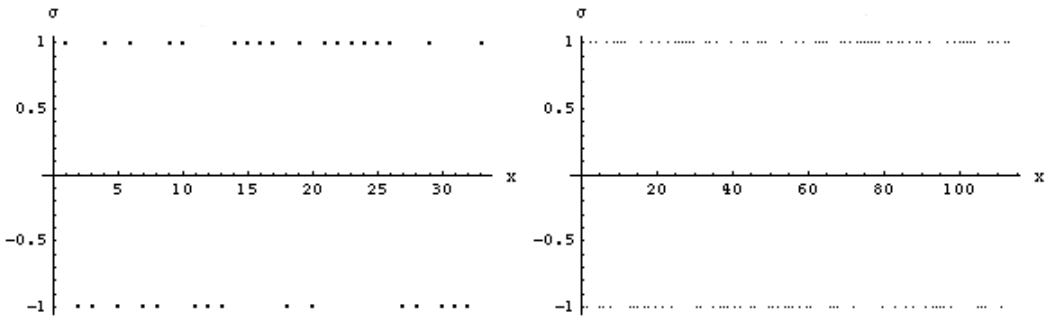

Figure 4.1: Ground state for $N = 33$ and $N = 113$.

4.5 Flipping spins from the ground state and statistics of levels

From now on we will restrict to $p = 2N + 1$ prime, with $p = 3\,(\mathrm{mod}4)$. We point out that this set has measure zero as a subset of the natural numbers. However, we have strong numerical evidence that some relevant properties that we are going to discuss hereafter, such as the behaviour of $m^0(N)$, the statistics of energy levels and the number of metastable states are somehow generic in N.

Let $\Omega_s \subset \Sigma_N$ be the subspace consisting of the $\binom{N}{s}$ configurations obtained by starting from the ground state σ^0 described above and flipping exactly s

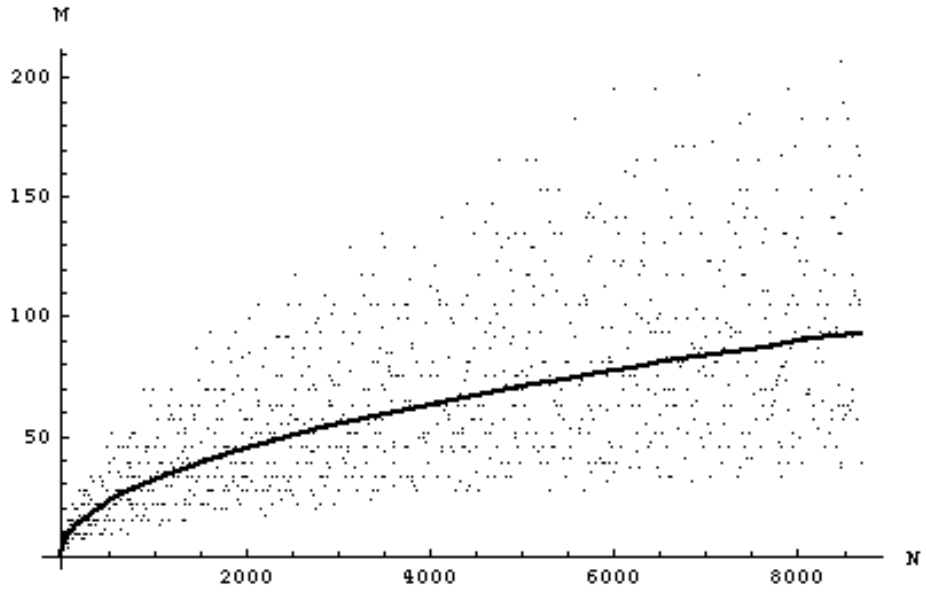

Figure 4.2: Total magnetization Nm^0 of the ground state versus N, $2N+1 = 4m+3$ prime. The continuous curve is $\sqrt{N}$.

different spins. Each point of Ω_s can thus be identified with a s-dimensional vector $\tau \in \{1, \ldots, N\}^s$ of the form $\tau = (x_1, \ldots, x_s)$, with $x_i \neq x_j$ for $i \neq j$, which specifies the positions of the flipped spins along the chain of length N. We then define the 'flipping' map $L_\tau : \Sigma_N \to \Sigma_N$ as:

$$(L_\tau \sigma)_x = \begin{cases} -\sigma_x, & x \in \tau, \\ \sigma_x, & x \notin \tau. \end{cases} \tag{4.38}$$

In this way we can write

$$\Omega_s = \{L_\tau \sigma^0\}_\tau. \tag{4.39}$$

The correspondence $\tau \to \sigma$ given by $\sigma = L_\tau \sigma^0$ is plainly one-to-one. Therefore in the sequel we shall freely identify a state $\sigma = L_\tau \sigma^0$ with the vector τ. Alternatively, we can proceed as follows. Define the *overlap* $q(\sigma)$ of a given configuration $\sigma \in \Sigma_N$ with respect to the ground state σ^0 as:

$$q(\sigma) = \frac{1}{N} \sum_{x=1}^{N} \sigma_x \sigma_x^0, \tag{4.40}$$

so that $q(\sigma^0) = 1$. Then

$$\Omega_s = \{\sigma \in \Sigma_N \,:\, q(\sigma) = 1 - 2\frac{s}{N}\} \tag{4.41}$$

The following straightforward calculation yields the energy values on the space Ω_s: using the definition of L_τ, the symmetry of J and the fact that the ground state σ^0 is an eigenvector of J to the eigenvalue 1 we have:

$$\begin{aligned}
H(L_\tau\sigma^0) &= -\frac{1}{2}\sum_{x\in\tau}\sum_{y\in\tau} J_{xy}\sigma_x^0\sigma_y^0 + \frac{1}{2}\sum_{x\in\tau}\sum_{y\notin\tau} J_{xy}\sigma_x^0\sigma_y^0 \\
&\quad + \frac{1}{2}\sum_{x\notin\tau}\sum_{y\in\tau} J_{xy}\sigma_x^0\sigma_y^0 - \frac{1}{2}\sum_{x\notin\tau}\sum_{y\notin\tau} J_{xy}\sigma_x^0\sigma_y^0 \\
&= -\frac{1}{2}\sum_{x,y=1}^{N} J_{xy}\sigma_x^0\sigma_y^0 + 2\sum_{x\in\tau}\sum_{y\notin\tau} J_{xy}\sigma_x^0\sigma_y^0 \\
&= -\frac{N}{2} + 2\sum_{x\in\tau}\sum_{y=1}^{N} J_{xy}\sigma_x^0\sigma_y^0 - 2\sum_{x\in\tau}\sum_{y\in\tau} J_{xy}\sigma_x^0\sigma_y^0 \\
&= -\frac{N}{2} + 2\sum_{x\in\tau}(\sigma_x^0)^2 - 2\sum_{x\in\tau}\sum_{y\in\tau} J_{xy}\sigma_x^0\sigma_y^0 \\
&= -\frac{N}{2} + 2s - 2\sum_{x\in\tau}\sum_{y\in\tau} J_{xy}\sigma_x^0\sigma_y^0.
\end{aligned} \tag{4.42}$$

Notice that for the Ising mean-field interaction: $J_{xy} = 1/N$, one finds

$$H(L_\tau\sigma^0) = -\frac{N}{2} + 2s - 2\frac{s^2}{N} = -\frac{N}{2}\left(1 - \frac{2s}{N}\right)^2. \tag{4.43}$$

It is now possible to study the distribution of the energy levels on the individual subspaces Ω_s, where $s = 0, 1, \ldots, N$. Let p_s be the probability distribution restricted on Ω_s, i.e.

$$p_s(C) = \binom{N}{s}^{-1} \sum_{\sigma\in C\cap\Omega_s} 1, \tag{4.44}$$

and let E_s denote the expectation wrt p_s. The n-th moment of the energy H on the subspace Ω_s is given by

$$\mathrm{E}_s(H^n) \equiv \int_{\Omega_s} H^n(\sigma)\, dp_s(\sigma) = \binom{N}{s}^{-1} \sum_{\tau\in\Omega_s} H^n(L_\tau\sigma^0), \tag{4.45}$$

so that the n-th moment $\mathrm{E}_N(H^n)$ of the energy on the whole configuration space Σ_N is

$$\mathrm{E}_N(H^n) \equiv \int_{\Sigma_N} H^n(\sigma)\, d\mathrm{P}_N(\sigma) = \frac{1}{2^N} \sum_{s=0}^{N} \binom{N}{s} \mathrm{E}_s(H^n). \tag{4.46}$$

A tedious but straightforward calculation (see Appendix A) yields the following expressions for the first two s-moments:

$$\mathrm{E}_s(H) = -\frac{N}{2}\left(1 - \frac{2s}{N}\right)^2, \tag{4.47}$$

$$\mathrm{Var}_s(H) \equiv \mathrm{E}_s(H^2) - (\mathrm{E}_s(H))^2 = \frac{4s(s-N)(2s^2 - 2sN + N)}{N^2(N-2)} \tag{4.48}$$

and consequently

$$\mathrm{E}_N(H) = -\frac{1}{2}, \qquad \mathrm{Var}_N(H) = \frac{N-1}{2}. \tag{4.49}$$

These results indicate that, at variance with the ferromagnetic case where the energy is constant on each subspace Ω_s, here there is a significant overlap between the distributions (for different s values) of the energy when restricted to Ω_s. In particular, from the expression of σ_s^2 we see that there can be a large number of states having small overlap with the ground state but nevertheless with energy very close to $-N/2$. For example we have $\mathrm{Var}_s(H)|_{s=N/2} \simeq N/2$, indicating that the energy restricted to the subspace $\Omega_{N/2}$ may fluctuate over the whole energy range. This simple phenomenon is intimately related to the existence of metastable states and it will prove crucial in the understanding of the zero temperature dynamics, as discussed below. Fig. (4.3) shows the distributions of the energy restricted to various subspaces Ω_s. Another quantity of interest is the specific magnetization $m(\sigma)$ of an arbitrary state $\sigma \in \Sigma_N$, given by:

$$m(\sigma) = \frac{1}{N} \sum_{x=1}^{N} \sigma_x, \tag{4.50}$$

In particular, given $\tau = (x_1, \ldots, x_s)$, we have

$$m(L_\tau \sigma^0) \equiv m(\tau) = m^0 - \frac{2}{N} \sum_{x \in \tau} \left(\frac{x}{p}\right). \tag{4.51}$$

Clearly,

$$\frac{1}{\binom{N}{s}} \sum_{\tau \in \Omega_s} \left(\sum_{x \in \tau} \left(\frac{x}{p}\right) \right) = \frac{1}{\binom{N}{s}} \sum_{x=1}^{N} \binom{n-1}{s-1} \cdot \left(\frac{x}{p}\right) = s \cdot m^0, \tag{4.52}$$

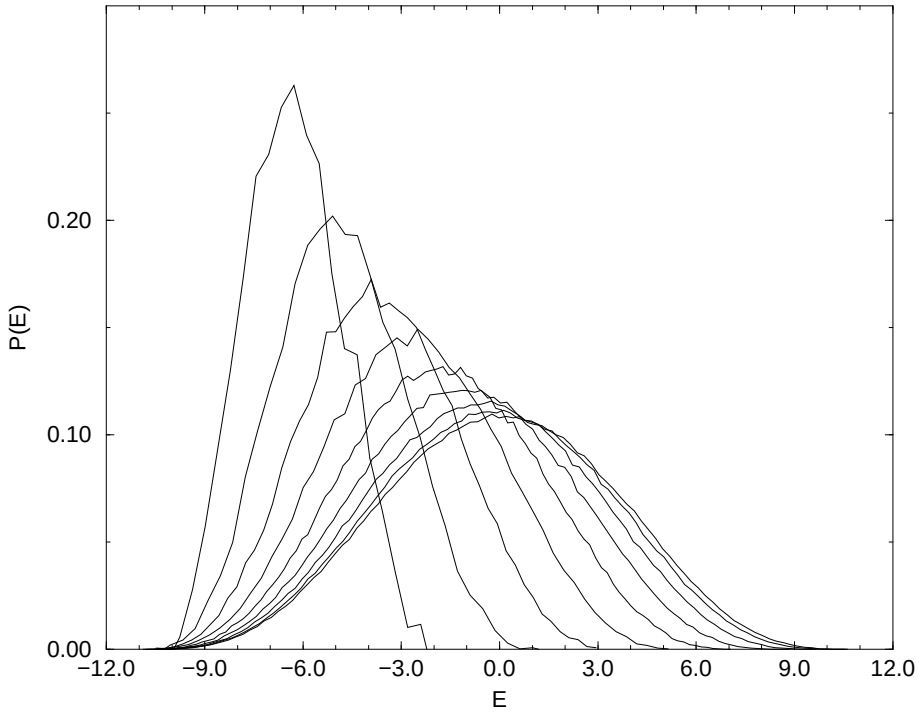

Figure 4.3: Distributions of the energy over the subspaces Ω_s. The size of the system is $N = 23$ and $s = 3, 4, \ldots, 11$ from left to right. The cases $s = 1$ and $s = 2$ behave in a similar way, but they are not plotted because of the small number of sample points for this lattice size N.

i.e.

$$E_s(m) \;=\; \frac{1}{\left(\begin{array}{c} N \\ s \end{array}\right)} \sum_{\tau \in \Omega_s} m(\tau) \;=\; m^0 \left(1 - 2\frac{s}{N}\right). \tag{4.53}$$

Moreover, we show in the Appendix B that

$$\mathrm{Var}_s(m) = \frac{4s(N-s)}{N^3(N-1)} + \frac{4s(s-1)}{N^3(N-1)} \cdot \sum_{x=1}^{p} \left(\frac{x}{p}\right) d_N(x), \tag{4.54}$$

where $d_N(x)$ is the integer valued function giving the number of elements $u \in \{1, \ldots, N\}$ such that $u^{-1}x \in \{1, \ldots, N\}$ (where u^{-1} denotes the inverse mod p of u). As will be discussed in Appendix B, $d_N(x)$ takes values around $p/4$ with rather

small fluctuations. Since $\sum_{x=1}^{p} \left(\frac{x}{p}\right) = 0$, the last term in (4.54) can be considered as a small correction to the constant value $4s(N-s)/N^3(N-1)$.

4.6 Zero temperature dynamics and metastable states.

We first introduce the following discrete 1−flip dynamics, given by:

$$\sigma(t+1) = \begin{cases} L_{\omega(t)}\,\sigma(t), & \text{if } H(L_\omega \sigma) < H(\sigma), \\ \sigma(t), & \text{otherwise,} \end{cases}$$

where, for each t, $\omega(t)$ is chosen randomly in $\{1,\ldots,N\}$ with uniform distribution. Choosing an initial condition $\sigma(0)$ at random with respect to P_N, one obtains a random orbit $\{\sigma(0),\sigma(1),\ldots,\sigma(\ell)\}$ for any realization $\{\omega(t)\}_{1\le t\le \ell}$ of length ℓ. As a consequence of the previous analysis, we might encounter the following two situations which effect the convergence of the dynamics to the ground state.

- On one hand, it may happen that starting from $\sigma(0)$ one reaches after t iterations a state $\sigma(t) \in \Omega_s$, of the form $\sigma(t) = L_\tau \sigma^0$ for some $\tau = (x_1,\ldots,x_s)$, such that $H(L_\tau\sigma^0) < H(L_\omega L_\tau \sigma^0)$ for any $\omega \in \{x_1,\ldots,x_s\}$.
- On the other hand one can reach $\sigma(t) \in \Omega_s$ such that for some $\omega \in \{1,\ldots,N\}$, $L_\omega\sigma \in \Omega_{s+1}$ and $H(L_\omega\sigma(t)) < H(\sigma(t))$. Namely, in order to decrease the energy, one must decrease the overlap with the ground state.

Due to the above observations, the overlap function $q(\sigma(t))$ between $\sigma(t)$ and the ground state is not in general monotonically non-decreasing along a given random orbit (this at variance with the Ising mean field model). In particular there might be metastable states [89]. Given $\omega \in \{1,\ldots,N\}$, we shall say that a configuration $\sigma \in \Sigma_N$ is ω-*stable* if

$$H(L_\omega\sigma) > H(\sigma). \tag{4.55}$$

We say that σ is 1-*flip stable* if it is ω-stable $\forall\omega \in \{1,\ldots,N\}$. Analougsly a configuration σ is said to be k-*flip stable* if its energy cannot be decreased by flipping any subset of k (or less than k) spins. It has been recently recognized [66] that generally for finite dimensional systems the zero temperature *metastable* states (i.e. solutions of TAP equations) coincide with ∞-*flip stable* configurations. However in mean-field models with infinite connectivity, like SK, due to the vanishing of

couplings in the thermodynamical limit, there is a degeneracy between *k-flip stable* for every finite k. Namely, in the limit $N \to \infty$, any k-flip stable configuration is also $k+1$-flip stable. In the present case the same argument of ref. [66] can be applied (since the couplings $J_{ij} = \mathcal{O}(1/\sqrt{N})$) so that *metastable* states can be studied just by considering 1-*flip stable* states. We denote here by $n(N)$ the total number of such metastable states as a function of N.

The main goal of this Chapter is to give an estimate of the number of metastable states for any given N. To this end we first performed some numerical investigations. For $N \leq 30$ we performed an exact enumeration of all configurations, whereas for larger N we run the zero temperature dynamics described above ("deep quench") for a number of realizations $\{\omega(t)\}$ as large as 10^8 for bigger sizes, keeping track of the metastable states. As shown in Fig. (4.4), the growth of these states is exponential for generic values of the N. The best numerical fit yields

$$n(N) \simeq C \cdot e^{0.28N}. \tag{4.56}$$

We remark that the same result has been obtained for the Random Orthogonal Model in Section (4.2) (see also [85]). The number of metastable states appears as a self-averaging property, that is shared by generic realization of a random orthogonal matrix.

4.7 Analytical estimate of the number of metastable states

We now proceed to give a partial justification of the numerical result of the previous Section by means of probabilistic arguments. First of all, we observe that from (4.42) one readily obtains that

$$H(L_\omega \sigma) \;=\; H(\sigma) \;+\; 2 \sum_{x \neq \omega} J_{x\omega}\, \sigma_x\, \sigma_\omega, \tag{4.57}$$

so that σ is ω-stable if and only if

$$(J\sigma)_\omega\, \sigma_\omega > J_{\omega\omega}. \tag{4.58}$$

Summing over ω and using (4.25) we see that if σ is 1-flip stable then

$$< J\sigma, \sigma > \;>>\; 1. \tag{4.59}$$

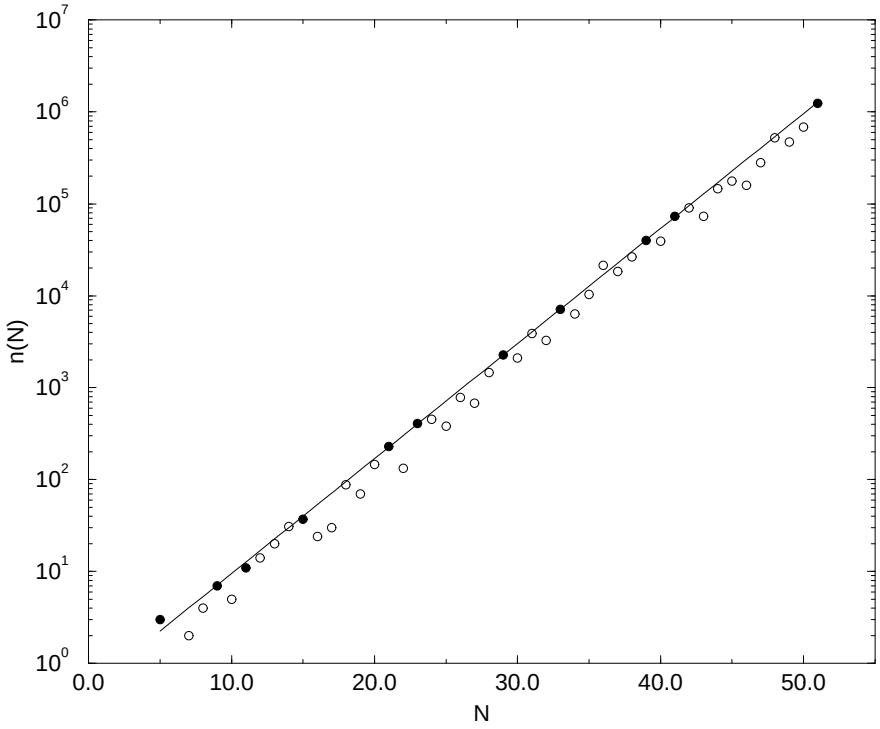

Figure 4.4: The number of metastable states $n(N)$ for N. The line represents the best fit $n(N) \approx e^{\lambda N}$ with $\lambda \approx 0.28$ for values of N such that $p = 2N + 1$ is a prime of the form $4m + 3$ (filled points). Other points are for generic integer N.

Recalling the expression (4.23) of the Hamiltonian we see that a necessary condition for $\sigma \in \Sigma_N$ to be 1-flip stable is that

$$H(\sigma) < \mathrm{E}_N(H) = -\frac{1}{2}\cdot \tag{4.60}$$

Let now $\tau = (x_1, \ldots, x_s)$ and $\omega \in \{1, \ldots, N\}$ be given. Using (4.57) and $J\sigma^0 = \sigma^0$, it is easy to see that if $\omega \notin \tau$ (i.e. $L_\omega \sigma \in \Omega_{s+1}$)

$$H(L_\omega \sigma) \;=\; H(\sigma) \;+\; 2\left(1 - J_{\omega\omega} - 2\sum_{x\in\tau} J_{x\omega}\,\sigma_x^0\,\sigma_\omega^0\right),$$

whereas, if $\omega \in \tau$ (i.e. $L_\omega \sigma \in \Omega_{s-1}$), we have

$$H(L_\omega \sigma) \;=\; H(\sigma) \;-\; 2\left(1 + J_{\omega\omega} - 2\sum_{x\in\tau} J_{x\omega}\,\sigma_x^0\,\sigma_\omega^0\right).$$

If we define

$$h(\tau,\omega) \;=\sum_{x\in\tau} J_{x\omega}\,\sigma_x^0\sigma_\omega^0, \tag{4.61}$$

we then see that a configuration $\sigma = L_\tau \sigma^0$ is ω-stable if and only if

$$\begin{cases} h(\tau,\omega) \;<\; \frac{1}{2}(1 - J_{\omega\omega}), & \text{if } \omega \notin \tau, \\ \\ h(\tau,\omega) \;>\; \frac{1}{2}(1 + J_{\omega\omega}), & \text{if } \omega \in \tau. \end{cases} \tag{4.62}$$

We now dwell upon the problem of characterizing the behaviour of the function $h(\tau,\omega)$ so as the condition (4.62) can be effectively used to estimate the number of metastable states. Let us rewrite $h(\tau,\omega)$ in the form

$$h(\tau,\omega) = \frac{2}{\sqrt{p}} \sum_{x\in\tau} \xi_x(\omega), \tag{4.63}$$

where

$$\xi_x(\omega) := \left(\frac{\omega x}{p}\right)\,\sin\left[\frac{2\pi\omega x}{p}\right]. \tag{4.64}$$

Now, having fixed τ and $x \in \tau$, we can view the function $\xi_x(\omega)$ defined in (4.64) as a random variable uniformly distributed on $\{1,\ldots,N\}$ and taking values in $[-1,1]$. Its mean and variance are easily computed:

$$E(\xi) = \frac{1}{N}\sum_{\omega=1}^{N}\left(\frac{\omega x}{p}\right)\,\sin\left[\frac{2\pi\omega x}{p}\right] = \frac{\sqrt{p}}{2N}, \tag{4.65}$$

and, using (4.25),

$$\mathrm{Var}(\xi) = \frac{1}{N}\sum_{\omega=1}^{N}\sin^2\left[\frac{2\pi\omega x}{p}\right] - \mu_x^2 = \frac{p}{4N}\left(1 - \frac{1}{N}\right). \tag{4.66}$$

Here we want to study the behaviour of the sum $\eta(\tau,\omega) := \sum_{x\in\tau}\xi_x(\omega)$. We remark that this sum, and thus $h(\tau,\omega) = 2\eta(\tau,\omega)/\sqrt{p}$, has to be regarded as a r.v. defined on the product of two probability spaces: for each fixed τ, it is the sum of the identically distributed random variables $\xi_x(\omega)$ on the space $\{1,\ldots,N\}$ with uniform distribution (this comes from the very definition of the zero temperature dynamics);

on the other hand, for each fixed ω, it can be regarded as a r.v. on Ω_s viewed as a probability space endowed with the distribution p_s. Its mean is given by (recall that the symbol E_s denotes the expectation wrt p_s):

$$\begin{aligned} \mathrm{E}_s(\eta) &= \binom{N}{s}^{-1} \sum_{\tau=(x_1,\dots,x_s)} \sum_{x\in\tau} \xi_x(\omega) = \binom{N}{s}^{-1} \sum_{x=1}^{N} \binom{N-1}{s-1} \xi_x(\omega) \quad (4.67) \\ &= \frac{s}{N} \sum_{x=1}^{N} \xi_x(\omega) = \frac{s\sqrt{p}}{2N}. \end{aligned}$$

which does not depend on ω and equals s times μ_x. Along the same lines one shows that

$$\mathrm{Var}_s(\eta) = \frac{sp}{4N}\left(1 - \frac{s}{N}\right). \tag{4.68}$$

Notice that unlike the means, here we have $\mathrm{Var}_s(\eta) \neq s \cdot \mathrm{Var}(\xi)$. This discrepancy comes from the fact that, for any fixed ω, the sequence $\xi_{x_1}, \xi_{x_2}, \dots, \xi_{x_s}$ is a sequence of distinct (and ordered) elements so that by no means we can view η as a sum of independent and identically distributed objects. Nonetheless, also supported by strong numerical evidence (see Fig. 4.5), we claim that a version of the central limit theorem is applicable so that when $N \to \infty$, $s \to \infty$ with $s/N \to \lambda$, we have

$$p_s\left(\alpha < \frac{\eta - \mathrm{E}_s\eta}{\sqrt{\mathrm{Var}_s\eta}} < \beta\right) \to \frac{1}{\sqrt{2\pi}} \int_\alpha^\beta e^{-y^2/2}\, dy. \tag{4.69}$$

Assuming the validity of (4.69), performing the change of variables $y = (x-\lambda)/\sqrt{\gamma}$, with $\gamma = \lambda(1-\lambda)$, and setting $a = \lambda + \alpha\sqrt{\gamma}$, $b = \lambda + \beta\sqrt{\gamma}$, we thus obtain an asymptotic gaussian distribution for $h(\,\cdot\,,\omega)$:

$$p_s\left(a < h(\tau,\omega) < b\right) \to \frac{1}{\sqrt{2\pi\gamma}} \int_a^b e^{-(x-\lambda)^2/2\gamma}\, dx. \tag{4.70}$$

Note that the r.h.s. does not depend on ω. One can actually say more: for any $\tilde\omega, \omega \in \{1,\dots,N\}$ we have $h(\tilde\omega^{-1}\tau, \tilde\omega\omega) = h(\tau,\omega)$. Therefore the set of values of $h(\,\cdot\,,\omega)$ on Ω_s does not depend on the choice of ω, i.e. $\{h(\tau,\omega)\}_{\tau\in\Omega_s} = \{h(\tau',\omega')\}_{\tau'\in\Omega_s}$, for all ω, ω'.

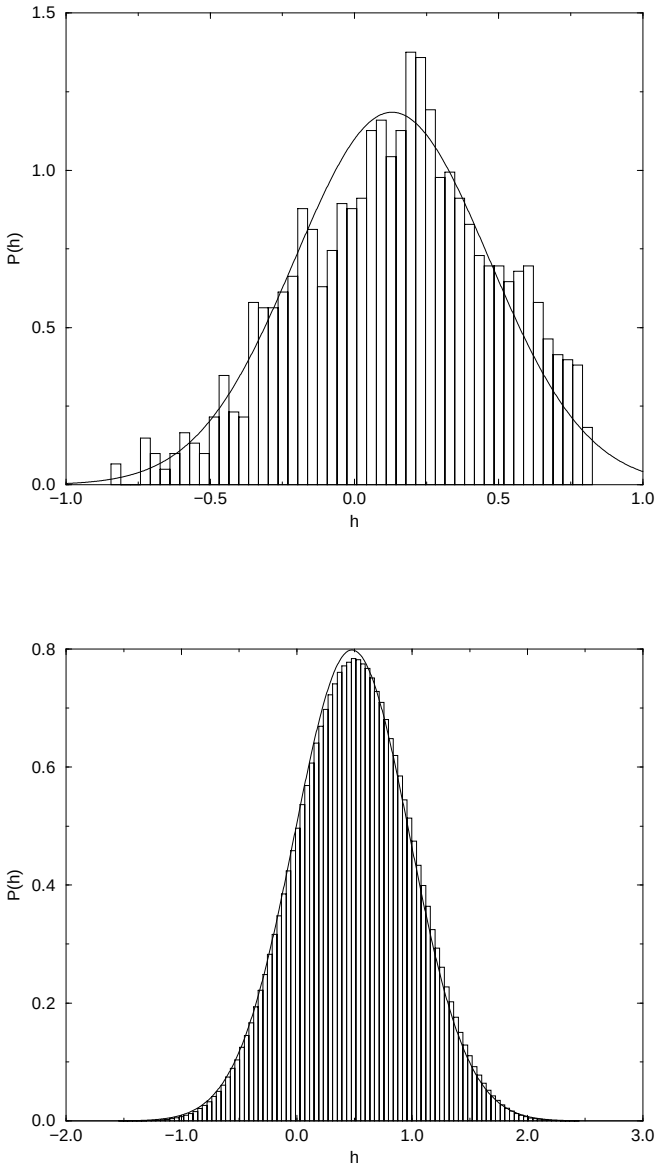

Figure 4.5: Distribution of the function $h(\tau, \omega)$ for a fixed $\omega \in \{1, \ldots, N\}$ and τ varying in Ω_s. Here $N = 23$ and $s = 3$ (left) and $s = 11$ (right). The solid line is the gaussian distribution in the r.h.s. of (4.70).

Having fixed an order for the lattice points $(\omega_1, \ldots, \omega_N)$, $\omega_j \neq \omega_k$, we now consider the following quantities:

$$\pi_{s,N}(\omega_k) = p_s\left(\{\sigma \in \Omega_s \,:\, H(L_{\omega_k}\sigma) \,>\, H(\sigma)\}\right), \tag{4.71}$$

the p_s-probability that a randomly chosen state $\sigma \in \Omega_s$ is ω_k-stable,

$$\begin{aligned}\pi_{s,N}(\omega_{k+1}|\,\omega_1, \ldots, \omega_k) \;\;=\;\; & p_s\left(\{\sigma \in \Omega_s \,:\, H(L_{\omega_{k+1}}\sigma) \,>\, H(\sigma)\right. \\ & \left.|\, H(L_{\omega_j}\sigma) \,>\, H(\sigma),\ \omega_j = \omega_1, \ldots \omega_k\right\}\Big), \end{aligned} \tag{4.72}$$

the conditional p_s-probability that a randomly chosen state $\sigma \in \Omega_s$ is ω_{k+1}-stable given that it is ω_j-stable for $j = 1, \ldots, k$, and

$$\pi_{s,N} = p_s\left(\{\sigma \in \Omega_s \,:\, H(L_\omega\sigma) \,>\, H(\sigma),\ \omega = \omega_1, \ldots, \omega_N\}\right), \tag{4.73}$$

the p_s-probability that a randomly chosen state $\sigma \in \Omega_s$ is 1-flip stable (i.e. stable for all possible flipping). Notice that by condition (4.62) the last quantity can be written as

$$\pi_{s,N} = \binom{N}{s}^{-1} \sum_{\substack{(x_1,\ldots,x_s)=\tau \\ (y_1,\ldots,y_{N-s})=\tau^c}} \prod_{i=1}^{s} \theta\left(h(\tau, x_i) > \frac{1 + J_{x_i x_i}}{2}\right) \prod_{j=1}^{N-s} \theta\left(h(\tau, y_j) < \frac{1 - J_{y_i y_i}}{2}\right). \tag{4.74}$$

The three quantities introduced above are related by the following identity:

$$\pi_{s,N} \;=\; \pi_s(\omega_1) \cdot \pi_s(\omega_2|\omega_1) \cdot \pi_s(\omega_3|\omega_1, \omega_2) \cdots \pi_s(\omega_N|\omega_1, \ldots, \omega_{N-1}) \tag{4.75}$$

and the total number of 1-flip stable states in Σ_N is, by definition,

$$n(N) = \sum_{s=0}^{N} \binom{N}{s} \pi_{s,N}. \tag{4.76}$$

We shall study the quantity $n(N)$ in the thermodynamic limit: $N \to \infty$, $s \to \infty$, with $s/N \to \lambda$ and $0 < \lambda < 1$. In this regime we write $\pi_{s,N} \equiv \pi_\lambda$ and apply Stirling's formula to obtain

$$\binom{N}{s} \sim \frac{e^{NF(\lambda)}}{\sqrt{2\pi N\lambda(1-\lambda)}}, \quad \text{with} \quad F(\lambda) = -\lambda \log \lambda - (1-\lambda)\log(1-\lambda). \tag{4.77}$$

Note that $F(\lambda)$ is concave and symmetric around $\lambda = 1/2$, with $F(1/2) = \log 2$. In this way we get for N large and $s \simeq \lambda N$ with λ ranging in the unit interval,

$$n(N) \simeq \int_0^1 \sqrt{\frac{N}{2\pi\lambda(1-\lambda)}}\, \exp\left[N\left(F(\lambda) + \frac{\log \pi_\lambda}{N}\right)\right] d\lambda. \tag{4.78}$$

It thus remains to estimate the probability π_λ. Let us consider first the unconditioned probability (4.71). According to (4.62) and the total probability formula we have:

$$\begin{aligned} \pi_{s,N}(\omega_k) &= \frac{s}{N}\, p_s\left(h(\tau,\omega_k) > \frac{1+J_{\omega_k\omega_k}}{2} \;\middle|\; \tau \ni \omega_k\right) \\ &+ \left(1-\frac{s}{N}\right) p_s\left(h(\tau,\omega_k) < \frac{1-J_{\omega_k\omega_k}}{2} \;\middle|\; \tau \not\ni \omega_k\right). \end{aligned} \tag{4.79}$$

Here s/N and $1 - s/N$ are the probabilities that $\tau \ni \omega_k$ and $\tau \not\ni \omega_k$, respectively. We can easily compute the conditional expectations

$$\mathrm{E}\left(h|\tau \ni \omega_k\right) = \binom{N-1}{s-1}^{-1} \frac{2}{\sqrt{p}} \sum_{\tau \ni \omega_k} \sum_{x \in \tau} \xi_x(\omega_k) = \frac{s-1}{N-1} - \left(\frac{s-N}{N-1}\right) J_{\omega_k\omega_k}\,, \tag{4.80}$$

and

$$\mathrm{E}\left(h|\tau \not\ni \omega_k\right) = \binom{N-1}{s}^{-1} \frac{2}{\sqrt{p}} \sum_{\tau \not\ni \omega_k} \sum_{x \in \tau} \xi_x(\omega_k) = \frac{s}{N-1}\left(1 - J_{\omega_k\omega_k}\right)\,. \tag{4.81}$$

In a similar way one can compute the variances $\gamma_+(\omega_k)$ and $\gamma_-(\omega_k)$ conditioned to the events $\{\tau \ni \omega_k\}$ and $\{\tau \not\ni \omega_k\}$. For N large and $s \simeq \lambda N$, retaining only terms $\mathcal{O}(1)$, one gets

$$\mathrm{E}\left(h|\tau \ni \omega_k\right) \simeq \mathrm{E}\left(h|\tau \not\ni \omega_k\right) \simeq \lambda, \qquad \gamma_-(\omega_k) \simeq \gamma_+(\omega_k) \simeq \gamma = \lambda(1-\lambda). \tag{4.82}$$

Moreover in the thermodynamic limit specified above we write $\pi_{s,N}(\omega_k) \equiv \pi_\lambda(\omega_k)$ and argue from (4.70) the following approximate expression for $\pi_\lambda(\omega_k)$:

$$\begin{aligned} \pi_\lambda(\omega_k) &\simeq \frac{\lambda}{\sqrt{2\pi\gamma}} \int_{1/2}^{\infty} e^{-(x-\lambda)^2/2\gamma}\, dx + \frac{(1-\lambda)}{\sqrt{2\pi\gamma}} \int_{-\infty}^{1/2} e^{-(x-\lambda)^2/2\gamma}\, dx \\ &= \frac{1}{2} + \left(\frac{1}{2} - \lambda\right) \mathrm{erf}\left(\frac{\frac{1}{2}-\lambda}{\sqrt{2\gamma}}\right) \end{aligned} \tag{4.83}$$

where we have denoted the error function by

$$\mathrm{erf}(z) = \frac{2}{\sqrt{\pi}} \int_0^z e^{-x^2}\, dx. \tag{4.84}$$

It is not difficult to check that the r.h.s. of (4.83) is convex and symmetric around $\lambda = 1/2$, where it reaches its minimum value equal to $1/2$.

Let us now come to $\pi_{s,N}$. In principle this quantity is to be computed by specifying the whole set of constraints embodied in (4.74) or, which is the same, by computing the conditional probabilities appearing in Eq.(4.75). However, this appears to be a difficult task. A first approach which drastically simplifies this task is to forget about the constraints implied by (4.74) and assume that (in the thermodynamic limit) the various ω-stability conditions become mutually independent, that is $\pi_\lambda(\omega_{k+1}|\omega_1, \ldots, \omega_k) = \pi_\lambda(\omega_{k+1})$, for all $k = 1, \ldots, N-1$, so that

$$\pi_\lambda = \prod_{k=1}^{N} \pi_\lambda(\omega_k). \tag{4.85}$$

Recalling Eq. (4.78) and (4.83), one is led to the following expression for $n(N)$:

$$n(N) \simeq \int_0^1 \sqrt{\frac{N}{2\pi\lambda(1-\lambda)}}\, \exp\Big(NG_1(\lambda)\Big)\, d\lambda, \tag{4.86}$$

where

$$G_1(\lambda) = F(\lambda) + \log\frac{1}{2} + \left(\frac{1}{2} - \lambda\right) \mathrm{erf}\left(\frac{\frac{1}{2}-\lambda}{\sqrt{2\gamma}}\right) \tag{4.87}$$

We show the shape of the the function $G_1(\lambda)$ in Fig. (4.6).

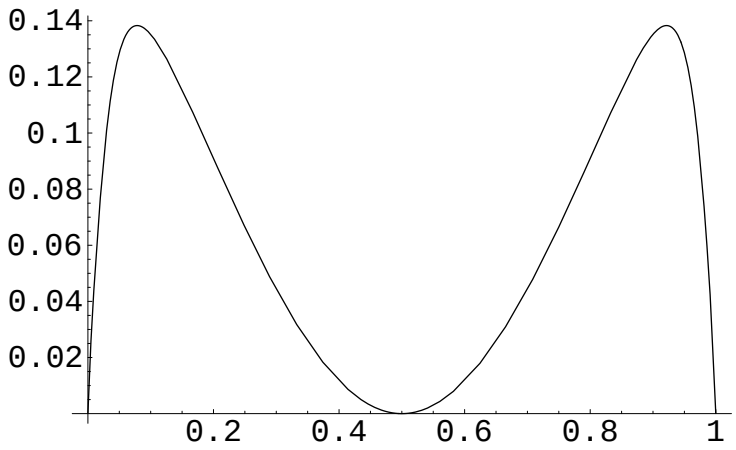

Figure 4.6: The function $G_1(\lambda)$ of equation (4.87) for $\lambda \in [0, 1]$.

Evaluating the integral (4.86) with the saddle-point method one gets

$$n(N) \simeq C\, e^{0.14N}. \tag{4.88}$$

Notice that the exponent is the half of what is observed numerically (cfr (4.56)). In the following Section we shall argue that (4.88) is indeed an estimate from below of the actual number of metastable states.

4.8 Numerical checks of the analytical estimate

The above discussion has been able to reproduce the exponential growth of the number of metastable states with the size of the system. To understand the discrepancy between the estimated exponent and the one measured numerically one should note that the nature of the interaction makes the conditional probabilities play a major role in the asymptotic of the number of metastable states. To be more precise, our approximation which assumes mutually independent individual ω-stability events, i.e. $\pi_\lambda(\omega_{k+1}|\omega_1,\ldots,\omega_k) \simeq \pi_\lambda(\omega_{k+1})$, is actually reasonable only for small value of k (this can be checked, for example, calculating the correlation functions). As numerical results shows, for large values of k the specific form of the interactions make these events strongly dependent. In Fig. (4.7) we show the function $P(k)$ providing the average of $\pi_\lambda(\omega_{k+1}|\omega_1,\ldots,\omega_k)$ over a large sample of different permutations $(\omega_1,\ldots,\omega_N)$ of the lattice points. The conditional probabilities $P(k)$ grow monotonically, almost linearly, from the initial (unconditioned) value up to a number close to 1. In other words, requiring that a large number k of spins produce an ω-stable state increases substantially the probability of doing the same for the remaining spins.

Another way of understanding the constructive effect of the correlations is the following. Consider again the function $h(\tau,\omega)$. Having fixed ω_{k+1}, we have already noticed that for s and N large enough the values of $h(\tau,\omega_{k+1})$ with $\tau \in \Omega_s$ are approximately distributed according to a gaussian probability density with mean $\lambda = s/N$ and variance $\gamma = \lambda(1-\lambda)$, regardless of the particular value of ω_{k+1}. Thus, in particular, the same distribution are expected to arise if one considers the values of $h(\tau,\omega_{k+1})$ constrained to the subsets of configurations such that $\omega_{k+1} \in \tau$, or $\omega_{k+1} \notin \tau$. On the other hand, if one picks $\omega_1,\omega_2,\ldots,\omega_k$ with $\omega_j \neq \omega_{k+1}$,

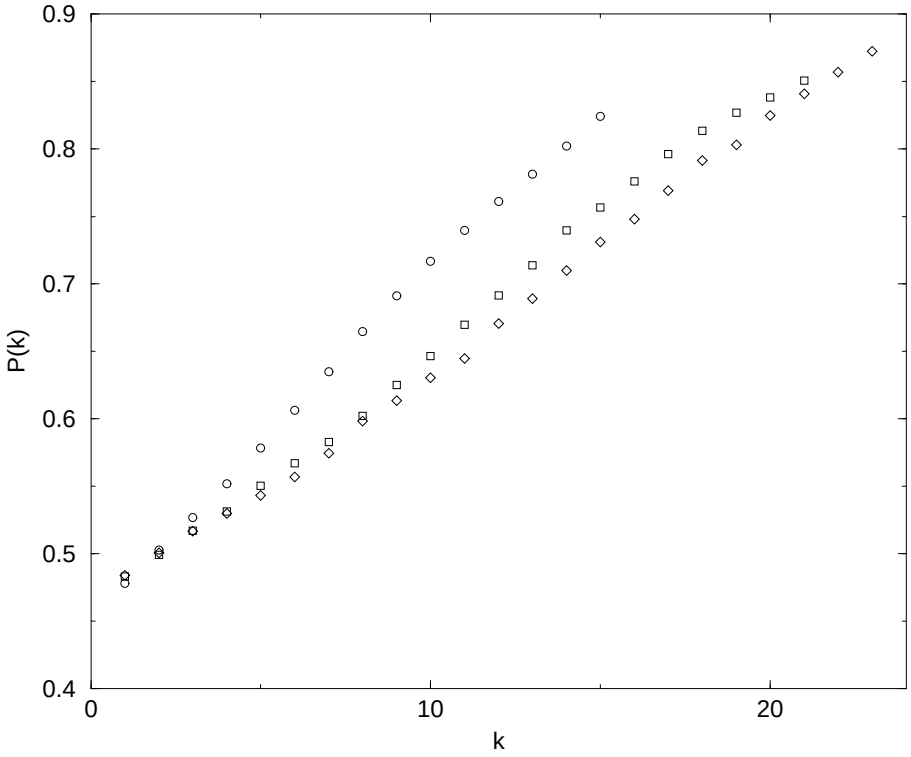

Figure 4.7: $P(k)$ versus k, for $N = 15(\text{circle}), 21(\text{square}), 23(\text{diamonds})$ and $s = [N/2]$. The conditional probabilities have been averaged over a sample of 10000 choices of $(\omega_1, \ldots, \omega_N)$.

$j = 1, \ldots, k$, and computes numerically the two conditional distributions of the values of $h(\tau, \omega_{k+1})$ given ω_1-stability, ... , ω_k-stability (again with the constraints $\omega_{k+1} \in \tau$ or $\omega_{k+1} \notin \tau$), one finds that their means move to opposite directions, thus increasing the probability of ω_{k+1}-stability (see (4.79)). This is shown in Fig. (4.8), where a system of size $N = 21$ and $s = 10$ is considered. The two central distributions correspond to the unconditioned cases, namely the values of $h(\tau, \omega)$ for $\tau \in \Omega_{10}$ with the only constraints $\omega \in \tau$ or $\omega \notin \tau$, respectively. Considering instead the values taken by h on the states τ which, besides the constraints specified above, are stable with respect the first 10 spins, one finds two distributions whose mean values have moved towards opposite directions. An averaged over ω has been performed.

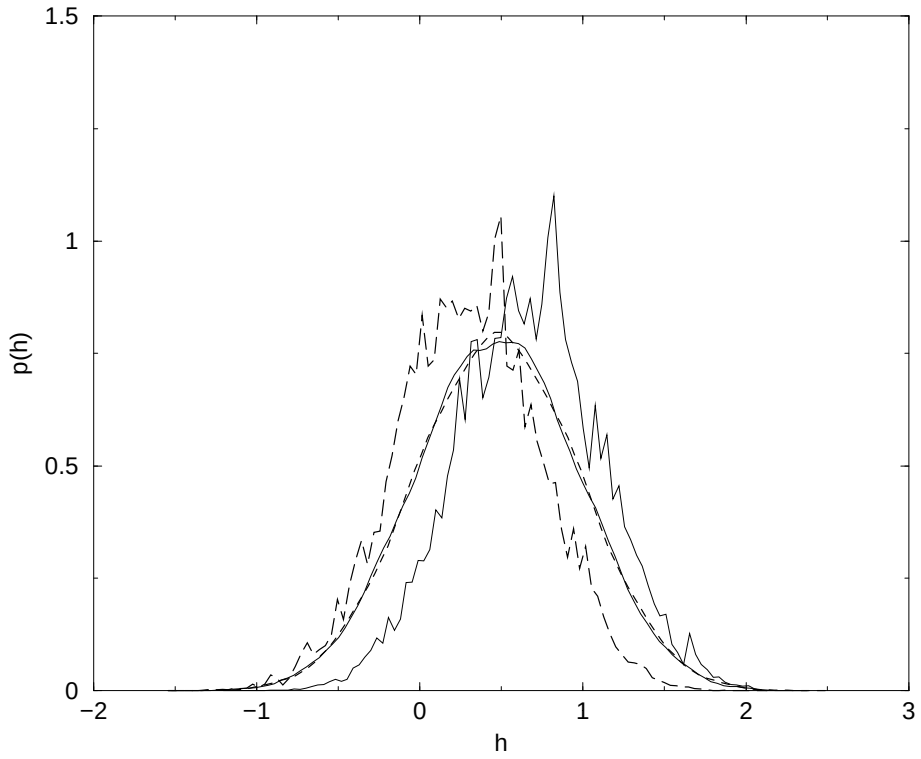

Figure 4.8: Graphs of the four distributions of the values of h described in the text.

4.9 Conclusions

We have investigated the statistical properties of energy levels and metastables states for a class of deterministic models, the most representative being the *sine* model [69], which have attracted much attention in recent years for their glassy behaviour despite the non-random nature of the interaction. We have pushed further on the analogy with glassy systems, proving a number of properties typical of disordered spin models. In particular, using number theoretic methods, we have described the energy (equivalently, free energy at $T = 0$) landscape as a function of configurations with a fixed overlap with the ground state. The analysis revealed the existence of states very different from the ground state but with energy arbitrarily close to it: this corresponds to the "chaoticity" property of spin-glasses systems, well established in long range models. More importantly, some of these states can be local energy minima (equivalently, 1-flip stable at $T = 0$). They are expected to have

a significant weight on the partition function in the low-temperature region, giving rise to the non-equilibrium behaviour observed in annealing Montecarlo experiments. We have been able to estimate the approximate number of these energy minima. The analytic computations, combined with the numerical findings, strongly support the conclusion that the bound (4.88) estimates from below the number of metastable states $n(N)$, proving their exponential increase with the size of the system.

A number of basic questions about metastability arises now in a natural way, such as computing the energy density distributions of metastables states, studying energy barriers among them and their attraction basins. These problems are currently under investigation using the approach developed in this work and will be addressed elsewhere.

Chapter 5

Chiral and spin order of the random XY model on a tube lattice

5.1 Introduction

It is well known that in isotropic vector spin-glasses, such as XY and Heisenberg models with quenched disorder, there can be two different types of phase transitions: the usual spin-glass ordering, associated with spin variables (S), and chiral-glass ordering, due to the so-called chiralities variables (C). In fact the system possesses two different symmetries, the Hamiltonian being invariant under global rotation of the spins and reflection about some arbitrary axis. Since the pioneering analysis of Villain [92] the possibility of a competition between spin and chiral ordering has been investigated both numerically and analytically. A first question is the lower critical dimensions (LCD) for the two transitions, in particular if they are the same or not. All attempts to prove rigorous results have failed [93, 94, 95]. Existing numerical simulations [96, 97, 98] agree that chiral order occur in three dimensions (so that $d_c = 3$), while much more controversial is the situation about spin ordering. Contrary to what has been the accepted belief for long time [96, 97], that is $d_s = 4$, recent numerical works considering larger sizes than previous ones [98], or new definition of defect energies in such a way to reduce the finite size corrections [99], have suggested that the LCD of XY spin glass may be close to three. In summary, the Ising behavior seen in experiments on many spin-glass

materials that are supposed to be described by the disordered $3D$ XY model is to be regarded as a still open problem: one possible scenario is that there exists a chiral-glass phase in the absence of spin-glass ordering, the another one is that the spin-glass critical temperature is actually different from zero. To gain some hints about low-temperature properties of the realistic three dimensional case, one and two dimensional models have been considered as well. It is well-established that a phase transition, either of spin or chiral type, occurs only a temperature $T = 0$. However there is a strong contradiction between analytical and numerical works. The former analyzed a one dimensional ladder lattice [100], a tube lattice [101] and a two dimensional system with special choice of disorder [102]. The outcome of these studies is a very plausible conjecture that chiral and spin glass correlation length exponents are the same below the LCD. On the other hand, basically all numerical experiments [96, 103, 104, 105, 98] have found two different exponents in two dimensions, $\nu_{SG} \sim 1.3$ and $\nu_{CG} \sim 2.6$. Only a very recent $T = 0$ defect energy scaling study, in which fluctuating twist boundary conditions are considered (see later), obtained an equality between the two exponents [106]. It is also worth mentioning that in four dimension, well above the LCD, a simultaneous ordering of spin and chirality has been revealed, with common critical temperature and critical exponents [107]. In the conflictual picture described above, it is desiderable to have a rigorous test of numerical simulations on some known analytic results, to understand their validity and limitations. This has been our principal motivation in deciding to study the XY random model on the tube lattice, for which it is available the theoretical analysis performed by Thill, Ney-Nifle and Hilhorst [101]. Also, since the tube is a $2 \times N$ lattice (it can be seen as a two dimensional lattice of which one dimension has been compactified), it has been possible to study fairly long chains and to study the effects of different twist boundary conditions (fixed or fluctuating).

5.2 The XY spin-glass model

The Hamiltonian of the XY spin-glass model with a bimodal distribution of couplings is

$$H = \sum_{\langle ij \rangle} J_{ij} S_i S_j \tag{5.1}$$

where the exchange interactions J_{ij} have values $\pm J$ and S_i is a unimodular two components vector on the site i of a given lattice of dimension d. We consider short-range interaction so that the sum is restricted to all pairs of nearest-neighbors sites. An equivalent formulation is

$$H = \sum_{\langle ij \rangle} J \cos(\theta_i - \theta_j - \pi_{ij}) \tag{5.2}$$

where $J > 0$ and θ_i is the phase of the spin, i.e. his angle with a fix direction. The random bond variables π_{ij} are responsible for frustration and take the values $\pi_{ij} = 0, \pi$ with equal probability, corresponding respectively to $+J$ ferro-magnetic and $-J$ anti-ferromagnetic couplings between neighbors spins. On each elementary plaquette of the lattice a frustration variable is easily defined:

$$f_r = \frac{1}{2\pi} \sum_r \pi_{ij} \tag{5.3}$$

where the sum is over the bonds in a clockwise direction. It is integer for unfrustrated plaquettes and half-integer for frustrated ones. Globally frustration variables satisfy, by construction, the condition

$$\sum_r f_r = 0 \tag{5.4}$$

Analougsly one can define the local chiral variable, that represents the sense of handedness of the spins at the corners of each plaquette:

$$c_r = 2^{-5/2} \sum_r (\delta(0, \pi_{ij}) - \delta(\pi, \pi_{ij})) \sin(\theta_i - \theta_j) \tag{5.5}$$

where again the sum runs over a directed contour of clockwise orientation and $\delta(m, n)$ is the Kronecker delta function ($\delta(m, n) = 1$ if $m = n$ and $\delta(m, n) = 0$ otherwise). In ground state configurations, chiralities takes value $c_r = 0$ on isolated unfrustrated plaquettes and $c_r = \pm 1/2$ on isolated frustrated ones. They are invariant under any global rotation of the spins, whereas they change sign under any global reflection about an arbitrary axis. Having defined the dynamical variables, spins and chiralities, one can introduce two correlation lengths ξ_s and ξ_c associated with them to measure the decay of correlation functions

$$\overline{\langle S_i \cdot S_{i+R} \rangle^2} \sim \exp(-|R|/\xi_s) \tag{5.6}$$

and

$$\overline{\langle c_i \cdot c_{i+R} \rangle^2} \sim \exp(-|R|/\xi_c) \tag{5.7}$$

Here, as usual, $\langle \cdots \rangle$ and $\overline{\cdots}$ denote a thermal and a disorder average, respectively. The appearance of a phase transition in the low temperature phase is signalled by a divergence of the correlation length that is expected to be of a power law type

$$\xi_s(T) \sim (T - T_s)^{-\nu_s} \qquad (T \to T_s) \tag{5.8}$$

and

$$\xi_c(T) \sim (T - T_c)^{-\nu_c} \qquad (T \to T_c) \tag{5.9}$$

Below the LCD of the system, one knows that $T_c = T_s = 0$, and ν_s, ν_c measure the eventually different ordering tendency.

5.3 Domain Wall Renormalization Group

A possible way of extracting the correlation lengths exponents is through a domain wall renormalization group analysis (DWRG). The general strategy of this approach is to study the effects of changing the boundary conditions (BC) on the ground state of a system of linear dimension L. Practically one has to calculate the ground state energy differences $\Delta E(L)$ passing from some reference boundary conditions (usually periodic) to different boundary conditions that introduce a defect or domain wall in the system. Then by analyzing the L-dependence of $\Delta E(L)$ averaged over disorder

$$\langle \Delta E(L) \rangle \sim L^{\theta} \tag{5.10}$$

one can measure the stiffness exponent θ, that, in the case of a $T = 0$ transition, is nothing else that the inverse of the correlation lengths exponent, $\theta = \nu^{-1}$. One crucial point in applying DWRG is the choice of BC. First of all we discuss periodic (P) boundary conditions, that are usually introduced to reduce unwanted surface effects, and we dwell on the requirement of compatibility of the ground state with boundary conditions.

To understand what we mean by a compatible ground state let us consider for a while the trivial case of an anti-ferromagnetic Ising model on a lattice. The couplings between spins $\sigma_i = \pm 1$ in the bulk are all negatives, so that in the energy

minimum configuration all spins are anti-parallel. Periodic boundary conditions imply $\sigma_{i+L\hat{\mu}} = \sigma_i$ where $\hat{\mu} = \hat{x}, \hat{y}, \ldots$ denotes the versors of the lattice in each direction. Moreover one has to specify how spins on opposite faces are coupled. It is very immediate to see that, in coupling spins on opposite faces, to have a compatible ground state one has to use a ferro- or anti-ferromagnetic bond according to the fact that L is odd or even. In a similar way in the XY model periodic boundary conditions are defined by requiring $\theta_{i+L\hat{\mu}} = \theta_i$. To define the interaction between sites on opposite faces one has to choose the global twist Δ_P^μ from one boundary to the opposite, where the twist in the μ direction is defined as the sum of the phase differences along a loop circling the lattice in that direction. Two possibilities are available:

- The first is simply to restrict the twist to be a integer multiple of 2π. This is basically equivalent to fix the twist $\Delta_P^\mu = 0$, since the lowest energy of the system $E_P(\Delta_P^\mu)$ is 2π periodic function in Δ_P^μ. This has been the standard choice in numerical simulations on XY model and we call it a *Random Twist* (RT) measurement for reasons that we explain in a while.

- On the other hand, it is easy to check that adding a twist different from zero on the μ direction is equivalent to make a gauge transformation on that direction by $\pi_{ij} \to \pi_{ij} + \Delta_P^\mu / L$. A more preferable possibility in choosing the twist is that in which it is not fixed to a constant but it is allowed to fluctuate. In particular to find the *true* ground state, compatible with periodic BC, it is convenient to fix the twist to the value $\Delta_P^\mu = \overline{\Delta_P^\mu}$ such that $E_P(\overline{\Delta_P^\mu})$ is a global minimum of the lowest energy. This second choice of a sample-dependent twist has been called *Best Twist* (BT) measurement and it is also more reasonable from a physical point of view, since in real experiments open boundary conditions are usually employed in which the twist can have any value.

The original problem is invariant under discrete gauge transformation modulo 2π so the RT measurement is performed in a random gauge while the BT measurement is done in the gauge which minimizes the energy. We denote by E_P^{RT} and E_P^{BT} the ground state energy of RT and BT measurements in periodic BC, respectively.

As said before, to apply DWRG one has to change boundary conditions in such a way to introduce a defect energy relative to the ground state. A spin

domain wall perpendicular to, say, the x direction is obtained by considering anti-periodic (AP) boundary conditions in that direction. This amounts to make a π rotation on boundary spins on the seam perpendicular to the x direction or, equivalently, to change the twist from the periodic value Δ_P^μ to the anti-periodic value $\Delta_{AP}^\mu = \Delta_P^\mu + \pi\delta(x,\mu)$. Since chiralities do not change passing to anti-periodic boundary conditions, this yields the energy with a spin defect. Two different spin domain wall energies are obtained, one in RT measurements

$$\Delta E_S^{RT} = |E_{AP}^{RT} - E_P^{RT}| \tag{5.11}$$

where E_{AP}^{RT} is the lowest energy with $\Delta_{AP}^\mu = \pi\delta(x,\mu)$, and another one in BT measurements

$$\Delta E_S^{BT} = E_{AP}^{BT} - E_P^{BT} \tag{5.12}$$

where E_{AP}^{BT} is the ground state with $\Delta_{AP}^\mu = \overline{\Delta_P^\mu} + \pi\delta(x,\mu)$. Averaging over disorder and and fitting to (5.10) one extract the two spin stiffness exponents θ_S^{RT} and θ_S^{BT}. Note that in the RT case the spin defect energy has been defined considering the modulus of the energy difference since there is no special preferences between periodic and anti-periodic boundary condition, so that a simple mean of the energy difference vanishes. This is not necessary in BT, where $E_{AP}^{BT} > E_P^{BT}$ in each sample since E_P^{BT} is the *true* energy minimum. Of course one does not expect the treatment of the boundary to affect the result in the infinite volume limit. However, since the constrains of manageable sizes in numerical simulation on XY model are usually very severe, different definition of boundary condition can led to very different estimate of critical exponents when using finite-size scaling. One expects that the RT value of the stiffness exponent coincide with the BT value at very large sizes, while they could be different for smaller systems as it is the case for the two dimensional model [99, 106]. It is our belief that the BT measurement is a better estimate of the true asymptotic value.

To study chiral order, a chiral domain wall is introduced in, say, the x direction considering reflective (R) boundary conditions [96]. This means that the spins in the first lattice iperplane perpendicular to the x direction interact with the images of the spin in the last lattice iperplane under reflection about an arbitrary axis. However, at variance with anti-periodic BC, it is not a priori clear how reflective BC probe the chiral order, due to the fact that in RT a spin domain wall superimposes

to the chiral domain wall, while in BT the periodic ground state may already trap a chiral defect. To overcome this difficulties an heuristic expression for the RT chiral domain wall was introduced in ref. [96]:

$$\Delta E_C^{RT} = |E_m - \langle E_m \rangle| \tag{5.13}$$

where $E_m = \min(E_P^{RT}, E_{AP}^{RT}) - E_R^{RT}$ with E_R^{RT} the RT ground state energy in reflective boundary condition. In the BT case it is enough to define

$$\Delta E_C^{BT} = |E_R^{BT} - E_P^{BT}| \tag{5.14}$$

where E_R^{BT} is the BT minimum in reflective boundary condition.

5.4 Coulomb gas representation

When looking for ground states energies, it is convenient to replace the cosine interaction in the original Hamiltonian (5.2) with a piecewise parabolic potential (this is the Villain formulation [108]) that is equivalent in the small temperature region

$$H = \frac{J}{2} \sum_{\langle ij \rangle} (\theta_i - \theta_j - 2\pi n_{ij} - \pi_{ij})^2 \tag{5.15}$$

with $n_{ij} = -n_{ji}$ any integer on the bond ij. In the following we set $J = 2$. Using a duality transformation [102, 109], it is possible to transform the problem in a Coulomb gas (CG) representation, in which the continuous variables θ_i on each sites are eliminated in favor of discrete vortex variables (charges) q_r on each plaquettes. These charges can assume any integer value and, in periodic boundary condition, they satisfy the charge neutrality condition $\sum_r q_r = 0$. Chiralities are obtained considering the sum of the frustration and vortex variables

$$c_r = f_r + q_r \tag{5.16}$$

Following Thill, Ney-Nifle and Hilhorst [101] the CG Hamiltonian for the tube lattice in P boundary conditions reads (by obvious notation, we denote by subscript 1 the bottom row of the tube and by 2 the up one):

$$H_P = \pi^2 \sum_{x,x'=1}^{N} \left(c_x^+ c_{x'}^+ U_P^+(x - x') + c_x^- c_{x'}^- U_P^-(x - x') \right)$$

$$+2\pi^2 N\left(q_y+f_y+\frac{1}{N}\sum_{x=1}^{N}x(c_{(x,1)}+c_{(x,2)})\right)^2$$
$$+\frac{8\pi^2}{N}\left(q_x+f_x+\frac{1}{2}\sum_{x=1}^{N}c_{(x,1)}+2c_{(x,2)}\right)^2 \tag{5.17}$$

where $c_x^{\pm}\equiv c_{(x,1)}\pm c_{(x,2)}$ are combinations of the two chiralities of the same column x, with $x=1,\dots N$ and

$$U_P^{+}(x-x')=\frac{1}{2N}\sum_{k_x\neq 0}\frac{e^{ik_x(x-x')}-1}{\sin^2(\frac{k_x}{2})} \tag{5.18}$$

$$U_P^{-}(x-x')=\frac{1}{2N}\sum_{k_x}\frac{e^{ik_x(x-x')}}{1+\sin^2(\frac{k_x}{2})} \tag{5.19}$$

where $k_x=2\pi n_x/N$ with $n_x=0,1,\dots,N-1$. The other two terms in Eq. (5.17) are corrections order $\mathcal{O}(1/N)$ that disappear in the thermodynamic limit, but that are important in finite size scaling as DWRG, also because they contain, besides the total electric dipole moment, the global frustration variables

$$f_x=\frac{1}{2\pi}\sum_{x=1}^{N}\pi_{(x,1)(x+1,1)}\quad f_y=\frac{1}{2\pi}\sum_{y=1}^{2}\pi_{(N,y)(N,y+1)} \tag{5.20}$$

which are related to the applied twist. The global charge q_x,q_y are restricted to be integer valued like the local charges. To obtain Hamiltonian in AP boundary conditions one has simply to put a twist of π, i.e. adding a term $1/2$ in the last term between brackets in Eq. (5.17), while the Hamiltonian in R boundary conditions is given by:

$$H_R=\pi^2\sum_{x,x'=1}^{N}\left(c_x^{+}c_{x'}^{+}U_R^{+}(x-x')+c_x^{-}c_{x'}^{-}U_R^{-}(x-x')\right) \tag{5.21}$$

where

$$U_R^{+}(x-x')=\frac{1}{2N}\sum_{k_x}\frac{e^{ik_x(x-x')}}{\sin^2(\frac{k_x}{2})} \tag{5.22}$$

$$U_R^{-}(x-x')=U_P^{-}(x-x') \tag{5.23}$$

and the charge obey a modified neutrality condition $(\sum_r q_r+2f_y)\bmod 2=0$. Note that in this case there are no boundary terms.

5.5 Numerical Results

We have performed numerical simulations to measure the spin and stiffness exponents. To find the ground state energies we used simulated annealing [110]. We repeated n_a times an annealing schedule starting from random initial configurations (corresponding to uniform infinite temperature measure), decreasing the temperature in n_s steps till very low temperature and accepting new configurations according to Metropolis algorithm. It is known that in frustrated systems the number of local minima of the energy increases exponentially with the size and that the free energy landscape is a corrugated function of the order parameters. In order to achieve the global minimum of the energy it is so necessary to consider increasing values of trials n_a and n_s, in such a way that there is the possibility for the system to not get trapped in the local valley of the free energy. The choice of their values has been made by trail and error. As a criterion we stopped our searches for ground states if doubling the number of annealings it did not give any improvement. We used $n_s = 10$, $n_a = 20$ for the smaller size ($L = 5$) and $n_s = 200$, $n_a = 1000$ for the bigger size ($L = 50$). For smallest sizes ($L \leq 10$) it has been possible to do an exact enumeration of all configurations, checking the efficiency of the algorithm. As a crude test, we verified that in BT measurements the condition $E_{AP}^{BT} > E_{P}^{BT}$ is always satisfied. Moreover, in some cases two runs for the same disorder realizations but with different sequences of random numbers were performed. Due to the very small magnitude of energy differences between different BC it was necessary to have a very large number of samples to obtain stable statistics. For each size $L \leq 35$ we considered 10240 samples, while for bigger sizes we reached 5120 disorder realizations.

In RT measurements we minimize the energy with respect to the chiralities c_r and to the global charges q_x and q_y, keeping fixed the global frustration variables. At variance in BT measurements we consider the optimal value of the twist, allowing the combinations $q_x + f_x$ and $q_y + f_y$ to vary over any integer or half-integer. The results of simulations are reported in Fig. (5.1). At variance with the prediction of analytical calculations [101], i.e. the stiffness exponents $\theta_s = \theta_c = -1.7972..$, in all cases we basically found $\theta_s = \theta_c \sim 1$, both in BT and RT measurements. More precisely, the results of the best fits on data of Fig. (5.1) are: $\theta_S^{RT} = -1.04 \pm 0.04$,

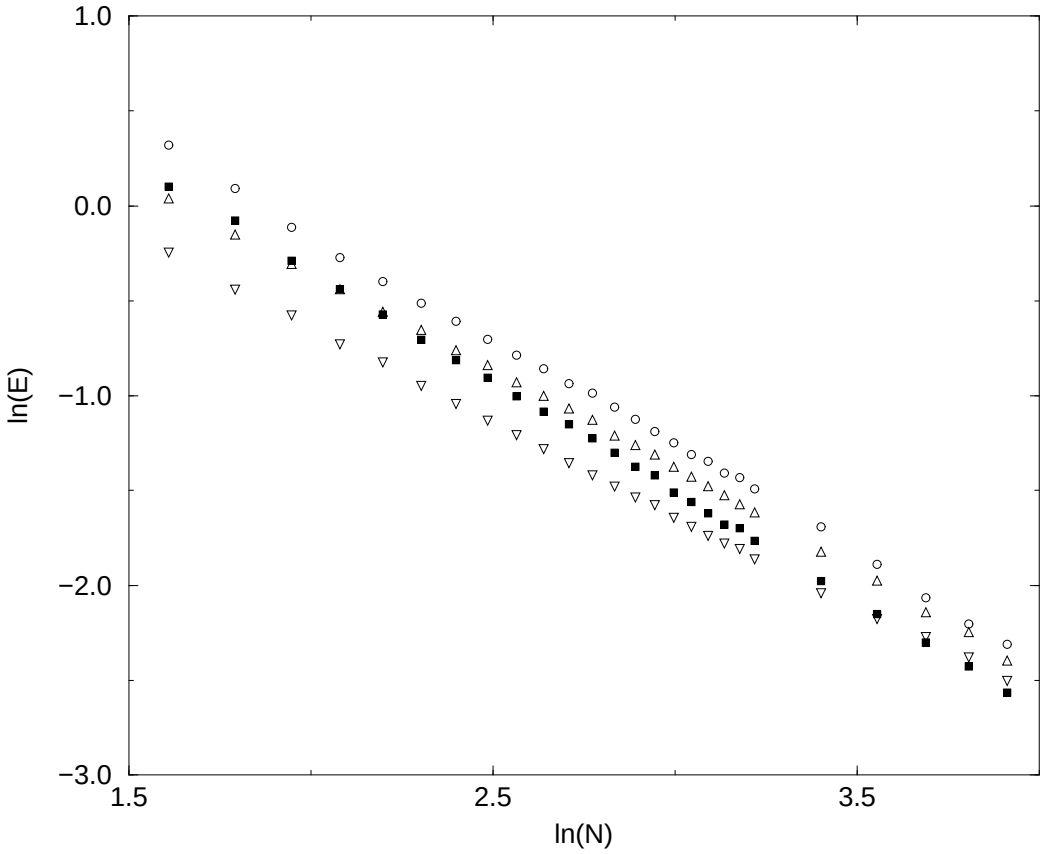

Figure 5.1: Spin and Chiral defect energies versus N: ΔE_S^{RT} (circles), ΔE_S^{BT} (squares), ΔE_C^{RT} (triangles up), ΔE_C^{BT} (triangles down) for $N = 5, \ldots, 25$ in steps of 1 and $N = 25, \ldots, 50$ in steps of 5.

$\theta_S^{BT} = -1.16 \pm 0.04$, $\theta_C^{RT} = -1.02 \pm 0.05$, $\theta_C^{BT} = -0.97 \pm 0.05$.

The observed discrepancy between theoretical predictions and numerical results is the signature that the derivation of Thill, Ney-Nifle and Hilhorst is incorrect. The proof of their results is in two steps: first they give a description of lowest energy states in the thermodynamic limit, proving a set of properties for ground states in different boundary condition; then they consider energy differences in the RT approach. To do this they estimated the bulk interaction potentials in Eq. ((5.18),(5.19)) in the infinite volume limit$N \to \infty$, (continuum limit on k_x), finding that in periodic boundary conditions, the charges c_x^+ interact via long-range Coulomb

potential

$$U_P^+(x-x') = -|x-x'|\left(1-\frac{|x-x'|}{N}\right) + E_+(N) \tag{5.24}$$

with $0 \leq |x-x'|/N \leq 1$, while the charges c_x^- affect each others by a short range dipolar interaction

$$U_P^-(x-x') = \frac{\sqrt{2}}{8}(3-2\sqrt{2})^{d(x,x\prime)} + E_-(N) \tag{5.25}$$

with $d(x,x\prime)$ the length of the shortest path between x and $x\prime$. Similar expression are obtained for reflective boundary conditions, Eq. ((5.22),(5.23)),

$$U_R^+(x-x') = \frac{N}{2}\left(1-\frac{2|x-x'|}{N}\right) + E_+(N) \tag{5.26}$$

$$U_R^-(x-x') = \frac{\sqrt{2}}{8}(3-2\sqrt{2})^{d(x,x\prime)}\sigma(x,x\prime) + E_-(N) \tag{5.27}$$

where $\sigma(x,x\prime) = -1$ if the shortest path between x and $x\prime$ crosses the rightest vertical bond and $\sigma(x,x\prime) = 1$ otherwise. The errors terms $E_\pm(N)$ are corrections of leading order $\mathcal{O}(1/N)$ due to the substitution of the summation with an integral in the complex plane. We point out that, while these finite size terms can be ignored in studying ground states in chosen boundary condition, they must be retained in considering ground states energy differences between different boundary conditions, since excitations involved are of higher order. Consistently we checked that the set of ground state properties proved in ref. [101] are verified also in numerical simulations. In particular in the energy minimum configurations the Coulomb energy is minimized independently of the other energies involved and the chiralities c_r take the values $0, \pm 1/2$, so that it is always possible to partition the non-zero chiralities into dipoles, grouping together two successive chiralities of opposite sign along the x-axis. On the other hand, besides the global spin-wave term in Eq. (5.17), we have individuated another finite size term $\mathcal{O}(1/N)$, i.e. the error $E_\pm(N)$ in estimates ((5.24), (5.25),(5.26) and (5.27)), that must be retained in analyzing how the system adjust to anti-periodic or reflecting BC starting from periodic BC.

The analysis of paragraph 4 of ref. [101] must therefore be modified in the following way. Let us denote the ground state configurations in P and AP boundary conditions by $c_x^\pm(P)$ and $c_x^\pm(AP)$, respectively. It still holds the distinction between even and odd number of frustrated plaquettes $(x,1)$ in the bottom line of the tube.

However in the even case the are two possibilities. The first one is to make vanish the global spin-wave term both in P and AP just reversing a sequence of dipoles, that costs an amount of energy $N^{-1.7972}$(see [101]). Since the chiralities configuration in P and AP are not the same, the energy difference will involve the contribution of $E_-(N)$, so that

$$\Delta E_{AP} \sim E_-(N) \sum_{x,x'} (c_x^-(AP)c_{x'}^-(AP) - c_x^-(P)c_{x'}^-(P)) + N^{-1.7972} \tag{5.28}$$

while the correction due to $E_+(N)$ can be ignored because of the neutrality condition $\sum_x c_x^+ = 0$. The other possibility is that the system choose to retain the same configuration in P and AP boundary conditions, so that the correction proportional to $E_-(N)$ are equal in both BC conditions and will cancel out considering the energy difference. However, in this case, either in P or AP the spin-wave term (i.e., the last term in Eq. (5.17)) is different from zero. As a result, in both the two described scenarios $\Delta E_{AP} \sim 1/N$, where ΔE_{AP} denotes both RT and BT measurements. Considering instead an odd number of frustrated plaquettes $(x, 1)$, the energy configuration will be the same in P and AP boundary conditions because the system is never able to let vanish the spin-wave term, so that the energy difference is always zero, $\Delta E_{AP} = 0$. This is exactly what we have observed in numerical simulations.

For what concern the chiral stiffness exponent, one has to note that, in general, in reflecting boundary conditions there are both the contribution of $E_\pm(N)$, since the charge neutrality condition is modified. As before, in passing from P to R boundary conditions, in the case of even number of frustrated plaquettes $(x, 1)$, a reversal of dipoles is involved, so that there is an amount of energy of order $1/N$ besides the excitation $N^{-1.7972}$. In case of odd number of frustrated plaquettes the global spin wave term never vanishes in PBC so that again $\Delta E_R = 1/N$.

5.6 Conclusion

Summarizing, we have studied a random XY spin-glass on a tube lattice. We have found a disagreement between numerical simulations and analytical predictions. We solved it noticing the lack in the theoretical analysis of correction terms $\mathcal{O}(1/N)$.

Nevertheless the main conclusion of ref. [101], i.e. the equality of the spin and chiral stiffness exponents, is confirmed by the numerical study, both in BT and RT measurements, giving support to the conjecture that spin and chiral correlation length exponents are the same below the lower critical dimension.

Chapter 6

Spin-glasses and portfolio optimization

6.1 Introduction

Portfolio theory is a basic pillar in economic analysis. It was originally proposed by Harry Markovitz [111] during the 50's. The approach was that the return of any financial activity is described by a random variable, whose expected mean and variance (interpreted as volatility) are assumed to be known (in some way or other) from its historical past. The selection of a particular portfolio is based on the mean-variance principle, *i.e.* if two portfolios are given, and the expected return of the first portfolio is higher than the second one; or the variance of the first portfolio is lower than the second one, we say that the first portfolio dominates the second; the latter being outside the decision field of a rational investor. Portfolio selection allows us to find the set of efficient portfolios, i.e. those portfolios not dominated by anything else. The rational investor eventually chooses among these (efficient portfolios), in a subjective manner, according to his/her preferences towards risk. Much criticism, over the years, has been addressed to Markovitz's model. For instance, the choice of variance as a signal of risk has been criticized on logical grounds: the model requires a quadratic utility function or a set of returns that must be normally distributed, but the two hypotheses are not mutually compatible. Criticism has also been made of other aspects of the original model. In spite of this, the Markowitz approach has been very successful, because of its ability to grasp the hard core of the problem of how to allocate wealth among alternative assets. Extended versions of the model (for

instance, in order to increase the number and types of assets considered; or to reduce computations for the estimated matrix of variance/covariances among returns), have almost continuously been introduced, and today various and updated versions of the original model are widely used by financial practitioners. Quoting from a successful fund management story [1]:

> Even if point estimates of risk and return variables fail to represent reality fairly, insofar as inputs stem from well-grounded interrelationships, the mean-variance optimization process produces valuable insight into efficient portfolio alternatives.

It is well-known that, in the case where short sales are allowed, it is straightforward to find an efficient investment strategy (basically one has to solve N equations in N unknowns, where N is the number of risky assets) [112, 113]. In practice, however, the short sales are usually allowed under very restricted legal conditions. Since the "shorted" security is "on loan" and has to be returned to the original owner at a preagreed date or demand, the lender must be protected against the eventuality of borrower's default. The short sales proceeds thus usually serve as collateral and are held on deposit with the lender. In addition to this collateral, the borrower is usually required to maintain a certain cash margin to ensure that the shorted security will be returned even if its market price rises. The incorporation of these constrains on the proceeds of short sales has been considered by Lintner [114, 115], who solved the problem assuming that the short sales proceeds plus 100 % margin are deposited with the stock owner, who pays interest on the deposited funds.

The general case where short sales are not allowed is usually very complicated. In this work we extend and generalize the traditional analysis (short-selling included), by considering the case of *futures markets*, where the short sale problem is regulated through the mechanism of margin accounts. Therefore a generalization of the usual portfolio optimization problem is tried out in a radically new setting: a hypothetical hedge-fund is considered, with the aim of optimizing its assets portfolio. Specifically - regarding the current state of the art in portfolio selection - the model for future markets allows for:

[1] David Swensen, *Pioneering Portfolio Management: An Unconventional Approach to Institutional Investment*, Free Press, 1999

- long-buying/short selling activities in equities,
- leveraging on margin accounts,
- a set of a (relatively) large number of assets to be prospected.

The main result we aim to discuss here is that the portfolio optimization problem in future markets naturally belongs to the realm of "complex" problems. In particular, a very large number of (quasi) equilibrium solutions coexists in the model and any procedure developed to reach a decision regarding the structure of the portfolio must face this problem. To be a little bit more precise, if we have N assets available to the investor, for a fixed expected return R, the number $n(N, R)$ of risk local minima grows exponentially in the number of assets, i.e.:

$$n(N, R) \sim e^{\omega(R)N}$$

where $\omega(R)$ is a positive number depending on return. Since we have this multiple equilibrium solution not equivalent among themself respect to the level of risk, we have to implement a second step in the solution procedure in order to get the global equilibrium. This conclusion is a direct consequence of the application of Lagrange optimization and the *non-linear* constraint on the total wealth in futures markets. The issue of non-unique equilibrium is a well-known chapter of economic analysis, particularly in models with money, increasing returns and imperfect competition [116] and a new line of research on equilibrium beliefs is being developed. However it should be emphasized that, in this work, the issue of multiple equilibrium solutions is discussed in a quite different setting. The underlying idea is that the selection of a *unique* optimum portfolio obtained from portfolio optimization in its current form (see for instance [112, 113]), works well only if we introduce drastic and perhaps unrealistic simplification. Enlarging the picture to a certain extent, by relaxing the most restrictive assumptions in line with the practical experience of fund management, when calculating the solution for the optimum portfolio, we reach rapidly the threshold of a so-called NP problem, an area of research currently still largely ignored in economic computation [117, 118]. We will deal in this work with the complexity of the problem for a concrete case of a portfolio made of 22 risky assets. We will explicitly show where complexity does arise and we will suggest the

necessity of using algorithms typical of the realm of other optimization problem (like the so-called "simulated annealing").

Our analysis is built on a seminal idea by Galluccio, Bouchaud and Potters [119], who have re-stated the problem of a solution to the portfolio optimization problem in futures markets in terms of a spin-glasses problem. For readers unfamiliar with this topic, spin-glasses is a branch of modern statistical physics of complex systems, originally related to magnetization of materials [2, 3]. We remained to the appendix for a brief introduction to spin glass theory and for an explanation of the connection to portfolio optimization.

The rest of the Chapter goes as follows. In Section (6.2) we define the model of portfolio optimization in future markets and we explain the non-linear constraint that is involved. A first analysis of the portfolio variance is presented in Subsection (6.2.1), showing the complexity of the problem compared to the usual case of *short sales* with a linear wealth constrain, while in Subsection (6.2.2) the general procedure and analytical calculation needed to construct the *efficient frontier* is obtained. We deal with a concrete example in Section (6.3), considering a portfolio of 22 assets on the Nasdaq Market and solving it by means of computer calculations. We show the multiple equilibrium solutions and we calculate the *efficient frontier*. The risk function as an exponential number of local minima and one needs to select by hand the lowest one. Moreover, there is the possibility that portfolios completely different among them correspond almost to the same value of the risk. Finally, in Section (6.4) we give some remarks on the vaiance/covariance matrix and in Section (6.5) we draw our conclusions.

6.2 The model

In this section, we present a model of portfolio optimization, where some traditional assumptions are relaxed. Specifically, in order to allow for the maximum flexibility in the model, a hedge-fund as rational investor agent is considered. Let us start from the standard definitions. We consider a portfolio $\mathcal{P}$ of N risky assets indexed by the subscript i which takes values $i = 1, \ldots, N$. The variance (i.e. risk) of the

portfolio is

$$\sigma_{\mathcal{P}}^2 = \sum_{i,j=1}^{N} C_{ij} p_i p_j = p^T C p \tag{6.1}$$

and the mean (i.e. expected average return)

$$R_{\mathcal{P}} = \sum_{i=1}^{N} p_i r_i = p^T r \tag{6.2}$$

where $p = (p_1, p_2, \ldots, p_N)$ are the shares of a given total wealth to be invested, and the external parameters are

r_i - the expected return on asset i,

C_{ij} - the matrix of variances ($i = j$) and covariances ($i \neq j$).

and we have introduced the usual vectorial notation with ^{T} to denote the transposed.

The aim of the optimization is to find the most efficient investment strategy, i.e. to evaluate proportions p of the total wealth W that minimize the risk $\sigma_{\mathcal{P}}^2$, for a given return $R_{\mathcal{P}}$ (or viceversa shares p that maximize the return $R_{\mathcal{P}}$ for a given level of risk $\sigma_{\mathcal{P}}^2$)). In other words, we would like to calculate the *efficient frontier*, that represents the relationship between the risk of the portfolio and the expected return of the portfolio itself having the best utility for the investor. Knowing the efficient frontier, once that a particular expected rate of return has been identified, we can determine the correspondent efficient portfolio; it is such that its variance (or riskiness) is a minimum. Therefore, once one of the two (either the risk or the return) has been chosen by the investor, the other variable is derived as a consequence.

Since long-buying and short-selling are allowed, and leveraging on margin accounts works, then the budget constraint is

$$\sum_{i=1}^{N} \Gamma \mid p_i \mid = W \tag{6.3}$$

where Γ is the (fixed) margin constraint and $p_i > 0$ or $p_i < 0$, depending on the sign of the contract (buy or sell respectively). The margin is assumed fixed for all operations, and it does not change over time according to price variations of the underlying assets. Moreover, the problem of issuing futures on behalf of the financial institution is not considered. Without loss of generality we can set $W/\Gamma = 1$, so that,

introducing the vector s whose components are $s_i = sign(p_i)$, the budget constrain becomes:

$$\sum_{i=1}^{N} \mid p_i \mid = p^T s = 1 \tag{6.4}$$

We remember the reader that the *sign* function is defined as $sign(x) = 1$ if $x > 0$ and $sign(x) = -1$ if $x < 0$.

6.2.1 "Complexity" of the model

Let us consider the problem of finding the minimum of the variance subjected to the only budget constraint (no fixed average portfolio return). In other words we want to minimize the portfolio variance Eq.(6.1) with the non-linear constrain given by Eq.(6.4). We introduce a Lagrangian function with one Lagrange multiplier μ:

$$L(p, \mu) = p^T C p - \mu(p^T s - 1) \tag{6.5}$$

Differentiating with respect to the $N + 1$ unknowns p and μ we obtain the following equations for the extreme points

$$p = \frac{1}{2}\mu C^{-1} s \tag{6.6}$$

$$p^T s = 1 \tag{6.7}$$

where C^{-1} is the inverse of the correlations matrix.
Inserting Eq.(6.6) in Eq.(6.7) we can solve for μ and then for p

$$\mu = \frac{2}{s^T C^{-1} s} \tag{6.8}$$

$$p = \frac{1}{s^T C^{-1} s} C^{-1} s \tag{6.9}$$

Applying the *sign* function to both sides of the last Equation, we finally obtain

$$s = sign(C^{-1} s) \tag{6.10}$$

where we have used the fact that, since C is a positive definite matrix, the same is true for C^{-1}, so that $s^T C^{-1} s > 0$ for every value of s.

The original problem has thus been mapped in finding the solution of Eq. (6.10): once the s_i that solve this Equation are known, the shares p_i can be calculated using Eq. (6.9),while the portfolio variance is given by

$$\sigma_{\mathcal{P}}^2 = \frac{1}{s^T C^{-1} s} \tag{6.11}$$

But solving Eq. (6.10) is a very tough task. It is exactly the same Equation that appears in spin-glasses theory when one looks for 1-flip stable configurations (see the Appendix). It is well-known in physics [2, 3] that Eq. (6.10) admits for a generic random matrix C^{-1} an exponential number of solution. Moreover these solutions are "chaotic", i.e. they are completely different one from another and they completely change varying the number of degree of freedom. In our case the matrix C^{-1} is not random but it is constructed from the hystorical datas. Nevertheless, since hystorical prices/returns movements are generated by market fluctuations,the correlation matrix C (and so its inverse C^{-1}) can be seen as a generic realization of some specific random matrix ensemble. In this way we can borrow the results from physics and directly draw some first conclusions (see also [119]):

- At variance with the usual case in which short sales are allowed, where we always find a minimization equation that admits a unique solution, in the present case of futures markets we have an exponential number of portfolios for which the risk function has a (local) minimum. So we face the embarace of which solution to choose and we need to calculate by hand the portfolio variance on each solution to find the true minimum.

- We can have very different portfolios corresponding to (local) risk minima having almost the same risk value.

- Adding one asset to the portfolio it radically change the shape of efficient investments.

6.2.2 Constructing the efficient frontier

In the previous Section we have shown how the complexity of the problem naturally arise in the minimization procedure for the case of the global minimum of the portfolio risk. This does not say nothing about the efficient frontier (even if it shows

the instability of rational investment decisions). To completely solve the problem, we have to repeat the minimization of the variance fixing the average return to the value R with an extra Lagrange multiplier ν.
Thus the problem is now to minimize Eq.(6.1) subject to Eq.(6.4) and to the additional constraint

$$R_{\mathcal{P}} = p^T r = R \tag{6.12}$$

We introduce the Lagrangian function

$$L(p, \mu) = p^T C p - \mu(p^T s - 1) - \nu(p^T r - R) \tag{6.13}$$

Differentiating with respect to the $N + 2$ unknowns p, μ and ν we obtain

$$\begin{aligned} p &= \frac{1}{2}\mu C^{-1} s + \frac{1}{2}\nu C^{-1} r \\ p^T s &= 1 \\ p^T r &= R \end{aligned} \tag{6.14}$$

Inserting the first equation in the second and the third, we can solve for μ and ν, and then for p. Defining

$$\begin{aligned} \alpha &= s^T C^{-1} s \\ \beta &= r^T C^{-1} s \\ \gamma &= r^T C^{-1} r \end{aligned} \tag{6.15}$$

we obtain the following expressions:

$$\begin{aligned} \mu &= 2\frac{\gamma - R\beta}{\alpha\gamma - \beta^2} \\ \nu &= 2\frac{R\alpha - \beta}{\alpha\gamma - \beta^2} \\ p &= \frac{\gamma - R\beta}{\alpha\gamma - \beta^2} C^{-1} s + \frac{R\alpha - \beta}{\alpha\gamma - \beta^2} C^{-1} r \end{aligned} \tag{6.16}$$

Applying the *sign* function to both sides of the last Equation and remembering that $s = sign(p)$ by definition, we finally obtain

$$s = sign\left(\frac{\gamma - R\beta}{\alpha\gamma - \beta^2} C^{-1} s + \frac{R\alpha - \beta}{\alpha\gamma - \beta^2} C^{-1} r\right) \tag{6.17}$$

This is the basic equation that substitute Eq.(6.10) in the case of a fixed average return R. If we now identify

$$\frac{\gamma - R\beta}{\alpha\gamma - \beta^2} C^{-1} \Longleftrightarrow J \tag{6.18}$$

$$\frac{R\alpha - \beta}{\alpha\gamma - \beta^2} C^{-1} r \Longleftrightarrow h \tag{6.19}$$

we establish a perfect analogy between the Equation to be solved for the portfolio optimization problem in future markets and the one for 1-flip stable states in spin glass models: J is the coupling matrix between spins and h is the external magnetic field.

The general procedure for tracing the N-stocks efficient frontier in the case of *future markets* thus can be summarized as follows:

1. Fix a certain value of the average expected portfolio return R.

2. For this return R solve the system of N equations (6.17) for the vector $s = (s_1, s_2, \ldots, s_N)$. In general the number of solutions n will be exponential in number of assets N: $n \sim e^{\omega N}$, where the exponential rate $\omega = \omega(R)$ depends on the fixed return R.

3. Calculate the value of the proportions investment $p = (p_1, p_2, \ldots, p_N)$ corresponding to each solution of step 2 through formula (6.16) and then the associated risk. Select the lowest value of the risk and the corresponding optimum portfolio investment.

4. Increase the return R by a certain (constant) amount and repeat the entire procedure from step 2 throught 4.

6.3 A worked example

In this Section we explicitly treat an example with real data: we demonstrate the "complexity" of our problem and we calculate the *efficient frontier* by means of computer calculations.

6.3.1 Data

We considered the case of a portfolio consisting of 22 risky assets. These risky assets are common stocks traded on the Nasdaq, chosen among the best and worst stocks in the period October 1, 1998 - November 13, 2000. An historical record of daily rates of return on these stocks for the 553 days of the period was used to estimate the relevant parameters - the mean return r_i and the variance/covariance matrix C_{ij}. The data source is *DataStream*. Calling $x(i,k)$ the prize of the i-th asset (where $i = 1, \ldots, 22$) at the k-th day (where $k = 1, \ldots, 553$), the formula used to estimate returns and covariances are:

$$r_i = \frac{x(i,553) - x(i,1)}{x(i,1)} \tag{6.20}$$

$$C_{ij} = \frac{1}{553} \sum_{k=1}^{553} x(i,k)x(j,k) \tag{6.21}$$

The estimated mean returns are given in Table (6.1) at the end of this Chapter, which also lists the stocks by name, while the variance/covariance matrix is splitted in Tables (6.2) and (6.3).

6.3.2 Multiple solutions

First of all we analyzed the whole set of possible choices that one obtains for a fixed value of the return on the portfolio composed by $N = 22$ assets. We choose to fix the average return to the value of the return of the Nasdaq index in the period we considered: $R = R_{NAS} = 0.84$ (i.e. 84%). Applying the "receipt" described in the previous Section, we found the solutions $\hat{s} = (\hat{s_1}, \hat{s_2}, \ldots, \hat{s_N})$ of the Eq.(6.17) doing an exhaustive enumeration of all the 2^N possible values of the N-dimensional vector s. We found 5625 $\hat{s}$ vectors that satisfy Eq.(6.17). From them we calculate the corresponding 5625 proportions $\hat{p}$ using Eq.(6.16) and the 5625 risk value $\hat{\sigma}^2$ using Eq.(6.1). These are the risk local minima. Then we selected by hand among them the global risk minimum, $\sigma^2_{MIN} = 0.15856$, and the corresponding efficient portfolio proportions p_{MIN}. The dependence of the number of solution $n(N,R)$ from the number of assets N and from the imposed average return R is investigated later. For the moment we focus our attention on the analysis of the risk local minima for the considered case $N = 22$, $R = R_{NAS} = 0.84$. We show how they are distributed

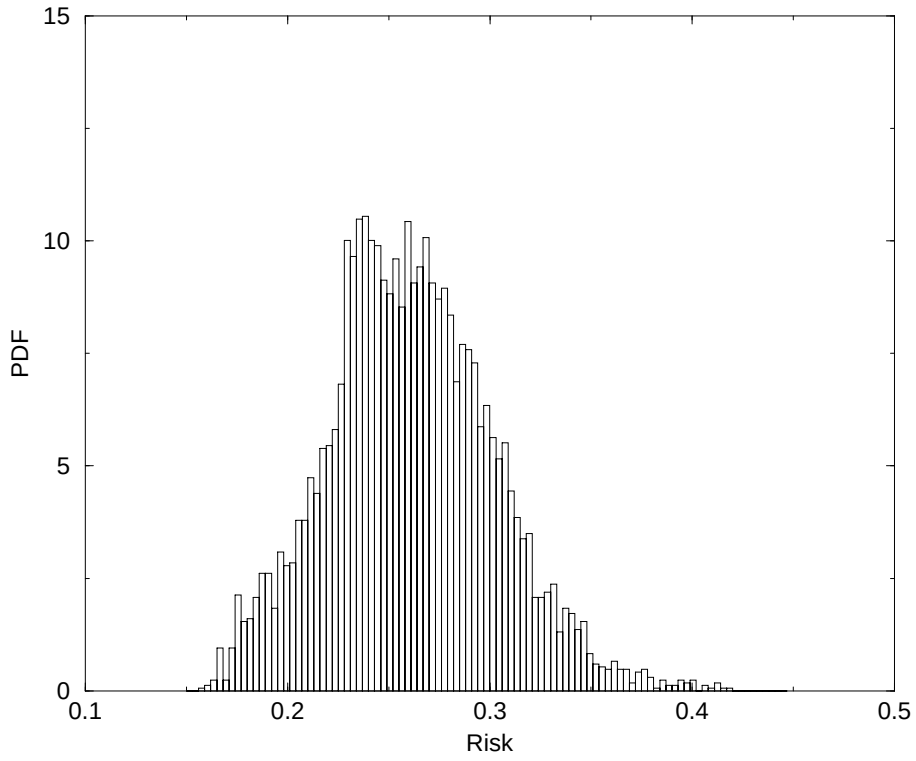

Figure 6.1: Histogram of the local risk minima. The number of assets is $N = 22$ and the fixed portfolio return is the Nasdaq return $R = R_{NAS} = 0.84$. *PDF* stands for Probability Distribution Function.

in Fig.(6.1), where we plot their probability distribution function, i.e the histogram normalized to have area 1. We see that most of the risk local minima have a risk value higher than the global risk minimum σ^2_{MIN}.

It is important to remark that the local minimum which corresponds to the maximum of the distribution shown in Fig. (6.1) are in fact the solutions that one would obtain with very "high probability". To be more precise, if one consider portfolio of some bigger dimension, just say 100 assets, then it would be impossible to compute exactly all the local minimum but instead one should rely on other methods. For example (but not only) one could implement algorithm developed in the realm of spin glass theory, aimed to freeze spin glass systems down to zero temperature in order to reach the real minimum (ground state). This rich class of algorithms can be roughly speaking addressed as the so called *simulated annealing*

techniques [110, 2]. If one try to implement this algorithms then it would almost impossible to end up on the efficient frontier, but instead one would almost surely converge to a portfolio solutions corresponding to an higher risk (see also Section (6.3.4)). Nevertheless we observe that there are also proportions $\hat{p}$, which can be very different among themselves and from p_{MIN} but with a risk value very close to lowest value of the risk σ^2_{MIN}. Suitable modifications of the previous general algorithm can eventually allow to reconstruct some of such *almost* optimal solutions.

From a practical point of view, this *quasi-degeneracy of the risk value with corresponding proportions p very far from each other* is the most interesting aspect of this work. In order to illustrate better this point, we use in simple terms a very important and not trivial *object* in spin glass theory, the so called *overlaps distribution*. To be more concrete, assume that for some reasons we know the global minimum solution $\bar{s} = \{\bar{s}_1, \ldots, \bar{s}_n\}$.[2] Moreover, let also denote by $\hat{s} = \{\hat{s}_1, \ldots, \hat{s}_n\}$ another local minimum solution. A simple number, which describe how different this two solutions are, can be defined basically by counting how many s_j's we must *flip* in order to go from one configuration to the other. This information is contained in the real number $-1 \leq q = q(\bar{s}, \hat{s}) \leq 1$ defined as:

$$q(\bar{s}, \hat{s}) \; = \; \frac{1}{n} \sum_{k=1}^{n} \bar{s}_k \hat{s}_k$$

In the left side of Fig.(6.2) we plot the probability distribution function of the numbers q_j's, obtained by measuring the overlap of any single local minimum with the global solution: $q_j = q(\bar{s}, \hat{s}^{(j)})$, where $\hat{s}^{(j)}$ runs over all possible 5625 solutions. In particular, this histogram show clearly that *most of* the solutions are in fact quite different from the one we would like to calculate a priori, i.e. $\bar{s}$.

Actually, a little bit more than this can be said. Roughly speaking, *in general* two different local solution might have almost the same risk level but in a strategic-economic context they can be totally different. This is shown in the right side of Fig.(6.2) , where the histogram of all the overlaps between different solutions is shown. Summarizing, a multiple choice is available to the investor and an irreducible component of randomness is present in the final decision. Moreover, it is likely that

[2]For simplicity, we consider only the sign of the proportions $s_j = \mathrm{sign} p_j$, but the same reasoning can be extended to the proportions themselves

traditional method for reconstructing the minimizing solution will lead the investor to be "trapped" into a quite different local minimum.

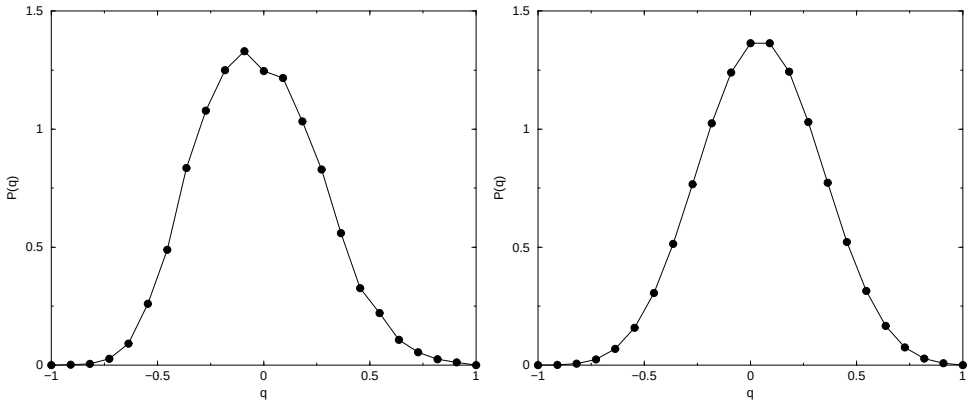

Figure 6.2: **Left:** the distribution of the overlap between the configuration s_{MIN} corresponding to the risk global minimum and the others configurations $\hat{s}$ corresponding to the risk local minima. **Right:** the distribution of the overlap between the all the configuration $\hat{\sigma}$ (including σ_{MIN}) corresponding to the risk local minima.

6.3.3 Exponential growth of solutions in the number of assets

The impossibility of taking a rational decision described in the previous paragraph get even worst if we consider the dependence of the solutions from the number of assets N. We performed numerical experiments varying N from 5 to 22 keeping the average return R fixed to R_{NAS}. For each value we calculate the number of local risk minima $n(N)$, i.e. the number of solutions of Eq. (6.17). As it is clear from Fig.(6.3) this number growths exponentially with the number of assets (note the lin-log scale in the graph). The best numerical fit yields $n(N) \sim \exp(0.419N)$.

This exponential growth of the number of risk local minima with the number of assets is the exact analog of the exponential growth of the number of local energy minima with the number of spins typical of the spin-glasses. From the economic point of view, the consequence of this growth is that the uncertain on taking a rational decision enlightened above get even bigger by increasing the portfolio dimension.

On the other hand the number of possible decisions decreases for increasing value of the fixed return R under which minimization is performed. We argue this fixing $N = 22$ and calculating the number of risk local minima varying the return R in the

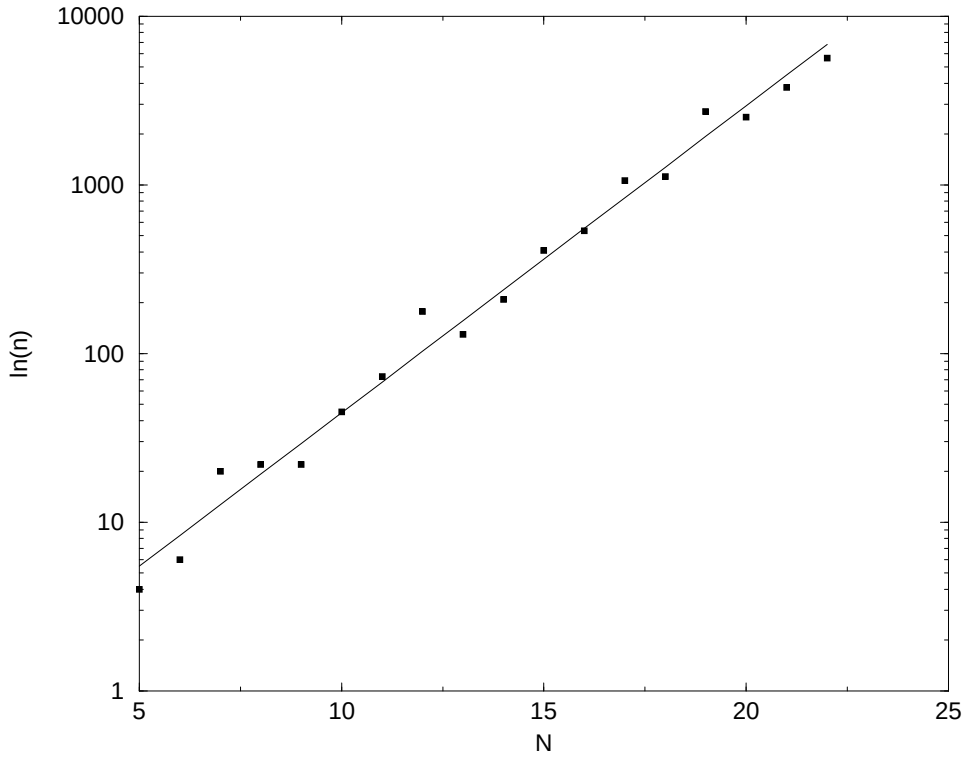

Figure 6.3: The number of local risk minima versus the number of assets N. The fixed average return is the Nasdaq return $R_{NAS} = 0.84$. The solid line is the best numerical fit $n(N) \sim \exp(0.419N)$

range $[0, 10]$ in constant steps of 0.1. In Fig.(6.4) we plot the number of solutions of Eq.(6.17) corresponding to each R value. We see that the local risk minimums decreases for increasing value of the return, becoming zero at $R \sim 7$. Above these threshold we do not find from Eq.(6.17) any portfolios satisfying both the budget and the return constrains. One should look for risk minima on the border of the manifold where Lagrange optimization is performed. We did not investigated this point further.

6.3.4 The efficient frontier

Here we use the data concerning the 22-stocks in order to compute the efficient frontier and two more related curves. More precisely, we first allow the averaged return to range from 0 to 7 in constant steps of 0.1 and for each value of the return we

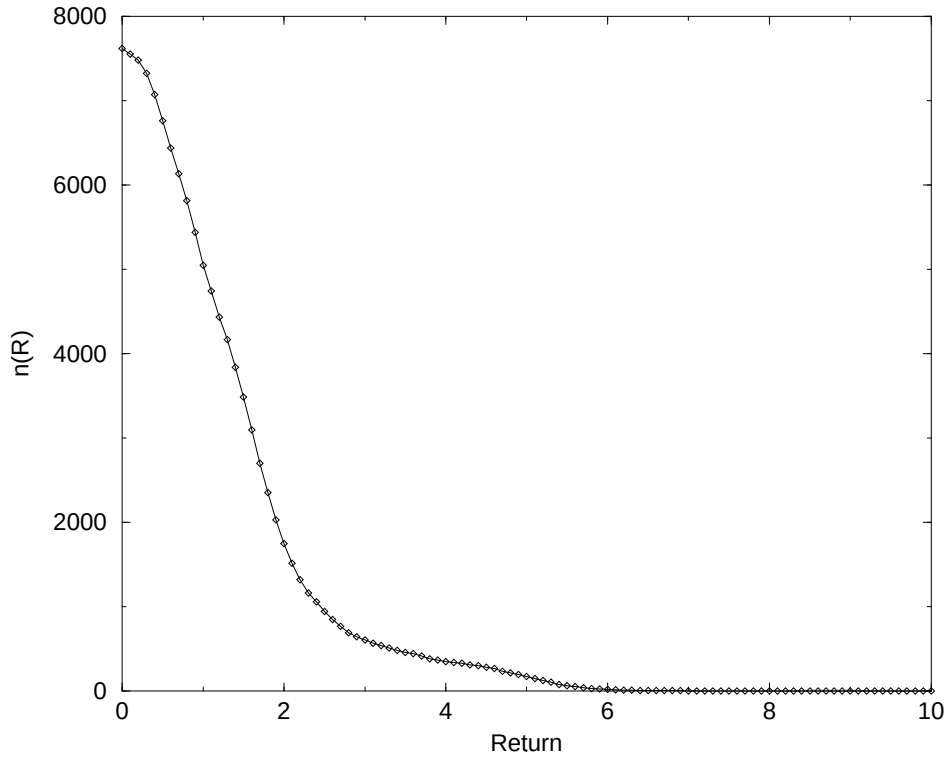

Figure 6.4: The number of local risk minima versus the average portfolio return. The number of assets is fixed to $N = 22$.

calculated the proportions p corresponding to the risk local minima. Then, among them we selected the one associated to the risk global minima and the one associated to the worst choice, namely the local minimum corresponding to the portfolio at the very right tail of Fig. (6.1) . Moreover, for a given fixed return, we also calculate the *averaged risk* $\bar{\sigma}^2$. Namely, if n is the total number of local minima and σ_j^2 are the associated risk minima ($j = 1, \ldots, n$), we define

$$\bar{\sigma}^2 \; = \; \frac{1}{n} \sum_{j=1}^{n} \sigma_j^2$$

By varying the return R, we use this data to reproduce a kind of *averaged* efficient frontier, which is shown in Fig. (6.5), together with the other two.

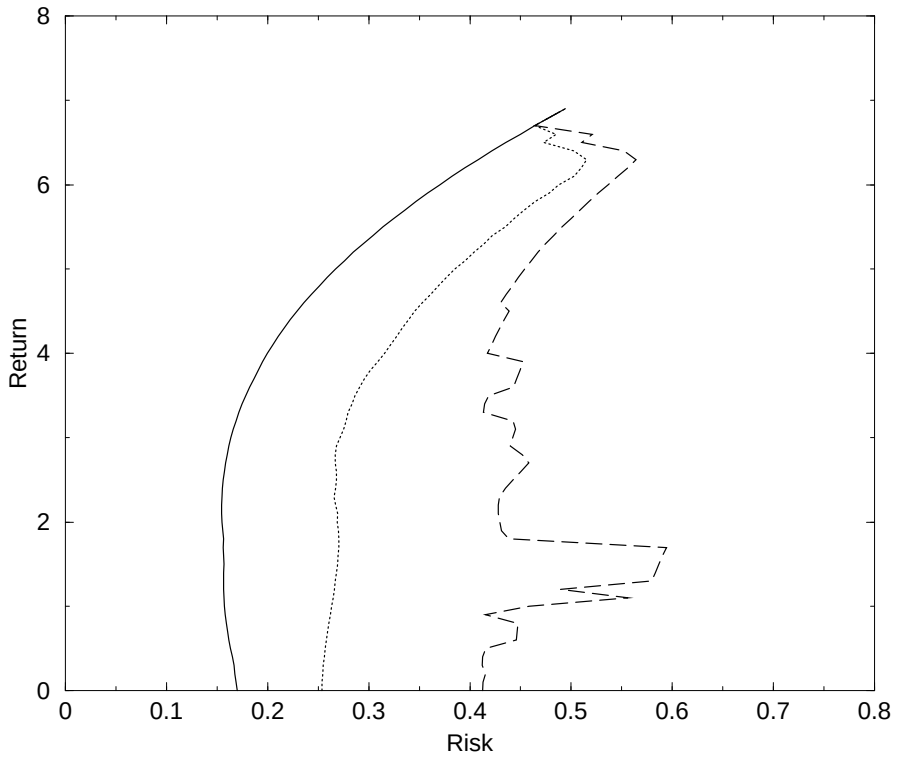

Figure 6.5: Efficient frontiers for the portfolio consisting of 22 assets. The continuous line is the *"best-efficient"* frontier corresponding to the lowest value between all the risk local minima. The dotted line shows the *"average-efficient"* frontier, i.e. it correspond to the average value of the risk between all the risk local minima. The dashed line is the *"worst-efficient"* frontier, constructed by using the higher values of the risk local minima for each fixed return.

6.4 A few remarks on the variances/covariances matrix

A few words of comment about the correlation matrix are in place. The computation of matrix C of variances/covariances between return variations of different assets is a key issue in the theoretical solution of the portfolio optimization problem. The study of these correlation matrices is a crucial problem in financial theory, both for developments of Markowitz's theory of optimal portfolios, and for problems (more recently introduced) of risk management, related to the so-called value at risk models. For covariance matrices used in value at risk models, the discussion is open to an almost continuous flow of new experiments, with an empirical evaluation

of the obtained results, based on a single case (for instance see [122]).

In ref. [119] a random matrix approach is proposed by Gallucio et al. as an alternative to well-established index models -originally presented by Markowitz himself and developed by Sharpe [112]. In this Section we try to comment about the random approach proposed by Galluccio et al. (cit), showing his richness from a theoretical point but also stressing the difficulties in concrete applications. Roughly speaking, these authors assume the matrix C of variance/covariance as random; in this way they can exploit a consolidated approach based on random matrix theory (see [123, 85]) to gain some information toward the solution of the problem. In particular, from an historical analysis on asset prizes variations in various Stock Markets, they argue that correlation matrix is a member of the so-called Exponential Orthogonal Ensemble. With this hypothesis, they are able to prove analytically the exponential increase of risk local minima, applying a well-known formula in spin glass theory, which allows to compute the total number of local energy minima by averaging over all possible *random realizations* of the model.

Assuming the matrix C as random is quite reasonable in terms of financial theory: prices/returns movements are in any case random, since they can be read as realization of a stochastic process, generated by market fluctuations. A second step consists in evaluating the significance of C not in terms of individual elements, but in terms of a matrix as a whole, i.e. by examining the spectrum of the eigenvalues/eigenvectors of the matrix itself. The main aim here is, roughly speaking, to separate the randomness contained in the data from the *real market* information. Let us consider a portfolio of N assets: the correlation matrix contains $N(N-1)/2$ entries, which must be computed from N time-series of length T. If T is small compared to N, one would expect that the determination of the covariance is most likely to be noisy, and therefore the empirical correlation matrix is to a large extent random; this implies that the structure of the matrix is dominated by measurement noise and real information are somewhat hidden in the data.

Therefore, and this is the second important point made by Galluccio et al., moving along this path, the theory of random matrices allows us to grasp some solid results. But clearly, a lot of further research must be done. A deep analysis of eigenvalues (and corresponding eigenvectors) performed in ref [124] sheds relevant light on the statistical properties of empirical correlation matrices. Along this

perspective, for instance, Galluccio et al. get some useful empirical results. In the case of the S & P500, less than 6 % of the eigenvectors, which are responsible for 26 % of the total volatility, appear to carry some information, and that is a surprising result. From this point of view, it should be stressed that Markovitz's portfolio scheme, based on a purely historical determination of the correlation matrix, proves particularly weak, since the elements of the matrix itself are dominated by noise.

Despite the above appreciations on the new random approach by Galluccio et al., it must be noted some unavoidable (at least for now) drawbacks of this approach. First of all, the identification of the random matrix ensemble to be considered is made only on the basis of the historical data analysis. It is nowadays clear that, to have a representation of correlations faithful to reality, future expectations must be included in the determination of the random matrix ensemble. Secondly, one has to note that the random approach could be useful in establishing average properties, like the exponential number of risk local minima, but it is not manageable from a practical point of view to exactly find the desired solutions.

In order to bring the analysis to a manageable framework, an alternative view to Galluccio's idea has been advanced in ref. [125] where a different deterministic approach to the treatment of correlations is introduced. This deterministic approach (up to this stage only a conjecture) moves from the recent discover in spin glasses theory that an exponential number of energy minima is not only typical of disordered spin systems, but can appear also in sufficiently complex deterministic models [85, 126]. Moreover the deterministic approach proposed in ref. [125] might be more suitable in an economic perspective, since it takes its roots in an expectation hypothesis (originally proposed by Krugman [120]) and allows for a portfolio strategy. It should be stressed, however, that both random and deterministic approaches reach exactly the same conclusions: a multiple equilibrium solution. The difference is in terms of their economic interpretation: the deterministic approach is more manageable for a strategy of investment activity; its underlying idea of an oscillatory behavior is coherent with other line of research in economic analysis (see [120]).

To summarize this section: matrix C of variances/covariances is a necessary component for calculating the optimum portfolios in a mean-variance framework; in fact the matrix is a set of correlation values (usually) calculated (in some way

or other) from the past; conventional economics analyzes -in terms of statistical significance- each element of the matrix, independently one by one. But if we consider the significance of the matrix as a whole, treating it as random, the whole picture is very different. On the other hand the application of a deterministic approach presents, from the economic viewpoint, some undoubtedly advantages. Clearly we have no chance of bypassing the multiple solutions setback, that is inherent in the complexity of the problem, but, knowing the actual solutions set we can try to develop a solution that allows for a strategy related to some form of rational behavior.

6.5 Conclusions

Originally hedge-funds were created on the basis of two fundamental aims: first, exploiting at the highest possible level financial leverage; secondly, in asset allocation planning, operating in financial markets according to a scientific approach. The first idea has proved very risky, as shown by some dramatic hedge-fund collapses (like the case of L.T.C.M.). The soundness of the second assumption (the scientific approach) has been challenged on theoretical grounds in this work. Investment activity is ontologically risky (in fact, in projecting future results, we must make use of the correlation matrix, which per s is derived, in one form or another, from the past). Moreover the hope for a rigorous approach is also fragile. The theory needs to be flexible enough to consider the problem of portfolio selection of some practical use for relatively highly sophisticated financial operators, such as hedge-funds. This implies the possibility to introduce a relatively wide range of hypotheses, not too far from concrete market situations, without necessarily being too simple.

We have presented here a model of portfolio optimization general enough to allow for: (a) a set of investments in equities through financial leverage (i.e. investment operations with margin accounts); (b) simultaneous long-buying and short-selling of the assets; (c) a relatively high number of assets involved. We have reached a couple of conclusions. Firstly, the model has a complex solution in terms of standard optimization method. Secondly, borrowing a suggestion from ref. [119], we get a solution by exploiting a hooking with the spin glass analysis. However, the solution obtained is still non conclusive, because in fact we have reached a multiple

equilibrium solution, where the number of equilibria is exponentially proportional to the number of assets involved, and each equilibrium can be chaotic (i.e. crucially depending on initial conditions) and very different one from the other, making the idea of rational behavior very awkward to interpret. This multiple equilibrium conclusion is general for a realistic and relevant example (portfolio optimization), and can easily be extended to other fields of economics, when the constraint for the objective function to be maxi/minimized is nonlinear. In more sophisticated language, this above picture is often referred to as a complex situation. It has been suggested how portfolio optimization in future markets should leave the traditional economic optimization procedure and enter instead the combinatorial optimization area.

Table 6.1: Rate of Return

	Name	*Symbol*	*Return*
1	Adobe	ADO	7.766
2	Amazon	AMA	0.626
3	Ameritrade	AME	3.585
4	Aol	AOL	2.926
5	Appmc	APP	33.602
6	Broadvis	BRO	23.269
7	Cisco	CIS	2.521
8	Cmgi	CMG	1.449
9	Dell	DEL	-0.216
10	Doubleclick	DOU	1.910
11	Ebay	EBA	5.429
12	Inktomy	INK	1.813
13	Intel	INT	0.831
14	Jdsuni	JDS	12.465
15	Microsoft	MIC	0.277
16	Oracle	ORA	4.500
17	Psinet	PSI	-0.721
18	Qualcomm	QUA	11.941
19	Sun	SUN	6.490
20	3com	TRI	2.456
21	Worldcom	WOR	-0.467
22	Yahoo	YAH	0.959
**	Nasdaq Index	NAS	0.839

	ADO	AMA	AME	AOL	APP	BRO	CIS	CMG	DEL	DOU	EBA
ADO	467.44	-101.38	-14.90	120.24	614.70	312.54	343.88	126.58	21.36	98.86	106.47
AMA	-101.38	384.43	114.03	230.24	-160.04	63.14	7.44	423.28	64.06	425.50	294.94
AME	-14.90	114.03	87.28	108.20	-29.15	-2.31	5.35	137.26	15.79	141.93	143.30
AOL	120.24	230.24	108.20	264.98	137.13	164.99	147.96	382.31	54.78	375.26	285.47
APP	614.70	-160.04	-29.15	137.13	923.25	448.33	483.33	233.44	19.96	153.08	140.94
BRO	312.54	63.14	-2.31	164.99	448.33	453.77	340.22	537.16	70.71	425.66	191.58
CIS	343.88	7.44	5.35	147.96	483.33	340.22	324.95	332.79	56.33	267.31	167.09
CMG	126.58	423.28	137.26	382.31	233.44	537.16	332.79	1180.10	132.61	1001.62	496.55
DEL	21.36	64.06	15.79	54.78	19.96	70.71	56.33	132.61	49.95	116.05	70.72
DOU	98.86	425.50	141.93	375.26	153.08	425.66	267.31	1001.62	116.05	935.10	474.98
EBA	106.47	294.94	143.30	285.47	140.94	191.58	167.09	496.55	70.72	474.98	460.16
INK	699.28	65.74	39.40	329.23	1032.80	811.58	724.30	906.35	162.38	716.08	478.03
INT	263.50	-24.51	-11.31	84.84	370.08	251.28	250.39	194.29	55.74	149.65	95.63
JDS	842.55	-79.14	-26.73	297.59	1230.08	866.05	788.90	788.30	110.09	602.30	319.04
MIC	-39.49	237.82	76.58	167.18	-57.25	121.63	58.59	424.14	63.57	390.36	203.60
ORA	279.11	-46.80	-15.51	79.95	399.73	251.41	245.64	185.60	33.10	133.50	81.28
PSI	19.69	124.33	44.26	101.39	45.21	158.31	93.89	342.56	45.94	287.42	151.06
QUA	575.69	245.55	53.92	419.03	818.39	845.70	657.78	1250.11	134.62	1083.78	474.85
SUN	701.05	-69.14	-3.23	249.81	1006.29	577.47	586.70	447.78	51.47	358.09	240.40
TRI	73.02	-34.03	-8.96	4.65	115.87	39.71	48.55	-4.98	-7.70	-14.37	-2.72
WOR	-135.91	140.80	56.35	62.55	-202.29	-57.08	-70.08	100.28	27.90	108.25	90.68
YAH	416.31	384.70	82.22	465.45	643.25	784.23	600.51	1309.43	189.44	1089.34	521.11

Table 6.2: Variance/Covariance matrix

	INK	INT	JDS	MIC	ORA	PSI	QUA	SUN	TRI	WOR	YAH
ADO	699.28	263.50	842.55	-39.49	279.11	19.69	575.69	701.05	73.02	-135.91	416.31
AMA	65.74	-24.51	-79.14	237.82	-46.80	124.33	245.55	-69.14	-34.03	140.80	384.70
AME	39.40	-11.31	-26.73	76.58	-15.51	44.26	53.92	-3.23	-8.96	56.35	82.22
AOL	329.23	84.84	297.59	167.18	79.95	101.39	419.03	249.81	4.65	62.55	465.45
APP	1032.80	370.08	1230.08	-57.25	399.73	45.21	818.39	1006.29	115.87	-202.29	643.25
BRO	811.58	251.28	866.05	121.63	251.41	158.31	845.70	577.47	39.71	-57.08	784.23
CIS	724.30	250.39	788.90	58.59	245.64	93.89	657.78	586.70	48.55	-70.08	600.51
CMG	906.35	194.29	788.30	424.14	185.60	342.56	1250.11	447.78	-4.98	100.28	1309.43
DEL	162.38	55.74	110.09	63.57	33.10	45.94	134.62	51.47	-7.70	27.90	189.44
DOU	716.08	149.65	602.30	390.36	133.50	287.42	1083.78	358.09	-14.37	108.25	1089.34
EBA	478.03	95.63	319.04	203.60	81.28	151.06	474.85	240.40	-2.72	90.68	521.11
INK	1876.60	569.78	1765.88	164.24	544.93	281.59	1528.09	1223.61	87.90	-124.90	1443.94
INT	569.78	223.00	615.17	25.51	195.23	64.88	428.18	440.61	34.70	-55.27	434.45
JDS	1765.88	615.17	2027.27	93.04	617.36	225.47	1592.54	1464.68	131.28	-215.37	1455.94
MIC	164.24	25.51	93.04	238.57	1.32	126.27	348.92	32.43	-19.72	95.61	421.19
ORA	544.93	195.23	617.36	1.32	199.65	49.37	454.69	464.19	43.85	-78.58	408.65
PSI	281.59	64.88	225.47	126.27	49.37	122.04	331.07	103.05	-7.51	44.91	367.91
QUA	1528.09	428.18	1592.54	348.92	454.69	331.07	1976.59	1113.31	66.54	-84.65	1652.27
SUN	1223.61	440.61	1464.68	32.43	464.19	103.05	1113.31	1184.34	120.84	-191.44	946.26
TRI	87.90	34.70	131.28	-19.72	43.85	-7.51	66.54	120.84	19.38	-33.61	41.72
WOR	-124.90	-55.27	-215.37	95.61	-78.58	44.91	-84.65	-191.44	-33.61	108.17	20.86
YAH	1443.94	434.45	1455.94	421.19	408.65	367.91	1652.27	946.26	41.72	20.86	1858.53

Table 6.3: Variance/Covariance matrix

Appendix A

Proof of formulas (4.47) and (4.48)

We sketch the basic steps of the calculation. Set

$$\alpha = -\frac{N}{2} + 2s \qquad\qquad c_j = \left(\begin{array}{c} N-j \\ s-j \end{array} \right).$$

We then have

$$\mathrm{E}_s(H^n) = \frac{1}{c_0} \sum_{\tau \in \Omega_s} \left(\alpha - 2 \sum_{x \in \tau} \sum_{y \in \tau} J_{xy} \right)^n = \frac{1}{c_0} \sum_{\tau \in \Omega_s} \sum_{k=0}^{n} \left(\begin{array}{c} n \\ k \end{array} \right) \alpha^{n-k} \left(-2 \sum_{x \in \tau} \sum_{y \in \tau} J_{xy} \right)^k .$$

For $n = 1$ we get

$$\begin{aligned} \sum_{\tau \in \Omega_s} \left(\sum_{x \in \omega} \sum_{y \in \omega} J_{xy} \right) &= \sum_{x=1}^{N} \sum_{y \neq x, y=1}^{N} c_2 J_{xy} \sigma_x \sigma_y + \sum_{x=1}^{N} c_1 J_{xx} \\ &= \sum_{x=1}^{N} \sum_{y=1}^{N} c_2 J_{xy} \sigma_x \sigma_y + \sum_{x=1}^{N} (c_1 - c_2) J_{xx} = c_2(N-1) + c_1, \end{aligned}$$

whereas for $n = 2$ we have

$$\begin{aligned} \sum_{\omega \in \Omega_s} \left(\sum_{x \in \omega} \sum_{y \in \omega} J_{xy} \right)^2 &= \sum_{z=1}^{N} \sum_{u \neq z; u=1}^{N} J_{zu} \sigma_z \sigma_u \left[\sum_{x \neq z,u; x=1}^{N} \sum_{y \neq z,u,x; y=1}^{N} c_4 J_{xy} \sigma_x \sigma_y \right. \\ &+ \sum_{y \neq z,u; y=1}^{N} c_3 J_{zy} \sigma_z \sigma_y + \sum_{y \neq z,u; y=1}^{N} c_3 J_{uy} \sigma_u \sigma_y + \sum_{x \neq z,u; x=1}^{N} c_3 J_{xz} \sigma_x \sigma_z + \sum_{x \neq z,u; x=1}^{N} c_3 J_{xu} \sigma_x \sigma_u \\ &+ \left. \sum_{x \neq z,u; x=1}^{N} c_3 J_{xx} + c_2 J_{zu} \sigma_z \sigma_u + c_2 J_{zz} + c_2 J_{uu} \right] + \sum_{z=1}^{N} J_{zz} \left[\sum_{x \neq z; x=1}^{N} \sum_{y \neq z, x; y=1}^{N} c_3 J_{xy} \sigma_x \sigma_y \right. \end{aligned}$$

$$
\begin{aligned}
&+ \quad \sum_{x\neq z;x=1}^{N} c_2 J_{xz}\sigma_x\sigma_z + \sum_{y\neq z;y=1}^{N} c_2 J_{yz}\sigma_y\sigma_z + \sum_{x\neq z;x=1}^{N} c_2 J_{xx} + c_1 J_{zz}\Bigg] \\
&= \quad c_4(N-1)(N-3) + 2c_3(N-1) + 2c_2(N-1) + c_1,
\end{aligned}
$$

which easily give the desired identities.

Appendix B

Proof of formula (4.54)

Let us first extend everything to the set $\{1, 2, \ldots, p-1\}$ which, p being prime, is a number field. Here we can exploit the multiplicative structure of the field and of the 'extended ground state' $\sigma^0_x = \left(\frac{x}{p}\right)$, $x = 1, \ldots, q$, with $q = p-1$. With slight abuse of notation we shall use the same symbols Ω_s, p_s and E_s to denote the corresponding extended quantities. It is immediate to see that $m(\sigma^0) = 0$ and

$$E_s(m) \;=\; \frac{1}{\left(\begin{array}{c} q \\ s \end{array}\right)} \sum_{\tau \in \Omega_s} \left(\frac{-2}{q} \sum_{x \in \tau} \left(\frac{x}{p}\right) \right) = 0.$$

In order to calculate the second moment we consider

$$\begin{aligned} \frac{1}{\left(\begin{array}{c} q \\ s \end{array}\right)} \sum_{\tau \in \Omega_s} \left(\sum_{x \in \tau} \left(\frac{x}{p}\right) \right)^2 \;&=\; \frac{1}{\left(\begin{array}{c} q \\ s \end{array}\right)} \sum_{\tau \in \Omega_s} \left(\sum_{x \in \tau^2} \left(\frac{x}{p}\right) \right) \\ &=\; \frac{1}{\left(\begin{array}{c} q \\ s \end{array}\right)} \sum_{x=1}^{q} c_p(x) \, \left(\frac{x}{p}\right) , \end{aligned}$$

where, for any given $\tau \in \Omega_s$, τ^2 is the collection, with multiplicity, of all possible products $x_j \cdot x_i$, $x_i, x_j \in \tau$ (all the operations are mod p). For example, if $\tau = \{x_1, x_2, x_3\}$ then $\tau^2 = \{x_1^2, x_2^2, x_3^2, x_1x_2, x_1x_3, x_2x_1, x_3x_1, x_2x_3, x_3x_2\}$. Also, for any given $x \in \{1, \ldots, q\}$,

$$c_p(x) \;=\; \sum_{\tau \in \Omega_s} \{\text{number of times } x \in \tau^2\} = \sum_{u=1}^{q} \sharp\{\tau \,|\, u \in \tau \text{ and } u^{-1}x \in \tau\}.$$

In particular, if $\left(\frac{x}{p}\right) = -1$ then $u \neq u^{-1}x$, $\forall u = 1, \ldots, q$, therefore

$$c_p(x) \;=\; \sum_{u=1}^{q} \left(\begin{array}{c} q-2 \\ s-2 \end{array} \right) \;=\; q \left(\begin{array}{c} q-2 \\ s-2 \end{array} \right).$$

If instead $\left(\frac{x}{p}\right) = 1$, then there exists $\bar{u}$ such that $\bar{u}^2 = x$, i.e.

$$c_p(x) \;=\; \sum_{u \neq \pm \bar{u}} \left(\begin{array}{c} q-2 \\ s-2 \end{array} \right) + 2 \left(\begin{array}{c} q-1 \\ s-1 \end{array} \right) \;=\; (q-2) \left(\begin{array}{c} q-2 \\ s-2 \end{array} \right) + 2 \left(\begin{array}{c} q-1 \\ s-1 \end{array} \right).$$

Putting everything together we get the following expression for the variance $\sigma_s^2(m)$:

$$\begin{aligned} \sigma_s^2(m) \;&=\; \frac{4}{q^2 \left(\begin{array}{c} q \\ s \end{array} \right)} \sum_{\tau \in \Omega_s} \left(\sum_{x \in \tau} \left(\frac{x}{p} \right) \right)^2 \\ &=\; \frac{4}{q^2 \left(\begin{array}{c} q \\ s \end{array} \right)} \left[-\frac{q^2}{2} \left(\begin{array}{c} q-2 \\ s-2 \end{array} \right) + \frac{q}{2}(q-2) \left(\begin{array}{c} q-2 \\ s-2 \end{array} \right) + q \left(\begin{array}{c} q-1 \\ s-1 \end{array} \right) \right] \\ &=\; \frac{4}{q \left(\begin{array}{c} q \\ s \end{array} \right)} \left[\left(\begin{array}{c} q-1 \\ s-1 \end{array} \right) - \left(\begin{array}{c} q-2 \\ s-2 \end{array} \right) \right] = \frac{4s(q-s)}{q^2(q-1)}. \end{aligned}$$

We now turn back to our the original lattice $\{1, \ldots, N\}$. Again we can write

$$\frac{1}{\left(\begin{array}{c} N \\ s \end{array} \right)} \sum_{\tau \in \Omega_s} \left(\sum_{x \in \tau} \left(\frac{x}{p} \right) \right)^2 \;=\; \frac{1}{\left(\begin{array}{c} N \\ s \end{array} \right)} \sum_{x=1}^{p} c_N(x) \left(\frac{x}{p} \right).$$

In this case, however, the multiplicity function $c_N(x)$ can not be handled as easily as before. In particular, given $x \in \{1, \ldots N\}$, we denote by $\Gamma(x)$ the set $= \{u_1, \ldots, u_{d_N(x)}\}$ given by the u's in $\{1, \ldots, N\}$ such that $u^{-1}x \in \{1, \ldots, N\}$. The cardinality $d_N(x)$ of the set $\Gamma(x)$ is a non trivial function of x. It is shown in Fig. B.1 for $1 \leq x \leq N$. If now $\left(\frac{x}{p}\right) = -1$, then clearly

$$c_N(x) \;=\; d_N(x) \cdot \left(\begin{array}{c} N-2 \\ s-2 \end{array} \right).$$

On the other hand, if $\left(\frac{x}{p}\right) = 1$ (i.e. $\bar{u}^2 = x$), then (note that either $\bar{u} \in \{1, \ldots, N\}$ or $-\bar{u} \in \{1, \ldots, N\}$)

$$c_N(x) \;=\; (d_N(x) - 1) \cdot \left(\begin{array}{c} N-2 \\ s-2 \end{array} \right) + \left(\begin{array}{c} N-1 \\ s-1 \end{array} \right).$$

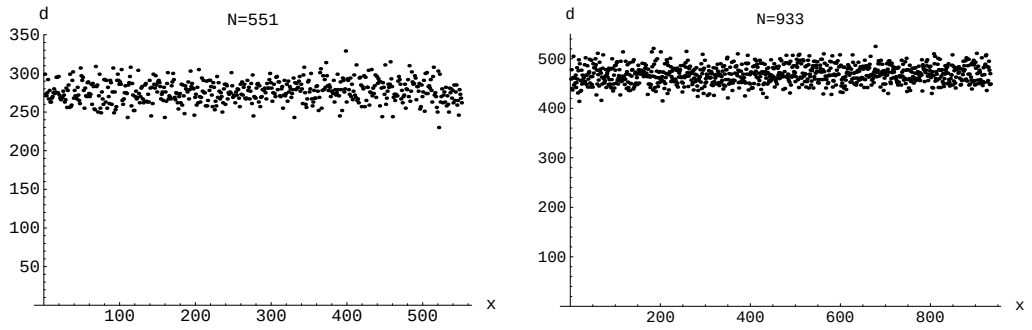

Figure B.1: The function $d_N(x)$ versus x, for $N = 551$ and $N = 933$

We can then use these informations and write

$$\begin{aligned}
\frac{1}{\left(\begin{array}{c} N \\ s \end{array}\right)} \sum_{\tau \in \Omega_s} \left(\sum_{x \in \tau} \left(\frac{x}{p}\right) \right)^2 &= \frac{1}{\left(\begin{array}{c} N \\ s \end{array}\right)} \sum_{x=1}^{p} c_N(x) \left(\frac{x}{N}\right) \\
&= \frac{1}{\left(\begin{array}{c} N \\ s \end{array}\right)} \left[- \sum_{\left(\frac{x}{p}\right)=-1} d_N(x) \cdot \left(\begin{array}{c} N-2 \\ s-2 \end{array}\right) + \right. \\
&\quad \left. + \sum_{\left(\frac{x}{p}\right)=1} \left((d_N(x)-1) \cdot \left(\begin{array}{c} N-2 \\ s-2 \end{array}\right) + \left(\begin{array}{c} N-1 \\ s-1 \end{array}\right) \right) \right] \\
&= \frac{1}{\left(\begin{array}{c} N \\ s \end{array}\right)} \left[\left(\begin{array}{c} N-2 \\ s-2 \end{array}\right) \cdot \sum_{x=1}^{p} d_N(x) \left(\frac{x}{p}\right) + \right. \\
&\quad \left. + \left(\left(\begin{array}{c} N-1 \\ s-1 \end{array}\right) - \left(\begin{array}{c} N-2 \\ s-2 \end{array}\right) \right) \cdot \sum_{\left(\frac{x}{p}\right)=1} 1 \right].
\end{aligned}$$

Finally, we have the following expression for the variance $\sigma_s^2(m)$ of the magnetization m over the space Ω_s:

$$\sigma_s^2(m) = \frac{4}{N^2} \, \mathrm{E}_s \left(\left(\sum_{x \in \tau} \left(\frac{x}{p}\right) \right)^2 \right) - \frac{4s^2 (m^0)^2}{N^2},$$

from which one easily gets formula (4.54).

Acknowledgments

First of all, I gratefully thank Professor S. Graffi for having suggested the research topics of this work. I acknowledge very much him, both for having giving me the possibility of working on such a fascinating subject like spin glasses and for having supported me also from the practical side. I am also indebted with M. Degli Esposti and S. Isola, with whom I seldom worked together in this years. Enthusiasm and excellent working conditions have always been typical properties of the mathematical physics research group at the Department of Mathematica of Bologna University.

Then it is pleasure to thank Prof. J. M. Kosterlitz that I visited throught the exchange program between the Bologna and Brown Universities. Discussing with him on different features of the problems has always been very illuminating. I appreciate a lot his kind hospitality, as well as the one of the Brown Physics Department where part of this work was performed. Some of the computations reported in this work were performed at the Theoretical Physics Computing Facility at Brown University.

Finally I am also in debt with prof. A. Schianchi with whom I worked on the "portfolio optimization problem". It has been nice to collaborate with him, as always it happens when people of different areas work together on a common topic.

Bibliography

[1] K. Binder and A. P. Young, "Spin glasses: experimental facts, theoretical concepts, and open questions", *Rev. Mod. Phys.* **58** 801 (1986)

[2] M. Mézard, G. Parisi and M. Virasoro, *Spin Glass Theory and Beyond*, World Scientific Publishing, Singapore (1987)

[3] K. H. Fisher and J. A. Hertz, *Spin glasses*, Cambridge University Press, Cambridge (1991)

[4] Debashish Chowdhury, *Spin Glasses and Other Frustated Systems*, Princeton University Press, Princeton (1986)

[5] M. A. Ruderman and C. Kittel, *Phys. Rev.* **96** 99 (1954)

[6] T. Kasuya, *Prog. Theor. Phys.* **16** 45 (1956)

[7] K. Yoshida, *Phys. Rev.* **106** 893 (1957)

[8] V. Cannella and J. A. Mydosh, *Phys. Rev. B* **6** 4220 (1972)

[9] C. A. M. Mulder, A. J. van Duyneveldt and J. A. Mydosh, "Susceptibility of CuMn spin-glass: frequency and field dependences", *Phys. Rev. B* **23** 1384 (1981)

[10] C. A. M. Mulder, A. J. van Duyneveldt and J. A. Mydosh, "Frequency and field dependence of the ac susceptibility of the AuMn spin-glass", *Phys. Rev. B* **25** 515 (1982)

[11] S. Nagata, P.H. Keesom and H. R. Harrison, *Phys. Rev. B* **19** 1633 (1979)

[12] L. Lundgren, P. Svedlindh and O. Beckman, "Experimental indication for a critical relaxation time in spin-glasses", *Phys. Rev. B* **26** 3990 (1982)

[13] L. Lundgren, P. Svedlindh, P. Nordblad and O. Beckman, "Dynamics of the relaxation time spectrum in a CuMn spin-glass", *Phys. Rev. Lett.* **51** 911 (1983)

[14] S. F. Edwards and P. W. Anderson, "Theory of spin glasses", *J. Phys. F: Metal Phys.* **5** 965 (1975)

[15] D. R. Sherrington and S. L. Kirckpatrich, "Solvable model of a spin-glass", *Phys. Rev. Lett.* **35** 1792 (1975)

[16] D. R. Sherrington and S. L. Kirckpatrich, "Infinite-ranged models of spin-glasses", *Phys. Rev. B* **17** 4384 (1978)

[17] J. R. L. de Almeida and D. J. Thouless, "Stability of the Sherrington-Kirkpatrick solution of a spin glass model", *J. Phys. A: Math. Gen.* **11** 129 (1978)

[18] D. J. Thouless, P. W. Anderson and G. Palmer, "Solution of 'Solvable model of a spin glass' ", *Phil. Mag.* **35** 593 (1977)

[19] H. J. Sommers, *Z. Phys. B* **31** 301 (1978)

[20] C. De Dominicis, *Phys. Rep.* **67** 37 (1980)

[21] T. Plefka, "Convergence condition of the TAP equation for the infinite-ranged Ising spin glass model", *J. Phys. A: Math. Gen.* **15** 1971 (1982)

[22] R. G. Palmer and C. M. Pond, *J. Phys. F.* **9** 1451 (1979)

[23] A. J. Bray and M. A. Moore, *J.Phys C: Solid State Phys.* **12** L441 (1979)

[24] A. J. Bray and M. A. Moore, "Metastable states in spin-glasses", *J.Phys C: Solid State Phys.* **13** L469 (1980)

[25] F. Tanaka and S. F. Edwards, "Analytic theory of the ground state properties of a spin glass. I. Ising spin glass", *J.Phys. F* **10** 2769 (1980)

[26] C. De Dominicis, M. Gabay, T. Garel and H. Orland, *J. Phys. (Paris)* **41** 923 (1980)

[27] P. Baldi and E. B. Baum, "Bounds on the size of ultrametric structures", *Phys. Rev. Lett.* **56** 1598 (1986)

[28] C. De Dominicis and A. P. Young, "Weighted averages and order parameters for the infinite range Ising spin glass", *J. Phys. A.: Math. Gen.* **16** 2063 (1983)

[29] K. Nemoto and H. Takayama, "TAP free energy structure of SK spin glasses", *J. Phys. C: Sol. St. Phys.* **18** L529 (1985)

[30] K. Nemoto and H. Takayama, *J. Magn. Matter* **54-57** 135 (1986)

[31] K. Nemoto, "A numerical study of the pure states of the Sherrington-Kirkpatrick spin glass model - a comparison with Parisi's replica-symmetry-breaking solution", *J. Phys. C: Sol. St. Phys.* **20** 1325 (1987)

[32] H. Sompolinsky and A. Zippelius, "Relaxational dynamics of the Edward-Anderson model and the mean field theory of spin glasses", *Phys. Rev. B* **25** 6860 (1982)

[33] A, Houghton, S. Jain and A. P. Young, "Role of the initial conditions in the mean field theory of spin glass dynamics", *Phys. Rev. B* **28** 2630 (1983)

[34] K. H. Fisher, . *Solid State Commun.* **18** 1515 (1976)

[35] A. Blandin, *J. Phys. C* **39** 1499 (1978)

[36] A. Blandin, M. Gabay and T. Garel, *J. Phys. C* **13** 403 (1980)

[37] A. J. Bray and M. A. Moore, *Phys. Rev. Lett.* **41** 1068 (1978)

[38] C. De Dominicis, M. Gabay and H. Orland, *J. Phys.* **42** L523 (1981)

[39] G. Parisi, "Toward a mean field theory for spin glasses", *Phys. Lett.* **73A** 203 (1979)

[40] G. Parisi, "A sequence of approximated solutions to the S-K model for spin glasses", *J. Phys. A: Math. Gen.* **13** L115 (1980)

[41] G. Parisi, "The order parameter for spin glasses: A function on the interval 0-1", *J. Phys. A: Math. Gen.* **13** 1101 (1980)

[42] G. Parisi, "Magnetic properties of spin glasses in a new mean field theory", *J. Phys. A: Math. Gen.* **13** 1887 (1980)

[43] G. Parisi, "Order parameter for spin-glasses", *Phys. Rev. Lett.* **50** 1946 (1983)

[44] C. De Dominicis and I. Kondor, "Eigenvalues of the stability matrix for Parisi solution of the long-range spin-glass", *Phys. Rev. B* **27** 606 (1983)

[45] M. Mezard, G. Parisi, N. Sourlas, G. Toulose and M. A. Virasoro, "Replyca simmetry breaking and the nature of the spin glass phase", *J. Phys.* **45** 843 (1984)

[46] M. Mezard and M. A. Virasoro, "The microstructure of ultrametricity", *J. Phys.* **46** 1293 (1985)

[47] A. P. Young, "Direct determination of the Probability Distribution for the Spin-Glass order Parameter", *Phys. Rev. Lett.* **51** 1206 (1983)

[48] B. Derrida, "Random-energy model: An exactly solvable model of disordered systems", *Phys. Rev. B* **24** 2613 (1981)

[49] D. J. Gross and M. Mezard, "The simplest spin glass", *Nucl. Phys. B* **240** 431 (1984)

[50] E. Gardner, "Spin glasses with p-spin interactions", *Nucl. Phys. B* **257** 747 (1985)

[51] D. Stariolo, "Ising spin glasses with multispin interactions", *Physica* **166A** 6229 (1990)

[52] A. Crisanti and H. J. Sommers, *Z. Phys. B* **87** 341 (1992)

[53] A. Crisanti, H. Horner and H. J. Sommers, *Z. Phys. B* **92** 257 (1993)

[54] D. S. Fisher and D. A. Huse, "Pure states in spin glasses", *J. Phys. A: Math. Gen.* **20** L997 (1987)

[55] D. A. Huse and D. S. Fisher, "Absence of many states in realistic spin glasses", *J. Phys. A: Math. Gen.* **20** L1005 (1987)

[56] D. S. Fisher and D. A. Huse, "Equilibrium behavior of the spin-glass ordered phase", *Phys. Rev. B* **38** 386 (1988)

[57] G. Toulouse, "Theory of the frustation effect in spin glasses: I", *Comm. Phys.* **2** 115 (1977)

[58] C. D. Mattis, *Phys. Lett.* **56A** 421 (1976)

[59] T. R. Kirkpatrick and P. G. Wolynes, "Connections between some kinetic and equilibrium theories of the glass transition", *Phys. Rev. A* **35** 3072 (1987)

[60] T. R. Kirkpatrick and P. G. Wolynes, "Stable and metastable states in mean-field Potts and structural glasses", *Phys. Rev. B* **36** 8552 (1987)

[61] T. R. Kirkpatrick and D.Thirumalai, "p-spin-interaction spin-glass models: Connections with the structural glass problem", *Phys. Rev. B* **36** 5388 (1987)

[62] T. R. Kirkpatrick and D.Thirumalai, "Mean-field Potts glass model: initial-condition effects on dynamics and properties of metastables states", *Phys. Rev. B* **38** 4881 (1988)

[63] T. R. Kirkpatrick and D.Thirumalai, *Transp. Theor. Stat. Phys.* **24** 927 (1995)

[64] F. H. Stillinger, T. A. Weber, *Science* **225** 983 (1984)

[65] M. Mèzard and G. Parisi, "Statistical physics of structural glasses ", *cond-mat/0002128*, to appear in the proceedings of the Trieste workshop on "Unifying Concepts in Glass Physics"

[66] G. Biroli and R. Monasson, "From inherent structures to pure states: some simple remarks and examples", *Europhys. Lett.* **50** 115 (2000)

[67] E. Marinari, G. Parisi and F. Ritort, Replica field theory for deterministic models (I): binary sequences with low autocorrelation", *J. Phys. A: Math. Gen.* **27** 7615 (1994)

[68] J. P. Bouchaud and M. Mézard, "Self-induced quenched disorder: a model for the glass transition", *J. Physique I* **4** 1109 (1994)

[69] E. Marinari, G. Parisi and F. Ritort, "Replica field theory for deterministic models (II): a non random spin glass with glassy behaviour", *J. Phys. A: Math. Gen.* **27** 7647 (1994)

[70] I. Borsari, M. Degli Esposti, S.Graffi and F.Unguendoli, "Deterministic spin models with a glassy phase transition", *J. Phys. A: Math. Gen.* **30** L155 (1997)

[71] M. E. J. Newman and C.Moore, "Glassy dynamics and aging in an exactly solvable spin model", *Phys. Rev. E* **60** 5068 (1999)

[72] M. J. E. Golay, "Sieves for low autocorrelation binary sequences" , *IEEE Trans. Inform. Theory* **IT23** 43 (1977)

[73] M. J. E. Golay, "The merit factor of long low autocorrelation binary sequences", *IEEE Trans. Inform. Theory* **IT28** 543 (1982)

[74] J. Bernasconi, "Low autocorrelation binary sequences: statistical mechanics and configuration space analysis", *J. Physique (Paris)* **48** 559 (1987)

[75] G. Migliorini and F. Ritort, "Dynamical behaviour of low-autocorrelation models", *J. Phys. A: Math. Gen.* **27** 7669 (1994)

[76] H. J. Sommers, "On the dynamic mean-field theory of spin-glasses" *Z. Physik* **B50** 97 (1983)

[77] I. Kondor and C. De Dominicis, "Ultrametricity and zero modes in the short-range Ising spin glass", *Europhys. Lett.* **2** 617 (1986)

[78] I. Borsari, S. Graffi and F. Unguendoli, "Ground states for a class of deterministic spin models with glassy behaviour", *J. Phys. A: Math. Gen.* **29** 1593 (1996)

[79] M. Degli Esposti, "Quantization of the orientation preservering automorphism of the torus", *Ann. Inst. H. Poincaré* **58** 7647 (1993)

[80] M. Degli Esposti, S. Graffi and S. Isola, "Classical limit for the quantized hyperbolic symplectomorphisms over the torus", *Commun. Math. Phys.* **167** 471 (1995)

[81] J. M. Kosterlitz, D. J. Thouless and R. C. Jones, "Spherical model of a spin-glass", *Phys. Rev. Lett.* **36** 1217 (1976)

[82] E. Marinari, G. Parisi and F. Ritort, "The fully frustrated simple hypercubic model is glassy and aging at large D", *J. Phys. A: Math. Gen.* **28** 327 (1995)

[83] I. Borsari, F. Camia, S. Graffi and F. Unguendoli, "Absence of glassy behaviour in the deterministic spherical and XY models", *J. Phys. A: Math. Gen.* **31** 1127 (1998)

[84] C. Itzykson and J. M. Drouffe, *Statistical field theory*, vol. II, Cambridge University Press, Cambridge (1988)

[85] G. Parisi and M. Potters, "Mean-field equations for spin models with orthogonal interaction matrices", *J. Phys. A: Math. Gen.* **28** 5267 (1995)

[86] A. Georges and J. S. Yedidia, "How to expand around mean-field theory using high-temperature expansions", *J. Phys. A: Math. Gen.* **24** 2173 (1991)

[87] G. H. Wannier, *Elements of Solide State Theory*, Cambridge University Press, Cambridge (1960)

[88] V.M. de Oliveira and J.F.Fontanari, "Landscape statistics of the p-spin Ising model", *J.Phys. A: Math. Gen.* **30** 8445 (1997)

[89] C. M. Newman and D. L. Stein, "Metastable states in spin glasses and disordered ferromagnets" *cond-mat/9908455*

[90] T. Apostol, *Introduction to Analytic Number Theory*, New York, Springer 1976

[91] Ya G. Sinai, *Probability Theory*, Springer-Verlag 1991.

[92] J. Villain, *J. Phys. C* **10** 4793 (1977); **11** 745 (1978)

[93] H. Nishimori and Y. Ozeki, *J. Phys. Soc. Jpn.* **59** 289 (1190)

[94] M. Schwartz and A. P. Young, *Europhys. Lett.* **15** 209 (1991)

[95] Y. Ozeki and H. Nishimori, "Lower critical dimension of the XY spin glass", *Phys. Rev. B* **46** 2879 (1992)

[96] H. Kawamura and M. Tanemura, *J. Phys. Soc. Jpn.* **60** 608 (1991)

[97] H. Kawamura, "Numerical studies of chiral ordering in three-dimensional XY spin glasses", *Phys. Rev. B* **51** 12398 (1995)

[98] J. Maucourt and D. R. Grempel, "Lower Critical Dimension of the XY Spin-Glass Model", *Phys. Rev. Lett.* **80** 770 (1998)

[99] J. M. Kosterlitz and N. Akino, "Numerical Study of Order in a Gauge Glass Model", *Phys. Rev. Lett.* **81** 4672 (1998)

[100] M. Ney-Nifle and H. J. Hilhorst, "Chiral- and spin-correlation functions in a random-bond XY ladder", *Phys. Rev. B* **48** 10254 (1993)

[101] M. J. Thill, M. Ney-Nifle and H. J. Hilhorst, "Chiral and continuous symmetry of an XY spin glass on a tube lattice", *J. Phys. A: Math. Gen.* **28** 4285 (1995)

[102] M. Ney-Nifle and H. J. Hilhorst, "Chiral and spin order in the two-dimensional $\pm JXY$ spin glass: Domain-wall scaling analysis", *Phys. Rev. B* **51** 8357 (1995)

[103] H. Kawamura and M. Tanemura, "Chiral order in a two-dimensional XY spin glass", *Phys. Rev. B* **36** 7177 (1987)

[104] P. Ray and M. A. Moore, "Chirality-glass and spin-glass correlations in the two-dimensional random-bond XY model", *Phys. Rev. B* **45** 5361 (1992)

[105] H. S. Bokil and A. P. Young, "Study of chirality in the two-dimensional XY spin glass", *J. Phys. A* **29** L89 (1996)

[106] J. M. Kosterlitz and N. Akino, "Numerical Study of Spin and Chiral Order in a Two-Dimensional XY Spin Glass", Phys. Rev. Lett. **82** 4094 (1999)

[107] S. Jain, "Chiral glass ordering in the XY spin glass in four dimensions", *J. Phys. A: Math. Gen.* **30** 8027 (1997)

[108] J. Villain, *J. Phys. (Paris)* **36** 581 (1975)

[109] A. Vallat and H. Beck, "Coulomb-gas representation of the two-dimensional XY model on a torus", *Phys. Rev. B* **50** 4015 (1994)

[110] S. Kirkpatrick, C. D. Gellat and M. P. Vecchi, *Science* **220** 671 (1983)

[111] H. Markovitz, *Portfolio selection: Efficient Diversification of Investments*, Wiley, New York (1959)

[112] E. J. Elton, M. J. Gruber, *Modern Portfolio Theory and Investment Analysis*, 5th ed., Wiley, New York (1995)

[113] H. Levy and M. Sarnat, *Portfolio and Investment Selection: Theory and Practice*, Prentice-Hall International, London (1984)

[114] J. Lintner, "The valuation of risk assets and the selection of risky investments in stock portfolios and capital budget", *Review of Econonomics and Statistics* (1965)

[115] J. Lintner, "The effect of short selling and margin requirements in perfect capital markets", *Journal of Financial and Quantitative Analysis*, 1173 (1971)

[116] C. Azariadis, *The problem of multiple equilibrium* Unpublished, University of California, Los Angeles (1992)

[117] M. R. Garey and D.S. Johnson, *Computers and Intractability: a Guide to the Theory of NP-Completness*, Freeman, San Francisco (1979)

[118] E. H. L. Aarts and J. K. Lenstra, Editors, *Local Search in Combinatorial Optimization*, John Wiley & Sons Ltd. (1997)

[119] S. Galluccio, J.P. Bouchaud and M. Potters, "Rational decision, random matrices and spin glasses", *Physica A* **259** 449 (1998)

[120] P. Krugman, "History versus Expectations", *Quarterly Journal of Economics CVI* 651 (1991)

[121] E. J. Elton and M. J. Gruber, "Modern Portfolio Theory, 1950 to Date", *Journal of Banking & Finance* **21**, 1743 (1998)

[122] C.O. Alexander and C.T. Leigh, "On the Covariance Matrices Used in Value at Risk Models", *The Journal of Derivatives Spring 1997*, 50 (1997)

[123] M. L. Mehta, *Random Matrices*, Academic Press, London. (1991)

[124] L.Laloux, P. Cizeau, J.P. Bouchaud, M. Potters, *Risk* **12** 69 (1999)

[125] A. Schianchi, "Portfolio optimization reconsidered: a generalization", unpublished (2000).

[126] M. Degli Esposti, C. Giardin, S. Graffi and S. Isola, 2000, "Statistics of energy levels and zero temperature dynamics for deterministic spin models with glassy behaviour", to be published on *Journal of Statistical Physics* (2001)